An-Najah National University
Faculty of Graduate studies

Nanoparticle CdS-Sensitized TiO_2 Catalyst for Photo-Degradation of Water Organic Contaminants: Feasibility Assessment and Natural-Dye Alternatives

By

Ahed Husni Abdel-Razaq Zyoud

Supervisor:
Prof. Dr. Hikmat Hilal

Co-supervisor:
Dr. Nidal Zatar

Submitted in Partial Fulfillment of the Requirements for the Ph.D. in Chemistry, Faculty of Graduate Studies, at An-Najah National University, Nablus, Palestine

2009

COMMITTEE DICISION

Nanoparticle CdS-Sensitized TiO_2 Catalyst for Photo-Degradation of Water Organic Contaminants: Feasibility Assessment and Natural-Dye Alternatives

By:

Ahed Husni Abdel-Razaq Zyoud

This Thesis was successfully defended on 11/ 08/ 2009 and approved by:

Committee Members	**Signatures**
1- **Prof. Hikmat S. Hilal, Ph.D.**, (Committee Chairman)	.....
2- **Dr. Nidal Zatar**, (Co-supervisor)	Nidal Zatar
3- **Dr. Ismail Warad**, (External Examiner)	.....
4- **Dr. Raqi Shubietah**, (Internal Examiner)	.....

DEDICATED

This thesis is especially dedicated to my wife (Asma), to my son (Waseem), and to my daughter (Lema)

ACKNOWLWDGEMENTS

I am indebted to my principal supervisor Prof. Dr. Hikmat Hilal. His brilliant academic guidance, continuous encouragement, patience, time, enthusiasm and support are greatly appreciated. I would also like to express my sincere appreciation and thanks to my co-supervisor Dr. Nidal Zatar for advice and guidance in times of need. Special thanks to my committee members, Dr. Ismail Warad, Dr. Raqi Shubaita for their effort and suggestions.

I would like to extend my appreciation and thanks to Prof. Dr. Guy Campet and to Dr. DaeHoon Park, both of ICMCB (University of Bordeaux), for assistance with XRD, TGA and SEM.

Thanks are due to French-Palestinian University Cooperation Program (Al-Magdisi) for financial support to this project and travel assistance to Bordeaux. I personally thank Mr. Sebastian Fagart and Ms. Mathilde Girardot for continued personal help.

Gift of free chemicals by Birzeit-Palestine Pharmaceutical Company is acknowledged.

I would like to thank Dr. Iyad Saadeddin for continued help through out this work. Thanks are also due to my friends Ahmed Hussen and Ghazi Noor.

I am deeply grateful to my parents, sisters and brothers for their support and encouragement all the time.

Finally, I would like to thank my wife, my son (Waseem), and to my daughter (Lema).

TABLE OF CONTENTS

CHAPTER 2

MATERIALS, EQUIPMENTS, PREPARATIONS AND CHARACTERIZATION TECHNIQUES FOR TiO_2/CdS SYSTEMS

CHAPTER 3

PHOTO-DEGRADATION OF METHYL ORANGE [MO] USING TiO_2/CdS

CHAPTER 4

PHOTO-DEGRADATION OF PHENAZOPYRIDINE USING TiO_2/CdS

CHAPTER 5

NATURAL DYE SENSITIZERS OF TiO_2 IN METHYL ORANGE AND PHENAZOPYRIDINE PHOTO-DEGRADATION: SCREENING STUDY USING ANTHOCYANIN DYE

LIST OF TABLES:

LIST OF FIGURES

LIST OF SCHEMES

LIST OF ABBREVIATIONS

Symbol	Abbreviation
UV	Ultraviolet
Vis.	Visible
MO	Methyl Orange
PhPy	Phenazopyridine
CBD	Chemical Bath Deposition
XRD	X-ray Diffraction
SEM	Scanning Electron Microscope
TGA	Thermal Gravimetric Analysis
AC	Activated Carbon
AOPs	Advanced Oxidation Processes
eV	Electron volt
SC	Semiconductor
e^-	Electron
h^+	hole
VB	Valence Band
CB	Conduction Band
E_g	band gap
E_{cs}	conduction band edge
E_{vs}	valence band edge
r	reaction rate

k_r	reaction rate constant
K	adsorption constant
C	contaminant concentration
t	time
E_a	activation energy
pH_{zpc}	pH of zero point charge
PL	photoluminescence
HMDE	Hanging Mercury Drop Electrode
FWHM	Full Width at Half Maximum
DSSC	Dyes Sensitized Solar Cells
HOMO	Highest Occupied Molecular Orbital
LUMO	Lowest Unoccupied Molecular Orbital

Nanoparticle CdS-Sensitized TiO_2 Catalyst for Photo-Degradation of Water Organic Contaminants: Feasibility Assessment and Natural-Dye Alternatives

By
Ahed Husni Abdel-Razaq Zyoud

Supervisor**: Prof. HiKmat Hilal Ph.D.**
Co-Supervisor**: Dr. Nidal Zatar**

ABSTRACT

The photocatalytic degradation of organic contaminants (like dyes, insecticide, pesticide, … etc) in water, using TiO_2 under UV are commonly used procedures. Modifying TiO_2 with CdS also a common technique used for water purification under visible light.

In this work both commercially and prepared TiO_2 were used for photo-degradation of both contaminates models (Methyl Orange MO and Phenazpyridine PhPy), $TiCl_3$ was used as a starting rote for preparation of rutile structure TiO_2 by hydrolysis. In order to sensitization of TiO_2 to photoexcited under visible light, A chemical path deposition method (CBD) was used to precipitate a nonsocial particles of CdS on TiO_2 particles surface. Sand was used as a supporting surface for the prepared catalyst. UV-visible scanning, photoluminescence measurements, XRD characterization, and SEM imaging were run for the prepared catalyst systems. The particles size of prepared CdS particle was found to be 20 nm.

The influence of the catalyst concentration, initial contaminant concentration and pH on photo-degradation rate were studied. Turnover number and Quantum yield were also calculated for comparison study. There is no observable increases in photo-degradation rate with increasing contaminants and catalyst concentration, but a decrease in the rate was observed, no effect to the temperature on the rate, also a higher photo-degradation rate for (MO & PhPy) was observed at higher pH degrees. Voltametric analysis shows almost complete CdS decomposition during the photo-degradation process.

Due to hazardous and toxicity of decomposed Cd^{2+} in the treated water, an alternative of natural nontoxic dyes (Anthocyanin) was used for the first time as a sensitizer for the rutile TiO_2. AC was also used as a supporting substrate. Electronic absorption spectra, FT-IR spectra, and TGA analysis were applied on the prepared TiO_2/Anthocyanine catalyst systems. A screen study was done to test the efficiency of the prepared sensitized catalyst, the catalyst was applied to photodegradate MO and PhPY. An observable efficiency was noted specially when using AC/TiO_2/Anthocyanin at low pH in photo-degradation of MO.

CHAPTER 1

GENERAL INTRODUCTION, LITERATURES SURVEY AND OBJECTIVES

1.1 Overview:

Purification of water, such as municipal wastewater, is conventionally achieved by combined processes usually including both physical and biological processes, such as flocculation, filtration and biological treatment[1-4]. These processes are relatively low in cost and well-established. However, such removal techniques are not able to remove low levels of toxic inorganic and organic contaminants. Chemical methods have been employed to remove low levels of toxic compound, and can involve the addition of powerful oxidants such as ozone or hydrogen peroxide. Advanced Oxidation Processes (AOPs) are characterized by generation of highly oxidizing hydroxyl radicals ($OH^{\bullet}$), leading to complete abatement of pollutants through mineralization to carbon dioxide, water, and inorganic ions such as nitrate, chloride, sulfate and phosphate [1-4], which are usually harmless compounds. Some chemical processes involve oxidizing chemicals alone, such as ozone and hydrogen peroxide, while others combine such chemicals with UV-visible light irradiation. Common photoassisted AOPs are UV/Fenton processes, Ozone/UV, H_2O_2/UV and photocatalysts [5].

Photocatalysts are categorized into homogeneous and heterogeneous systems. TiO_2 based processes are the fastest growing techniques in the last forty years [6-9]. TiO_2 is activated by near UV radiation, and partly by sunlight which slightly includes near UV. Electrons (reducing species) and holes (oxidizing species) are generated when TiO_2 is irradiated. Oxidizing species such as the $OH^{\bullet}$ could be also generated by interaction between holes and OH^-, such a technique may replace expensive and hazardous oxidizing chemicals in the processes[6]. Illuminated TiO_2 is one of the most powerful oxidants due to the high oxidizing potential of holes in the valence band formed by photoexcitation [10-12]. Owing to its outstanding photocatalytic activity, excellent chemical and photochemical stability, non toxicity and low cost, TiO_2 can be used at commercial scale. TiO_2 based photocatalysts have been used for water purification, sterilization [13-14], and waste water treatment [12].

TiO_2 photocatalysis has focused on the oxidation of organic pollutants. This is because most of pollutants are organic in nature. Inorganic soluble and higher oxidation states, could also be reduced to insoluble forms for subsequent removal [15-20].

Photocatalytic processes have evolved into a possible commercial technique in water remediation. The idea began when Fujishima and Honda (1972) demonstrated water photolysis into hydrogen and oxygen gas by irradiation of TiO_2 electrode connected to a platinum counter electrode. Many review papers on photocatalytic remediation processes have been

presented in recent years [5-11]. Literature provides extensive details on various aspects of photocatalytic processes.

TiO_2 (band gab 3.2 eV) can only be activated by near UV irradiation (wavelength less than 380 nm), which represents less than 5% of the total solar spectrum at the earth crust. Many workers investigated the enhancement of the photo-response of TiO_2 in the visible region. Methods used include the coupling with a semiconductor which is sensitive to visible light (small band gab), such as CdS [20]. Other methods include dye sensitization of TiO_2 [21] and ion implantation into the TiO_2 crystal matrix [11].

During the last decade, thousands of references and related patents, on heterogeneous photocatalytic removal of hazardous compounds from water and air appeared. A variety of organic molecules can be photocatalytically oxidized and eventually mineralized according to the following general reaction [6, 11-14, 23-25, 29-30].

$$\textit{Organic Molecules} + O_2 \quad (TiO_2) \rightarrow CO_2 + H_2O + \textit{Mineral Acids} \quad (1.1)$$

An abbreviated list of compounds that have been demonstrated to be degradable via reaction (1.1) is given in Table (1.1). Often, local pollution problems impel researchers to investigate the degradability of a particular compound, and new compounds are continually being added to the list [11].

Table 1.1: Different photodegraded contaminants with different semiconductors.

Degraded substance	Catalyst used	Region	Ref.
Phenol, Chlorinated Phenols,	TiO_2-rotating disk pellets	UV	26

4-Chlorophenol (4-CP), 2,4-Dichlorophenol (2,4-DCP), 2,4,6-Trichlorophenol (2,4,6-TCP), 2,3,6-Trichlorophenol (2,3,6-TCP), 2,3,5-Trichlorophenol (2,3,5-TCP), Pentachlorophenol (PCP), and γ-isomer of 1,2,3,4,5,6 Hexachlorocyclohexane (Lindane),	on stainless steel supports (SS),		
Chlorinated Phenols, CO_2, Rhodamine-6G and Phenol, Oxidation of C_2H_4, Photoxidation of Propane, Freon 12, 1,2-Dichloroethane, Chloroform	TiO_2-SiO_2 mixed oxide sol-gel, precipitation, sol-gel/co-precipitation, co-precipitation, impregnation	UV	27
2,4-Dichlorophenoxyacetic acid (2,4-D) [Herbicide]	TiO_2/UVA/O_3, Fe(II)/UVA/O_3 ,	UVA	28
Acrinathrin, Avermectine B1, Endosulphan, Formetanate, Imidacloprid, Lufenuron, Methamidophos, Oxamyl, Pyrimethanil, Propamocarb [Pesticides]	TiO_2	UV	29
Phenol, Phenolic compounds	TiO_2 thin films prepared by direct current dc supports such as glass, silicon, alumina, glass coated Indium tin oxide	UV	30
17-β-Oestradiol	TiO_2 immobilized in Ti-6Al-4V alloy	UV	31
Propoxur, 2-Isopropoxyphenol, 1,2-Dihydroxybenzene, Isopropoxy-Dihydroxybenzene	2,4,6-triphenylpyrylium-Zeolite Y as photocatalyst	UV	32
Sulfide, Etanethiol	Cobalt(II) 2,9,16,23-tetrasulphophthalocyanine & cobalt(II) 2,4,16,23-tetra(chlorosulphonyl)phthalocyanine bonded to TiO_2 matrix by sol-gel		33
2-Chlorophenol, 2-Nitrophenol	TiO_2	UVA	34
CBr_4	TiO_2	UV	35
Trichloroethylene in gas phase	TiO_2 supported on glass bead	UVA	36
Phenol	TiO_2 anatase	UVA	37
Phenol	TiO_2/AC	UV	38
Formaldehyde	TiO_2	UV	47
Para-hydroxybenzoic acid	TiO_2	UV	36
2,4-Dichlorophenoxyaceticacid, & Benzofuran	TiO_2	UV	37
Organic pollutant , Phenol , Chloro Phenol, Trichloroethylene,	TiO_2, modified with 8-hydroxyquinoline (HOQ)	Vis	39
Dye-sensitized TiO_2 solar cells		Vis	40
Tamaron 50®	AC/ TiO_2/dye	Vis	41

Chlorophenoxyacetic acid, Methyl Parathion	TiO_2 sensitized by Zeolite Y (TPY)	Vis	29
N,N,N',N'-Tetraethylrhdamine (Rhodamine B) (RB)	TiO_2 colloidal solution	UV vis	42
4-Chlorophenoxyacetic acid	TiO_2/2,4,6-Triphenylpyrylium ion (TP^+) supported on amorphous Sand	UV/ vis	43
Phenol	TiO_2/dye	vis	44

1.2 Semiconductor Photocatalysis:

1.2.1 Electronic Properties of Semiconductors:

Semiconductors (SC) could be photo-excited by absorbing light at suitable wavelengths to generate two types of electronic carriers in a process called (electron-hole pair generation). Electrons $\mathbf{e^-}$ represent the reducing species and holes $\mathbf{h^+}$ represent the oxidizing species.

$$\textbf{Semiconductor (SC)} + \textbf{photon } (\boldsymbol{hn}) \rightarrow \textbf{SC } (\mathbf{e^- + h^+})$$

The bonding and electron distribution in a solid material is often described by the band theory [45]. Valence Band (VB) refers to highest filled aggregate of orbitals, whereas the Conduction Band (CB) refers to the lowest empty band associated with the first exited state. The forbidden energy domain between conduction band and valence band is called the band gap (E_g). For many compounds, as the number of nonnumeric units in a particle increases, the band gap decreases (Figure 1.1). Photoexcitation involves the promotion of an electron $\mathbf{e^-}$ from the valence band (VB) to the conduction band (CB). This occurs as a result of absorption of a photon of energy exceeding the band-gab ($hn > E_g$) by the semiconductor. This simultaneously generates a hole $\boldsymbol{h^+}$ in the valence band. A hole can be

rationalized as an empty level in the valence band or a valence bond with an electron missing [45].

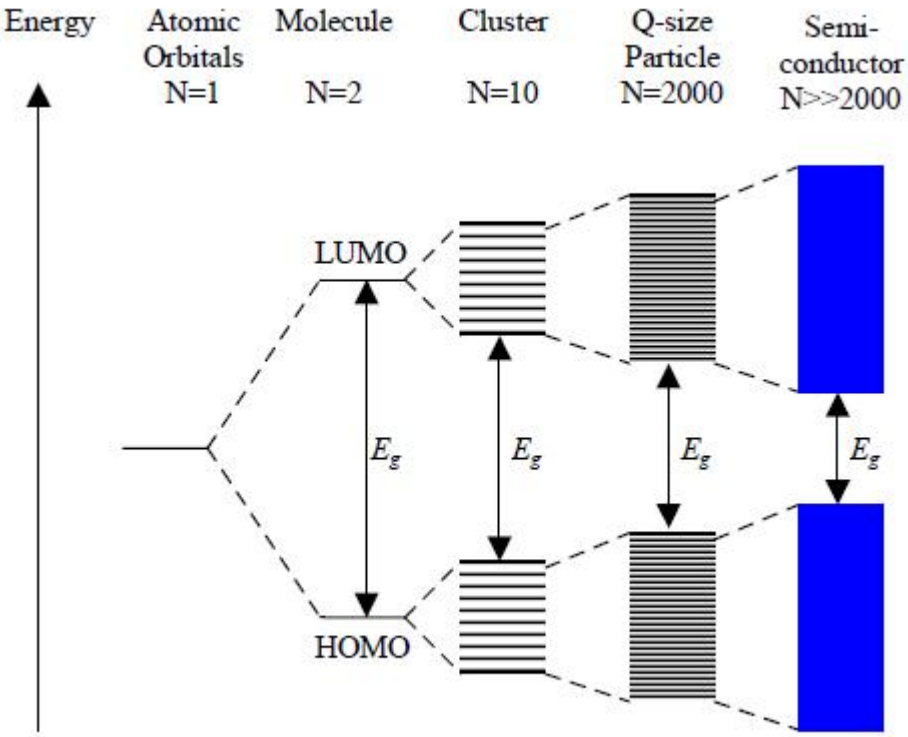

Figure 1.1: The effect of the increase in the number (N) of nonnumeric units from unity to cluster of more than 2000 on the electronic structure of a semiconductor compound [45].

Semiconductors can be categorized into two main types: intrinsic and extrinsic semiconductors. An intrinsic semiconductor contains negligible concentrations of defects and impurities. Small band-gap semiconductors can be thermally excited, leading to electron-hole pair generation, giving rise to electrical conductivity. Extrinsic semiconductors have impurities added to their lattice and contain defects. If accepter impurities are present in the extrinsic semiconductor, the semiconductor is termed as a ***p-type*** semiconductor. Acceptor impurities have a deficit of electrons and hence result in an excess of holes in the semiconductor. Hence, a p-type

semiconductor has a Fermi level just above its upper valence band edge. The Fermi level (E_f) shall be defined as the top of the available electron energy levels at low temperatures. For an ***n-type*** semiconductor, the majority charge carriers are electrons due to the presence of donor impurities. Donor impurities contribute extra electrons to the intrinsic semiconductor. The resulting semiconductor has electrons as its majority charge carriers, and its Fermi level is just below its lower conduction band edge [45].

1.2.2 Photo-Effect on TiO_2 Semiconductor:

As photo-excitation of n-type semiconductor TiO_2 with photons ($h\nu > E_g$) occurs, electrons are excited from the valance band (VB) to the conduction band (CB), producing holes in the valance band (Figure 1.2). Under the influence of electric field, it has been suggested that most generated holes occur at the surface, while the minority of the electrons are transferred through the bulk of the TiO_2 particle. The prolonged irradiation could result in the accumulation of electrons in the interior. This could cause flattening of the band near surface and the narrowing of the space charge layer, easing the transfer of electrons from the interior to the surface [47]. The generated $\mathbf{e^-}$ and $\mathbf{h^+}$ can take part in processes as illustrated in Figure (1.2). Electron hole recombination may occur in the bulk (reaction **1a**) and/or at the surface (reaction **1b**). The successfully transferred electrons and holes to the TiO_2 surface behave as follows: The electrons may reduce an electron acceptor A^+ (reaction **2a**) while the holes may oxidize an electron

donor D (reaction **2b**) [10]. The redox reactions **2a** and **2b** are desirable to the destruction of organic and inorganic pollutants via oxidation and reduction processes respectively. These processes are believed to occur mainly on the TiO_2 surface. The presence of the $\mathbf{A^+}$ and **D** species on the TiO_2 surface is hence imperative to the capture of $\mathbf{e^-}$ and $\mathbf{h^+}$ respectively.

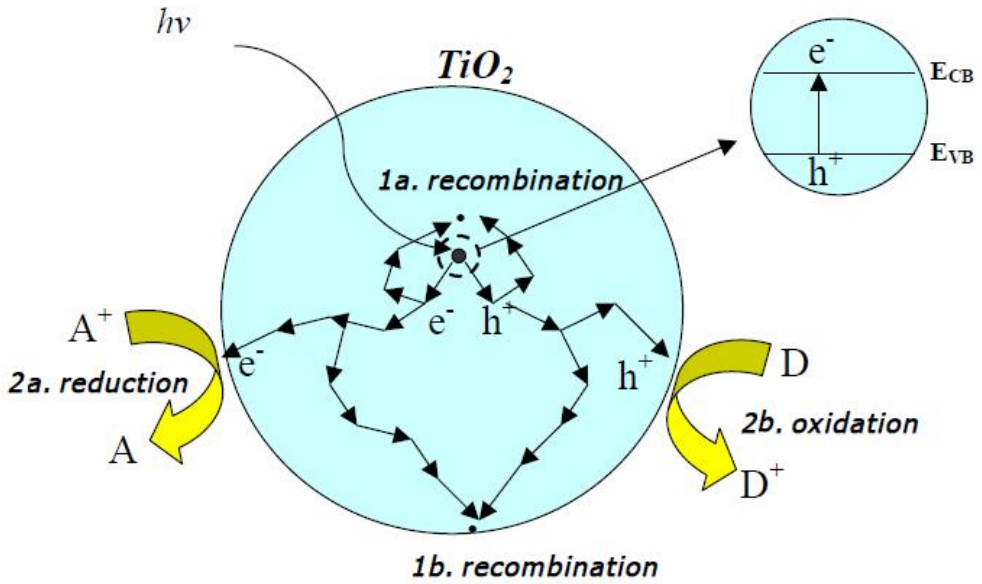

Figure 1.2: Possible pathways of main charge carriers occurring in a TiO_2 particle following photo-excitation [48].

1.2.3 Redox Power of Semiconductors:

Semiconductors may absorb light with (hv > Eg), producing photo-electrons and photo-holes. The generated electrons and holes quickly relax to the bottom of the conduction band and the top of the valence band respectively by dissipating their extra kinetic energy in the form of ***phonons***. The generated electrons and holes can be used to drive a redox reaction. Thermodynamically, the energy level of the conduction band edge

(E_{cs}) is a measure of the reduction strength of electrons in the semiconductor, and the valence band edge (E_{vs}) is a measure of oxidation power of the holes in the semiconductor [21]. Different semiconductors possess different band edge energy levels. Higher (more positive) valence band edge potentials have higher oxidizing power for their holes. A thermodynamically favorable semiconductor toward photo-degradation of different organic compounds is one with a valence band edge having a relatively high positive potential. On the other hand, small band-gap semiconductors have better light absorption match with solar light emission spectrum. Figure (1.3) shows the band-gap and band edges of common semiconductors in contact with aqueous media at pH ~0.0 [48].

From a utilization of solar energy point of view, small band gap semiconductors would be preferred. However, small band gap semiconductors normally do not have highly positive valence band potentials. They also suffer serious chemical and/or photo-chemical corrosions [49].

The selection of semiconductor photo-catalysts, depending on the application, often involves the compromise between a number of factors, such as high oxidizing power, good solar light coverage, and chemical & photochemical stability.

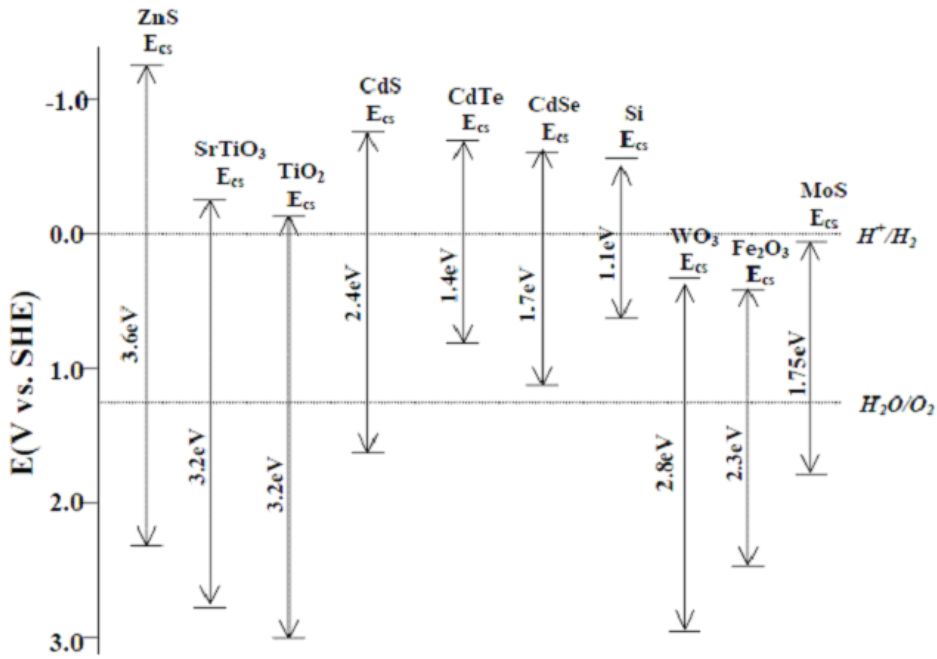

Figure 1.3: Energy-level diagram for various semiconductors showing relative energy positions of VB and CB edges in aqueous media at pH 0.0 [48].

TiO_2 is among the few semiconductors that have high oxidizing power ($E_g \approx 3.1$ eV) and good chemical and photochemical stabilities. Its poor solar light coverage has been treated by sensitizing with other small band-gap semiconductors or dyes [50-51], and by natural dyes as in the potential work of this thesis.

1.2.4 Semiconductor Nano-Particles:

An increase in the band gap of the semiconductor with decrease in the particle size is defined as quantization effect. Nanoparticles of semiconductors display unique size-dependent properties (quantization effect) that alter their photochemical, photophysical, optical and electrochemical responses [52]. Both large band gap (e.g., ZnO, TiO_2, SnO_2

and WO_3) and small band gap (e.g., CdSe, CdS) semiconductors display this property. Charge generation, separation, retention and transfer across a semiconductor and its surroundings are greatly affected by quantization effect [53-57]. Surface bound species, such as surrounding electrolytes, sensitizers, metals and dyes, determine the mechanism of charge transfer at the semiconductor/surrounding interface. Photo-induced excitation leads to charge separation in the semiconductor followed by electron and/or hole transfer to the surroundings dictated by the energetic of the system. Furthermore, defects or vacancies are created in the semiconductor largely due to the method of synthesis. Such defects affect photo-electrochemical and photo-catalytic behaviors of the semiconductor.

Two major drawbacks of any individual large band-gap semiconductor have been identified as, recombination of photo-generated charges (electron and holes) and limited light harvesting ability. These factors are limit the commercial usage of the semiconductor. A semiconductor can be sensitized using another semiconductor (TiO_2/CdS and TiO_2/CdSe) [52], or dyes (TiO_2/Azo dyes) [58]. Charge recombination can be minimized using metal deposits (Ag, Pt, Ru) [59-60]. The metal inhibit recombination of the photogenerated charges by releasing charges at solid/liquid interface. Thus both drawbacks of the semiconductor can be effectively overcome depending on the material used to create composite with a semiconductor [60].

1.2.5 Titanium Dioxide TiO_2:

TiO_2 has three different crystal phases: rutile (the most common form), anatase and brookite. Rutile is the thermodynamically stable form of TiO_2, into which anatase and brookite convert when heated above 500°C or 750°C, respectively [6, 24]. Studies indicate that the anatase form shows the highest $OH^{\bullet}$ formation rates [60]. Many studies show that there is optimum composition of anatase-rutile that gives better results in photo-degradation of organic pollutants [62]. In rutile the octahedra are not regular**,** showing a slight orthorhombic distortion, whereas in anatase and brookite the octahedra of oxygen atoms are significantly distorted, so that their symmetry is lower than orthorhombic. The modifications differentiate in the number of sharing edges with neighboring octahedra [63]. Due to these differences, rutile and anatase show different densities and other physical properties. Some of these differences are represented in Table (1.2). The band gap for TiO_2 semiconductor crystalline phases for rutile and anatase are 3.02 eV and 3.23 eV, corresponding to photons of wavelength 413 nm and 388 nm, respectively [5]. Anatase shows the highest photo-catalytic activity, followed by rutile. Brookite is rarely used in photo-catalytic studies, because it is the most unstable form and is very difficult to prepare [64]. Most TiO_2 photocatalytic studies have been carried out using pure anatase form, pure rutile form or a mixture of both forms [64]. Anatase form of TiO_2 gets over rutile form in photo-catalytic activity. This is because in the rutile, the excess charge carriers tend to have higher recombination rates than in anatase [66]. Crystal structures for rutile, anatase and brookite titanium dioxide are shown in (Figure 1.4)

Table 1.2: Properties of anatase and rutile structures of TiO_2[66]

Properties	Rutile	Anatase	Brookite
Lattice constant a (A^o)	4.59	3.78	9.18
Lattice constant b (A^o)	4.59	3.78	5.45
Lattice constant c (A^o)	2.95	9.52	5.15
Specific gravity	4.2 – 4.3	3.82 – 3.97	3.9 – 4.1
Index of refraction	2.74	2.52	2.58
Hardness (Mohs scale)	6.0 – 6.5	5.5 – 6.0	5.5 – 6.0
Melting point	1858 C^o	1858 C^o	1858 C^o

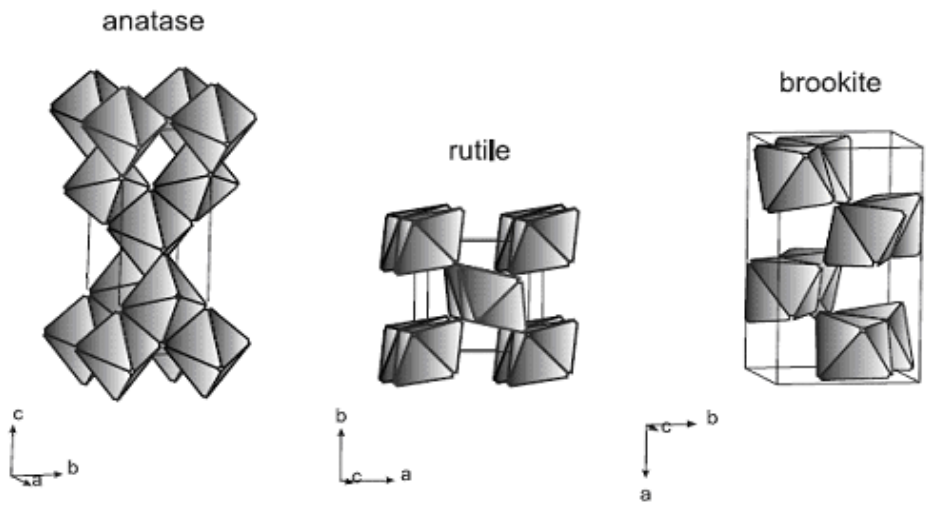

Figure 1.4: TiO_6 octahedra representing the different modifications of TiO_2 (anatase, rutile and brookite)

1.2.6 General Mechanisms for Semiconductor Photocatalysis:

The process for heterogeneous photo-catalysis by semiconductors starts with electron-hole pair generation in the semiconductor particles. Upon excitation, the separated electrons and holes may follow several pathways. The migration of electrons and holes to the semiconductor surface will further promote electron transfer to adsorbed organic or inorganic species. The electron transfer process is more efficient if the species are readily adsorbed on the surface. While at the surface, the semiconductor can donate electrons to an electron acceptor (usually oxygen molecule). A hole can migrate to the surface where an electron from a donor species can

combine with the surface hole to oxidize the donor species. The probability and rate of the charge transfer processes for electrons and holes depend on the redox potential levels of the adsorbate species and on edge positions for VB and CB. Electron and hole recombination competes with charge transfer to adsorbed species (Figure 1.2). Recombination of the separated electron and hole can occur inside the bulk or at the surface of semiconductor particle accompanied with heat releasing [23]

1.2.6.1 Titanium Dioxide TiO_2 Photocatalytic Mechanism:

TiO_2 photo-catalytic reaction mechanism is still being investigated, but a simplified primary photo-catalytic mechanism is believed to involve multiple processes [67]. These include light and semiconductor interactions, photo-generated electron/hole interactions with the semiconductor (at the surface and in the bulk), and photo-generated electron/hole capture at the interface. The in-solution reaction mechanisms depend on the organic compounds involved. The in-semiconductor mechanisms are basically the same regardless of type of organic compounds involved. Based on laser flash photolysis measurements, general mechanisms and time characteristics of various steps involved in the heterogeneous photocatalysis at TiO_2 have been suggested by Hoffmann [21]. Steps and their characteristic times are listed in Table (1.3).

According to this general mechanism, the overall photo-catalytic quantum efficiency is controlled by: competition between the recombination of the charge carriers ($\mathbf{e^-}$ & $\mathbf{h^+}$) and trapping of charge carriers on one hand, and

competition between recombination of trapped charge carriers and interfacial charge transfer (capture of charge carriers) on the other hand. Therefore if the surface of the catalyst is covered with pollutants, the direct oxidation by positive holes could be the major oxidation pathway, since the adsorption of organic compounds on the surface of the catalysts is the prerequisite step for direct charge transfer. On the other hand, direct oxidation by hydroxyl radicals requires the adsorption of water or hydroxide ions on the surface to form the hydroxyl radicals.

Table 1.3: General mechanism of semiconductor photocatalysis at TiO_2 [21].

Primary process	Characteristic times
Charge carrier generation	
$TiO_2 + h\nu \rightarrow h_{vb}^+ + e_{cb}^-$	Fast (fs)
Charge-carrier trapping	
$h_{vb}^+ + >Ti^{IV}OH \rightarrow \{>Ti^{IV}OH^{\bullet}\}^+$	Fast(10ns)
$e_{cb}^- + >Ti^{IV}OH \rightarrow \{>Ti^{III}OH\}$	Shallow trap(100ps) dynamic equilibrium
$e_{cb}^- + >Ti^{IV} \rightarrow >Ti^{III}$	Deep trap (10ns) irreversible
Charge-carrier recombination	
$e_{cb}^- + \{>Ti^{IV}OH^{\bullet}\}^+ \rightarrow >Ti^{IV}OH$	Slow (100ns)
$h_{vb}^+ + \{>Ti^{III}OH\} \rightarrow >Ti^{IV}OH$	Fast (10ns)
Interfacial charge transfer	
$\{>Ti^{IV}OH^{\bullet}\}^+ + Red \rightarrow >Ti^{IV}OH + Red^{\bullet+}$	Slow (100ns)
$\{>Ti^{III}OH\} + Ox \rightarrow >Ti^{IV}OH + Ox^{\bullet-}$	Very slow (ms)

Note: *h_{vb}^+: photoholes, e_{cb}^-: photoelectrons, >TiOH: TiO_2 surface group, Red: Reductant, Ox: Oxidant.*

The suggested mechanisms for contaminant degradation by photoexcited semiconductor are divided into the following categories:

A) Adsorption: For a catalytic reaction to occur, at least one and frequently all of the reactants must become attached to the surface (adsorption). Adsorption takes place by physical adsorption or chemisorption. Literature referred UV/TiO_2 photo-degradation process to Langmuir adsorption model, which postulated that:

1. All catalyst surface sites are identical and have same adsorption activity.
2. There is no interaction between adsorbed molecules.
3. All same molecules adsorb by same mechanism; and adsorbed complexes have same structures.
4. The extent of adsorption is less than one complete mono-molecular layer on the surface.

B) Direct photo-catalytic pathway

The mechanism of Langmuir-Hinshelwood photo-catalytic reaction, which occurs at a photo-chemically active surface after photo-excitation of the catalyst and producing electrons-holes is described as follows:

$$M_{(\text{Contaminant Molecule})} + S_{(\text{Semiconductor surface})} \leftrightarrow M_{ads\ (\text{adsorbed Molecule})}$$

(adsorption / desorption Langmuir equilibrium)

$$Catalyst + hn \rightarrow e^- + h^+$$ (Photoexcitation of the catalyst)

$$M_{ads} + h^+ \rightarrow M^+_{ads}$$ (Hole trapping by adsorbed molecules)

$$M^+_{ads} + e^- \rightarrow M_{ads}$$ (Decay of the reactive state)

$$M^{+}_{ads} \rightarrow product + S_{\text{(Semiconductor surface)}} \qquad \text{(Chemical reaction)}$$

The photo-excitation of the catalyst produces electrons and holes. The carrier (hole) may be trapped by the adsorbed molecule to form a reactive radical state, whose decay occurs through recombination with an electron. The chemical reaction yields the products and regenerates the original state of the catalyst surface (S).

1.3 Kinetics of Photo-Catalytic Degradation:

1.3.1 Experimental Parameters Effects:

Several photo-catalytic chemical and physical parameters were studied. Such parameters include: Oxygen, pH, initial contaminant concentration, catalyst dosage, agitation rate, temperature, light wavelength, and light intensity. Many workers investigated the effects of such parameters on the photo-catalytic rate [11, 69-72]. Herrmann (1999) summarized these effects via plots of rates versus parameters involved as shown in Figure (1.5) [11].

1.3.1.1 Effect of Catalyst Amount on Reaction Rate:

The initial reaction rates were found to be directly proportional to catalyst amount. However, above a certain value of the mass of catalyst, the reaction rate level plateau-off, decrease or becomes independent of the amount of loaded catalyst, as shown in Figure (1.5). This limit depends on reaction conditions and photo-reactor geometry. The limit was found to be 2.5 mg TiO_2 per ml solution. This indicates maximum amount of catalyst

particles at entire surface exposed, and at higher amounts screening effect occurs. Screening masks part of the photo-sensitive surface [11]. Bangun & Andesina suggested increased agglomeration of particles, due to greater particle-particle interactions at high catalyst amount, and that optimum catalyst loading would be a function of pH [73]

1.3.1.2 Effect of Wave Length on Reaction Rate:

As shown in Figure (1.5), the variation of the reaction rate as a function of the wavelength follows the absorption spectrum of the catalyst. The threshold wavelength corresponds to catalyst energy band gap, so that TiO_2 requires $\lambda<400$ nm [11]. The Figure shows that with shorter wave length, the rate remains constant.

1.3.1.3 Effect of Initial Contaminant Concentration on Reaction Rate:

With respect to heterogeneous catalysis, the contaminant molecules have to be adsorbed on the catalyst surface active sites, the adsorption of contaminant molecules and the availability of active sites are important parameters for photo-catalytic reactions and mechanisms [11, 74]. The rate of photo-degradation reaction is proportional to the rate of adsorption of contaminant molecules which is also proportional to the available active sites. As the reaction proceeds, the amount of adsorbed contaminant molecules will decrease until the contaminant is consumed.

The kinetic models for photo-catalytic reactions are derived based on the classical Langmuir-Henshelwood heterogeneous catalytic model, which assumes that the reaction occurs on the surface and the reaction rate (r) is

proportional to the fraction of surface active sites by the contaminant concentration (θ) :

$$r = -\frac{dC}{dt} = k_r q = k_r \frac{KC}{1+KC}$$

where k_r is the reaction rate constant, K is the adsorption constant and C is the contaminant concentration at any time t.

For dilute solutions ($C < 10^{-3}$M), $KC << 1$ and the reaction is of the apparent first order. At higher concentrations ($C > 5 \times 10^{-3}$ M), $KC >> 1$ and the reaction rate is maximum and of zero order with respect to contaminant [11].

1.3.1.4 Effect of Temperature on Photo-Degradation Rate:

The photo-catalysis activity of TiO_2 is usually found to be particularly not affected by temperature, and the apparent activation energy $\mathbf{E_a}$ is often very small (a few kJ/mol) in the moderate temperature range (20 – 80 ^oC). At lower temperatures, near to 0 ^oC, the photocatalytic activity decreases and the $\mathbf{E_a}$ increases as shown in Figure (1.5). The lowering in the photocatalytic activity is due to desorption of the final products, while the rise in the E_a tends to the heat of adsorption of the products [11].

1.3.1.5 Light Intensity:

The effects of light intensity and wavelength have also been another area of research in this field. A low level light intensity was found to exhibit a linear relationship with the rate of degradation while at intermediate light intensity the degradation rate was found to depend on the square root of the

light intensity. The rate was however independent of the light at very high intensities (Figure 1.5) [11].

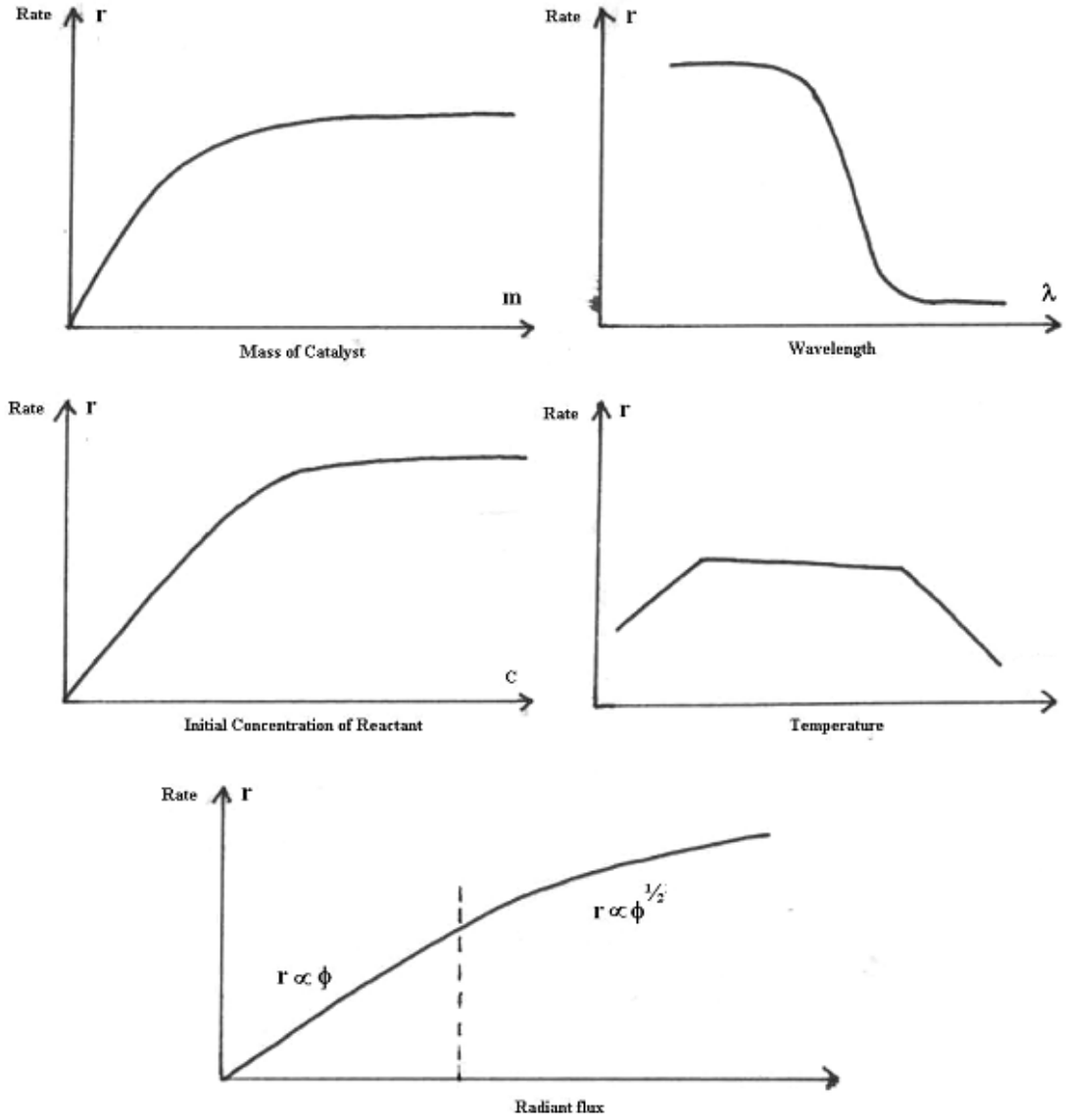

Figure 1.5: Influence of the different physical parameters that govern the reaction rate (generally comprised between 0.1 – 1 mM): (a) mass of catalyst; (b) wavelength; (c) initial concentration of reactant; (d) temperature and (e) radiant flux [11].

1.3.1.6 Effect of pH on Photo-Degradation Rate:

Hoffmann *et al*. [77] reported that the pH of zero point charge for TiO_2 (pH_{zpc}) is ~ 6.25, calculated from the pK_{a1} and pK_{a2} of acid-base equilibria of TiO_2 contacted with aqueous media:

$$>TiOH_2^+ \;\; « \;\; >TiOH + H^+ \qquad pK_{a1} = 4.5$$

$$>TiOH \;\; « \;\; >TiO^- + H^+ \qquad pK_{a2} = 8.0$$

Below pH_{zpc} the surface of TiO_2 is positively charged, while above this pH the surface is negatively charge. Hoffmann *et al*. [77] proposed a model to describe the distribution of different TiO_2 surface species (>TiOH, $>TiOH_2^+$, $>TiO^-$) with pH as shown in Figure (1.6).

The pH would greatly influence the photo-catalytic oxidation kinetics of strong adsorbates. However, the complexity involved in the substrate/surface coordination and in the subsequent photo-catalytic oxidation steps make it difficult to identify what effect of the original substrate adsorption has on its photo-catalytic oxidation kinetics. In some cases the pH greatly affected photo-catalytic reaction rates [78], while in most cases, the rate of photo-catalytic reaction is only weakly dependent on the solution pH [79-83].

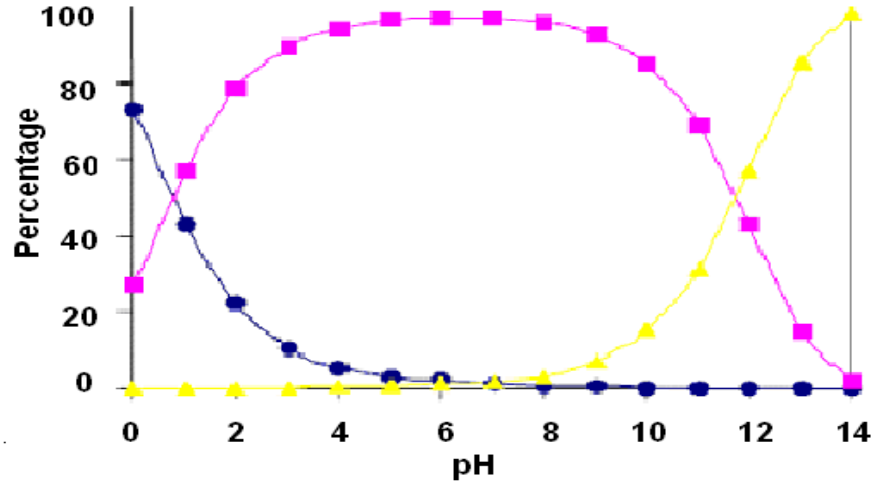

Figure 1.6: The distribution of TiO_2 surface species with pH, (■) >TiOH, (●) >$TiOH_2^+$, (▲) >TiO^-.

1.4 Sensitization of TiO_2: Composite Semiconductor and Dye Sensitization:

As mentioned previously, TiO_2 absorbs only in the near UV irradiation, which only constitutes less than 5% in sunlight irradiation. Thus the quantum efficiency is very low under visible light irradiation. Coupling TiO_2 with CdS semiconductor (E_{bg} = 2.2 eV) is a technique used to sensitize TiO_2 to work under visible irradiation. The sensitizer semiconductor must have a narrower band gap with higher conduction band edge than that of TiO_2. The concept of sensitization which has been investigated by Spanhel et al is explained in Figure (1.7) [83]. CdS absorbs in the visible light (λ<~560 nm) to excite the electrons to the conduction band. Due to the relative positions of the TiO_2 and CdS conduction bands, the electrons from the conduction band of CdS could be transferred to that of attached TiO_2. The electrons would then reduce species (such as oxygen or metal ions) at the TiO_2 back surface. While the remaining holes in the valence band of the CdS could oxidize the contaminants molecules. To be

oxidized, the contaminant molecule must have an oxidation potential comparable or less positive than CdS valence band edge.

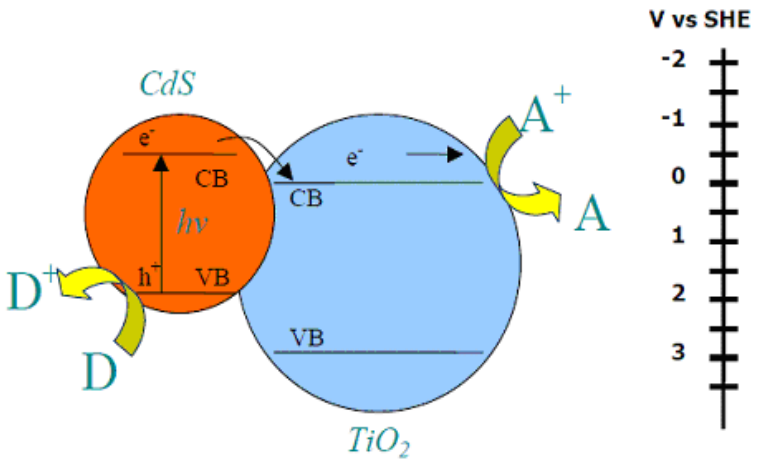

Figure 1.7: Sensitization in a TiO_2/CdS system

Another approach used to sensitize TiO_2 is molecular dye-sensitization technique. This technique involves addition of dyes into the TiO_2 photocatalytic system. The reaction pathway of the combined rule of the TiO_2/Dye photosensitized reaction has been described by Kamat, (Figure 1.8) [84]. In order to achieve sensitization, the dye must possess oxidative energy level more negative than the conduction band of TiO_2 when excited by visible light. The excited electron, in the dye molecule LUMO, moves to the conduction band of TiO_2, and subsequently reduces an electron acceptor (such as oxygen). Unoccupied (empty) orbitals in the HOMO of the dye will oxidize the contaminant molecules. As mentioned above, the contaminant molecule to be oxidized must have an oxidizing potential comparable or less positive than dye HOMO.

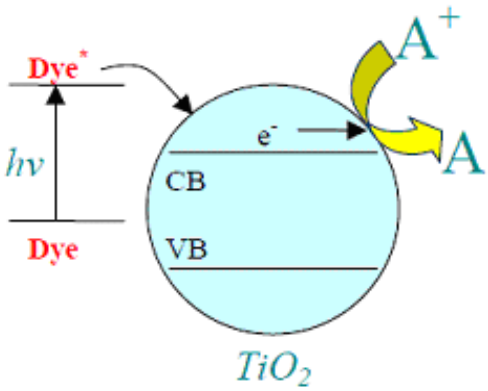

Figure 1.8: Sensitization of TiO_2 with molecular dye systems.

Zhang *et al* found that only 10% of the photo-excited electrons could be used for reduction while the others recombine with the dye itself [85].

1.5 General Objectives:

1.5.1 Strategic Objectives:

This work aims at finding a suitable dye that would sensitize TiO_2 in degrading organic contaminants under solar simulator light, taking into account efficiency, recyclability, cost and environmental safety.

1.5.2 Technical Objectives:

The technical objectives of this study are:

1- Sensitizing of rutile TiO_2 by short band gab nanoparticles CdS toward photocatalytic activity.

2- Investigating the efficiency of the prepared sensitized CdS@TiO_2 toward photo-degradation of Methyl Orange which is commonly studied contaminant model in literature, for comparison purposes.

3- Studying the efficiency of CdS@TiO_2 towered photo-degradation of Phenazopyridine (which has not been studied earlier using TiO_2 systems).

4- Testing the possibility of decomposition of CdS during the photo-degradation process, and determination the amount of leaching out Cd^{2+} ions in treating solution during the process.

5- Studying the effect of different parameters, such as pH, temperature, contaminant concentration and loaded catalyst on photo-degradation efficiency.

6- Substrate the CdS@TiO_2 catalyst on water non soluble sand, in order to recovery the used catalyst, and to see if it reduced the leaching out of Cd^{2+} during the photo-degradation process.

7- Screening study for using safe non toxic natural dyes (Anthocyanin) for sensitizing TiO_2 to photodegrade contaminants under visible light.

8- Supporting the prepared TiO_2/Anthocyanin catalyst onto activated carbon, in order to observe if AC could increase the efficiency of photo-degradation of contaminant.

References:

1. P. Pichat, Partial or complete heterogeneous photocatalytic oxidation of organic compounds in liquid organics or aqueous phases, *Catal. Toda.y*, **19** (1994) 313-334.

2. I. K. Konstantinou, V. A. Sakkas, T. A. Albanis, Photocatalytic degradation of the herbicides propanil and molinate over aqueous TiO_2 suspensions: identification of intermediates and the reactionpathway. *Appl. Catal., B*, ***34*** **(**2001**)** 227-239.

3. C. Maillard, C. Guillard, P. Pichat, The degradation of nitrobenzene in water by photocatalysis over TiO_2: kinetics and products; simultaneous elimination of benzamide or phenol or Pb^{2+} cations, *New J. Chem*., **18** (1994) 941-948.

4. V. Maurino, C. Minero, E. Pelizzetti, M. Vincenti, Photocatalytic transformation of sulfonylurea herbicides over irradiated titanium dioxide particles,*Colloid. Surface A*, **151** (1999) 329-338.

5. D. Chem, M. Sivakumar, A. K. Ray, heterogeneous photocatalysis in Environmental Remediation, *Dev. Chem. Eng. Miner. Process*, **8** (2000) 505-550.

6. A. Mills, S. Le Hunte, An Overview of Semiconductor Photocatalysis, *J Photoch. Photobio. A*, **108** (1997) 1-35.

7. J. Robertson, Semiconductor photocatalysis: an environmentally acceptable alternative production technique and effluent treatment process, *J. clean. prod.*, **4** (1996) 203-212.

8. A. Hagfeldt, M. Gratzel, Light-induced redox Reaction in Nanocrystalline Sysrtems, *Chem. Rev.*, **95** (1995) 49-68.

9. G. D. Surender, G. P. Fotou, S. E. Pratsinis, Titania-based Aqueous Phase Photocatalytic Remediation Processes: Strategies for Enhancement of Quantum Efficiency, *Trends Chem. Eng.*, **4** (1998) 145-159.

10. M. I. Litter, Review: Heterogeneous Photocatalysis Transition metals Ions in Photocatalytic Systems, *Appl. Catal. B*: *Environ.*, **23** (1999) 89-114.

11. J. M. Herrmann, Heterogeneous Photocatalysis: Fundamentals and Applications to the removal of Various types of Aqueous Pollutants, *Catal. Today*, **53** (1999) 115-129.

12. O. Legrini, E. Oliveros, A. M. Braun, Photochemical Processes for Water Treatment, *Chem. Rev.*, **93** (1993) 671–698.

13. D. F. Ollis, E. Pelizzetti, and N. Serpone, Heterogeneous photocatalysis in the environment: application to water purification, in Photocatalysis, Fundamentals and Applications, *John Wiley & Sons*, New York, NY, USA, **Chapter 18** (1989), pp. 603–637.

14. N. Serpone, D. Lawless, R. Terzian, C. Minero, E. Pelizzetti, M. Schiavello, editors. Photochemical conversion and storage of solar energy. *Dordrecht: Kluwer Academic Publishers*, (1991) 451-475.

15. D. Lawless, A. Res, R. Harris, N. Serpone, C. Minero, E. Pelizzetti, , and H. Hidaka, Removalof toxic metal from solutions by photocatalysis using irradiated platinized titanium dioxide: removalof lead. *Chim. Ind.* **72** (1990) 139-46.

16. H. Reiche and A. J. Bard, Heterogeneous Photosynthetic Production of Amino Acids from Methane-Ammonia-Water at Pt/TiO . Implications in Chemical Evolution, *J. Am. Chem. Soc.*, **101** (1979) 3127.

17. L. D. Lau, R. Rodriguez, S. Henery , D. Manuel, Photoreduction of Mercuric Salt Solutions at High pH, *Environ. Sci. Technol.*, **32** (1998) 670.

18. N. Serpone, Y. K. Ah-You, T. P. Tran, R. Harris, E. Pelizzetti, H. Hidaka, AM1 simulated sunlight photoreduction of Hg(II) andCH_3Hg(II) chloride salts from aqueous suspensions of titanium dioxide. *Sol. Energy*, **39** (1987) 491-498.

19. K. Tennakone, , and U. S. Ketipearachchi, Photocatalytic Method for Removal of Mercury From Contaminated Water, *Appl. Catal., B, Environ.*, ***5*** *(1995) 343-349.*

20. D. Robert and S. Malato, Solar photocatalysis: a clean process for water detoxification, *Sci. Total Environ.*, **291** (2002) 85–97.

21. M. R. Hoffmann, S. T. Martin, W. Y. Choi, D. W. Bahnemann, Environmental applications of semiconductor photo-catalysis, *Chem. Rev.*, **9** (1995) 69-96.

22. D. F. Ollis, H. Al-Ekabi (Eds.), Photocatalytic Purification and Treatment of Water and Air, *Elsevier Science Publishers: Amsterdam*, (1993) pp. 193-205.

23. A. Linsebigler, G. Lu, J. T. Yates, Photocatalysis on TiO_2 surfaces: principles, mechanisms, and selected results, *Chem. Rev.* **95 (**1995) 735-758.

24. U. Stafford, K. A. Gray, P. V. Kamat, Photocatalytic degradation of organic contaminants: Halophenols and related model compounds, *Heterogen. Chem. Rev.*, **3** (1996) 77-104.

25. D. D. Dionysiou, A. P. Khodadouse *etal*, Continuous-mode photocatalytic degradation of chlorinated phenols and pesticides in water using a bench-scale TiO_2 rotating disk reactor, *Applied Catalysis B: Environmental*, **24** (2000) 139-155.

26. X. Gao, I. E. Wachs, Titania-Sand as catalysts: molecular structural characteristics and physico-chemical properties, *Catalysis Ttoday*, **51** (1999) 233-254.

27. E. Piera, J. C. Calpe, E. Brillas, X. Domènech, J. Peral, 2,4-Dichlorophenoxyacetic acid degradation by catalyzed ozonation: TiO_2/UVA/O_3 and Fe(II)/UVA/O_3 systems, *Appl. Catal. B: Environ.*, **27** (2000) 169-177.

28. S. Malato, *et al*, Photocatalysis with solar energy at a pilot-plant scale: an overview, *Appl. Catal. B: Environ.*, **25**, (2000), 31-38.

29. D. Dumitriu, A. R. Bally, C. Ballif, et al., Photocatalytic degradation of phenol by TiO_2 thin films prepared by sputtering, *Appl. Catal. B: Environ***.,** **25** (2000) 83-92.

30. H. M. Coleman, B. R. Eggins, J. A. Byrne, F. L. Palmer and E. King, Photocatalytic degradation of 17-β-oestradiol on immobilised TiO_2**,** *Appl. Catal. B*: *Environ.*, **24** (2000) L1-L5.

31. A. Sanjuan, G. Alvaro, G. Mercedes, S. A. Hermenegildo, Degradation of propoxur in water using 2,4,6-triphenylpyrylium-Zeolite Y as photocatalyst: Product study and laser flash photolysis, *Appl. Catal. B: Environ.*, **25** (2000) 257-265.

32. T. Stuchinskaya, N. Kundo, L. Gogina; U. Schubert, A. Lorenz, V. Maizlish, Cobalt phthalocyanine derivatives supported on TiO_2 by sol-gel processing - Part 2. Activity in sulfide and ethanethiol oxidation**,** *J. Mol. Catal. A: Chem.*, **140** (1999) 235-240.

33. Kuo-Hua Wang, Yung-Hsu Hsieh Ming-Yeuan Chou and Chen-Yu Chang, Photocatalytic degradation of 2-chloro and 2-nitrophenol by titanium dioxide suspensions in aqueous solution**,** *Appl. Catal. B: Environ.*, **21** (1999) 1-8.

34. P. Calza, C. Minero, A. Hiskia, E. Papacostantinou, E. Pelizzetti, Photolytic and photocatalytic decomposition of bromomethanes in irradiated aqueous solutions**,** *Appl. Catal. B: Environ.*, **12** (1999) 191-202.

35. K. Wang, H. Tsai, Y. Hsieh, The kinetics of photocatalytic degradation of trichloroethylene in gas phase over TiO_2 supported on glass bead, *Appl. Catal. B: Environ.*, **17** (1998) 313-320.

36. I. Ilisz, A. Dombi, Investigation of the photodecomposition of phenol in near-UV-irradiated aqueous TiO_2 suspensions. II. Effect of charge-trapping species on product distribution, *Appl. Catal. A: Gen*, **180** (1999) 35-45.

37. J. Matos, J. Laine, J.Herrmann, Synergy effect in the photocatalytic degradation of phenol on a suspended mixture of titania and activated carbon, *Appl. Catal. B: Environ.*, **18** (1998) 281-291.

38. D. Chatterjee, A. Mahata, Photoassisted detoxification of organic pollutants on the surface modified TiO_2 semiconductor particulate system, *Catal. Commun.*, **2** (2001) 1-3.

39. S. Y. Huang, G. Schlichthörl, A. J. Nozik, M. Grätzel, A. J. Frank, Charge Recombination in dye-Sensitized Nanocrystalne TiO_2 Solar Cells, . *Phys. Chem. B*, **101** (1997) 2576–2582.

40. L. Majad, Dye-Modified Nano-Crystalline TiO_2 surfaces in Light Driven Water Purification From Organic Contaminants. *Ph. D. Thesis An-Najah N. University*, (2005).

41. P. Qu, J. Zhao', T. Shen, H. Hidaka, TiO_2-assisted photo-degradation of dyes: A study of two competitive primary processes in the degradation of RB in an aqueous TiO_2 colloidal solution, *J. Mol. Catal. A: Chem.*, **129** (1998) 257-268.

42. A. Sanjuán, G. Aguirre, M. Alvaro, H. García, 2, 4, 6-Triphenylpyrylium ion encapsulated in Y zeolite as photocatalyst. A co-operative contribution of the zeolite host to the photo-degradation of 4-chlorophenoxyacetic acid using solar light, *Appl. Catal. B: Environ.*, **15** (1998) 247-257.

43. D. Chatterjee, A. Mahata, photo-assisted detoxification of organic pollutants on the surface modified TiO2 semiconductor particulate system, *Catal. Commun.*, **2** (2000) 1-3.

44. M. R. Huffmann, S. T. Martine, W. Choi, D. W. Bahnemann, Environmental Applications of Semiconductor Photocatalysis, *Chem. Rev.*, **95** (1995) 69-96.

45. V. Parmon, A. V. Emeline, N. Serpone, Glossary of Terms in Photocatalysis and Radiocatalysis, *Int. J. Photoenergy*, **4** (2002) 91-131.

46. R. Memming, Photochemical Utilization of Solar Energy. Photochemistry and Photophysics, *Floridea: CRC Press*, **3** (1990).

47. A. L. Linsebrigler, G. Lu, and J. T. Yates, Jr., Photocatalysis on TiO_2 Surfaces: Principles, Mechanisms, and Selected Results, *Chem. Rev.*, **95** (1995) 735-758.

48. N. Serpone, E. Pelizzeti, Photocatalysis, Fundamentals and Applications, *John Wiley & Sons: New york, Brisbane*, (1989).

49. Y. V. Pleskov, Y. Y. Gurevich, Semiconductor Photoelectrochemistry; *Consultants Bureau: New York, London*, (1986).

50. T. A. Gad-Allah, S. Kato, S. Satokawa, T. Kojima, Role of core diameter and Sand content in photocatalytic activity of $TiO_2/SiO_2/Fe_3O_4$ composite, *Solid State Sci.*, **9** (2007) 737-743.

51. S. Hotchandani, P.V. Kamat, Charge-transfer processes in coupled semiconductor systems. Photochemistry and photoelectrochemistry of the colloidal CdS-ZnO system, *J. Phys. Chem.*, **96** (1992) 6834-6839.

52. P.V. Kamat, *et al.*, Semiconductor nanoparticles, in Handbook of Nanostructured materials and nanotechnology, *H. Nalwa, Editor., Academic Press: New York*, (1999) 292-344.

53. J. Z. Zhang, Ultrafast studies of electron dynamics in semiconductor and metal colloidal nanoparticles: Effect of size and surface, *Account Chem. Res.*, **30** (1997) 423-429.

54. L.M. Peter, Dynamic Aspects of Semiconductor Photoelectrochemistry, *Chem. Rev.*, **90** (1990) 753-769.

55. P. V. Kamat Interfacial charge transfer processes in colloidal semiconductor systems. *Prog. React. Kinet.*, **19** (1994) 277-316.

56. P. V. Kamat, Electron Transfer Processes in Nanostructured Semiconductor Thin Films, in Nanoparticles and Nanostructural Films, *J.H. Fendler, Editor, Wiley-VCH: New York*. (1998) 207-233.

57. J. Z. Zhang, Interfacial Charge Carrier Dynamics of Colloidal Semiconductor Nanoparticles. *J. Phys. Chem. B*, **104** (2000) 7239-7253.

58. M. Graetzel and A. J. McEvoy, Principles and Applications of Dye Sensitized Nanocrystalline Solar Cells (DSC), *Asian J. Energ. Environ.*, **5** (2004) 197-210.

59. G-J. Yang, C-J. Li, X-C. Huang, C-X. Li, and Y-Y. Wang, Influence of Silver Doping on Photocatalytic Activity of Liquid-Flame-Sprayed-Nanostructured TiO_2 Coating, *J. Therm. Spray Techn.*, **16** (2007).

60. B. Tian, T. Tong, F. Chen, J. Zhang, Effect of Water Washing Treatment on the Photocatalytic Activity of Au/TiO_2 Catalysts, *Acta Physico-Chimica Sinca*, **23** (2007) 978−982.

61. K. Tanaka, T. Hisanaga, A. rivera, Efect of Crystal Form of TiO_2 on the Photocatalytic Degradation of Pollutants, Phoocatalytic

treatment of Water and Air, *Elsevier Science Publishers, B.V. Amsterdam*, (1993) 169-178.

62. R. A. Rovira, Influence of Structure and UV-Light Absorption on the Electrical Conductivity of TiO_2 and Comparison with its Catalytic Activity , *Ph. D. thesis, University of Hannover*, (2005).

63. H. Kominami, J-I. Kato, S-y. Murakami, Y. Ishii, M. Kohno, K. Yabutani, T. Yamamoto, Y. Kera, M. Inoue, T. Inui and B. Ohtani., Solvothermal Syntheses of Semiconductor Photocatalysts of Ultra-high Activities: *Catal. Today*, **84** (2003) 181-189.

64. T. Ohno, K. Sarukawa, M. Matsumura, Photocatalytic Activity of Pure Rutile Particles Isolated from TiO_2 powder by Dissolving the Anatase Component in HF Solution, *J. Phys. Chem. B*, **105** (2001) 2417-2420.

65. K-M. Schindler and M. Kuns, Charge-Carrier Dynamics in TiO_2 Powders. *J. Phys. Chem.*, **94** (1990) 8222-8226.

66. A. Fujishima**,** K **.**Hashimot**,** T **.**Watanabe**,** TiO_2 Photocatalysis Fundamentals and Application, *BKC Inc.*, (1999) 125.

67. H. Al-Ekabi, B. Buttere, D. Delany, W. Holden, T. Powell, , and J. Story, The Photocatalytic Destruction of Gaseous Trichloroethylene and Trichloroethylene Over immobilized Titanium-Dioxide, Photocatalytic Purification and treatment of water and Air, *Elsevier Science Publishers, B.V. Amsterdam*, (1993), 719-725.

68. N. Serpon, and A. V. Emeline, Suggested terms and definitions in photocatalysis and radiocatalysis, *Int. J. Photoenergy*, **4** (2002) 91-131.

69. D. Chen, , A. K. Ray, Photocatalytic Kinetics of phenol and its Derivatives over UV irradiated TiO_2, *Appl. Catal. B: Environ.*, **23** (1999) 143-157.

70. J. Lea, A. A. Adesina, The Photo-oxidative Degradation of Sodium Dodecyl Sulphate in Aerated Aqueous TiO_2 Suspension, *J. Photoch. Photobio. A*, **118** (1998) 111-122.

71. R. W. Matthews, Kinetics of Photocatalytic Oxidation of Organic Solures over Titanium Dioxide, *J. Catal.*, **111** (1988) 264-272.

72. V. Augugliaro, V. Loddo, L. Palmisano, M. Schiavello, Performance of Heterogeneous Photocatalytic Systems: Influence of Operational Variables on Photoactivity of Aqueous Suspension of TiO_2, *J. Catal.*, **153** (1995) 32-40.

73. J. Bangun, A. a. adesina, The Photo-degradation Kinetics of Aqueous Sodium Oxalate Solution using TiO_2 Catalyst, *Appl. Catal. A: Gen.*, **175** (1998) 221-235.

74. V. Parmon, A. V. Emeline, N. Serpone, Glossary of terms in Photocatalysis and Radiocatalysis, *Int. J. Photoenergy*, **4** (2002) 91-131.

75. DF Ollis, E. Pellizzetti, N. Serpone, Destruction of Water Contaminants. *Environ. Sci. Technol.*, **25** (1991) 1523-1528.

76. C. Korman, D. W. Bahnemann, M. R. Hoffmann, Photolysis of chloroform and other organic molecules in aqueous titanium dioxide suspensions, *Envion. Sci. Technol.*, **25 (**1991) 494-500.

77. M.R. Hoffmann, S.T. Martin, W.Choi and D.W. Bahnemann, Environmental Applications of Semiconductor Photocatalysis, *Chem. Rev.* **95** (1995) 69-96.

78. Jiang, D.; Zhao, H.; Jia, Z.; Cao, J.; John, R. J., Photoelectrochemical behavior of methanol oxidation at nanoporous TiO2 film electrodes, *J. Photochem. Photobio* A, **144** (2001) 197-204.

79. A. E. Regazzoni, P. Mandelbaum, M. Matsuyoshi, S. Schiller, S. Bilmes A., M. A. Blesa, Adsorption and Photooxidation of Salicylic Acid on Titanium Dioxide: A Surface Complexation Description. *Langmuir*, **14** (1998) 868-874.

80. Harada, H., Ueda, T., Sakata, T., Semiconductor effect on the selective photocatalytic reaction of .alpha.-hydroxycarboxylic acids, *J. Phys. Chem.*, **93** (1989) 1542-1548.

81. F. Sabin, T. Turk, A. J. Vogler, Photo-oxidaton of organic compounds in the presence of titanium dioxide: determination of the efficiency, *J. Photochem. Photobiol. A*, **63** (1992) 99-106.

82. T. L., Rose, C. J. Nanjundiah, Rate enhancement of photooxidation of cyanide anion with titanium dioxide particles, *Phys. Chem.*, **89** (1984) 3766-3771.

83. L. Spanhel, H. Weller, A. Henglein, Photochemistry of semiconductor Colloids. 22. Electron Injection from Iluminated CdS into Attached TiO_2 and ZnO particles, *J. Am. Chem. Soc.*, **109** (1987) 6632-6635.

84. P. V. Kamat, Photoelectrochemistry in Particulate Systems. 9. Photosensitized Reduction in aColloidal TiO_2 System using Anthracene-9-carboxylic Acid as the Sensitizer, *J. Phys. Chem.*, **93** (1989) 859-864.

85. F. J. Zhang, L. Z. Zhao, T. Shen, H. Hidaka, E. Pelizzetti, N. Serpone, Photoassisted degradation of dye pollutants TiO_2 dispersions under irradiation by visible light, *J. Mol. Catal. A: Chem.*, **120** (1997) 173–178.

CHAPTER 2

MATERIALS, EQUIPMENTS, PREPARATIONS AND CHARACTERIZATION TECHNIQUES FOR TiO_2/CdS SYSTEMS

2.1 Materials and Chemicals:

Commercial Rutile TiO_2 powder (less than 500 nm in diameter) was purchased from Aldrich. Rutile TiO_2 was intentionally used here due to its known lower catalytic activity compared to Anatase TiO_2 [1-3]. Thus it is here desirable to enhance the activity of the less active Rutile system.

Thiourea, $CdCl_2$ and organic solvents were all purchased from either Aldrich-Sigma Co. or Frutarom Co. in pure form. $TiCl_3$ and Methyl Orange were purchased from Aldrich. Phenazopyridine hydrochloride was kindly

donated Berziet-Palestine Pharmaceutical Company. High surface area AC was purchased from Aldrich. *Hibiscus (Karkade)* for natural dye extraction was purchased from local markets.

2.2. Equipment: Apparatus and Methods

2.2.1 Irradiation Sources: UV-range radiation was obtained using an Oriel 500 W Hg/Xe lamp, equipped with a Universal Arc Lamp Housing, Model 66901, Oriel Instruments). The lamp specifications are shown in Table (2.1). Unless otherwise stated the lamp was operated at 150 W power. The light intensity at the solution surface was measured using a luxmeter and found to be 0.0032 W/cm^2 (Figure 2.1).

Table 2.1: Arc lamp description [4]

Model No.	Oriel-66142
Description	500 W Hg (Xe)
Average life (hours)	400
Suggested power range (W)	400-500
Typical voltage (VDC)	26
Typical current (ADC)	19

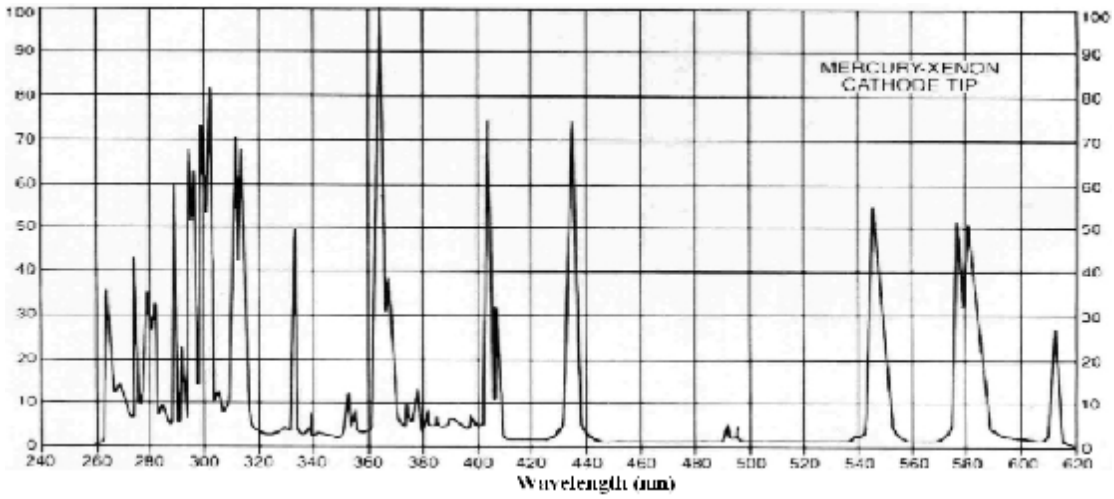

Figure 2.1: Typical spectral irradiance of Hg/Xe Lamp.

Solar simulated radiation was obtained using a 50 W Xenon lamp equipped with housing and a concentrating lens (Leybold Didacitic Company, model 45064). The lamp has a high stability and an intense coverage of wide spectrum. The light intensity at the solution surface was measured by using luxmeter and found to be 0.0212 W/cm^2 (Figure 2.2).

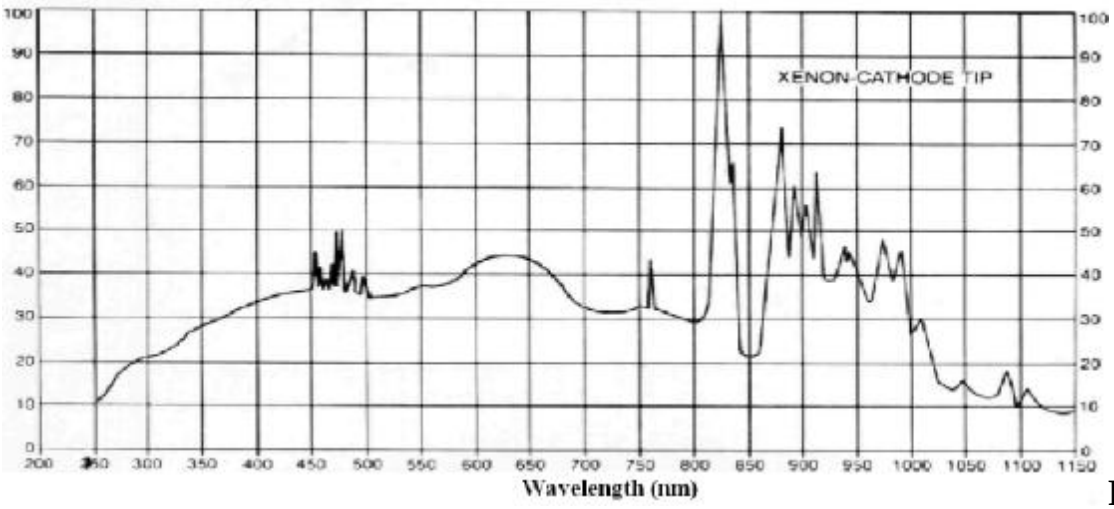

Figure 2.2: Typical spectral irradiance of Xe Lamp.

2.2.2 Absorption Spectrophotometry:

A Shimadzu UV-1601 spectrophotometer, equipped with a thermal printer Model DPU-411-040, Type 20BE, was used for electronic absorption spectra; measurements. The spectrophotometer was used to measure remaining contaminant concentrations during photo-degradation experiments. It was also used to measure solid state spectra for different catalyst systems.

2.2.3 Fluorescence Spectrometry:

A Perkin-Elmer LS50 Luminescence Spectrophotometer was used to measure emission fluorescence spectra for different catalyst systems. Emission spectra was also measured for a number of reagents. Emission spectra was used to measure semiconductor catalyst band gap. The wavelength of the photoluminescence peak was taken to be the wavelength of the band gap for the quantum wells, as reported in literature [5]

2.2.4 Voltametry:

Pol 150 with MDE 150 which was purchased from radiometer company, were used for voltametry analysis, the voltametry analysis was applied to determined Cadmium ions Cd^{+2} and the photo-degradation remaining (like SO_4^{-2}, $S_2O_3^{-2}$, NO_3^-, ….. etc).

2.2.5 Photo-catalytic Reactor:

Photo-degradation reactions were conducted in a magnetically stirred double-walled condenser cell equipped with a thermostat water flow. The reactor walls were covered with aluminum foil to reflect astray light and to protect persons from the harmful UV-light. The source of light was adjusted above the reactor cell at a suitable height (Figure 2.3).

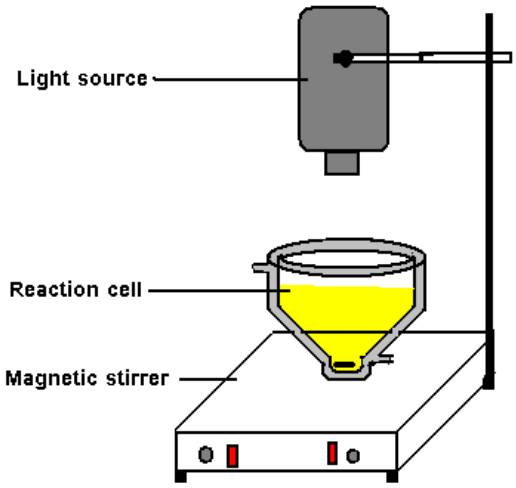

Figure 2.3: Arrangement of photocatalytic reactor**.**

2.3 General Photo-Degradation Procedure:

Photo-catalytic experiments were conducted as follows: A known amount of catalyst was loaded in the reactor. A known volume of contaminant solution with fixed initial concentration was added. The reaction mixture was stirred vigorously for 60 minutes in dark, after covering the vent of the reaction cell with aluminum foil. The cover was then removed, and 2 ml of liquate was taken and kept in dark for further analysis.

The reaction mixture was exposed to the direct light with continuous stirring. Aliquots (2 ml) were aspirated at specified time and kept in dark for analysis of contaminant.

2.3.1 Contaminant Concentration Measurement:

This study involved two contaminants. The first contaminant is Methyl Orange [**MO**], its molecular structure and spectrum are represent in Scheme (2.1). The other contaminant is Phenazopyridine hydrochloride

[**PhPY**]. Phenazopyridine is a pharmaceutical drug, with a specifically local analgesic effect. It is often used to alleviate pains, irritation, discomfort, or urgency caused by urinary tract infections, surgery, or injury to the urinary tract. Its molecular structure and spectrum are shown in Scheme (2.2). Both contaminant concentrations were analyzed spectrophotometrically, using pre-constructed calibration curves. The aspirated samples in each experiment, syringed out at certain time intervals, were centrifuged at 5000 rpm for 5 minutes. The supernatant was transferred to the spectrophotometer cell, and the absorbance was measured for each contaminant at the proper wavelength (λ_{480nm} for Methyl Orange and λ_{430nm} for Phenazopyridine)

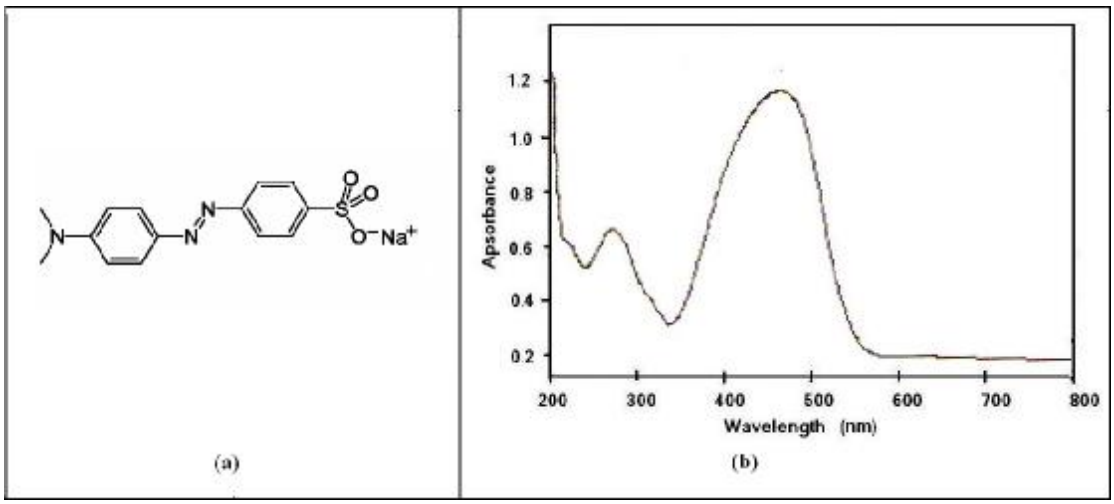

Scheme 2.1: a) Methyl Orange structure b) Methyl Orange UV-Vis spectrum.

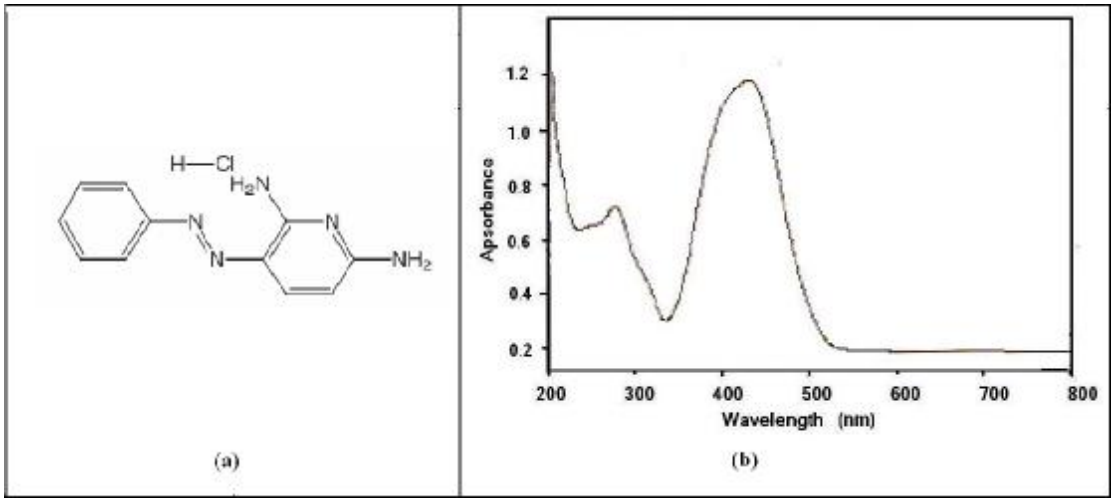

Scheme 2.2: a) Phenazopyridine hydrochloride structure b) Phenazopyridine hydrochloride UV-Vis spectrum**.**

2.3.2 In-solution Cadmium Ion Determination:

During photo-degradation process, CdS sensitizer gave Cd^{2+} ions in the solution. The free Cd^{2+} ion concentration was determined using anodic stripping differential pulse voltametry. The technique was conducted on a hanging dropping mercury electrode (MDE150**)** connected to a PC controlled Polarograph (POL150). Supporting electrolyte (10 ml of 0.1M HCl solution) was added, followed by 100 µL of the solution taken from reaction mixture. Hanging Mercury Drop Electrode (HMDE) method was followed. The analysis parameters were: initial potential -700 mV, final potential -400 mV, purging time 30 sec., deposition time 20 sec., scan rate 20 mV/sec., pulse height 25 mV.

2.4 Catalyst Preparation:

2.4.1 Naked Titanium Dioxide:

Commercial rutile TiO_2 was described above, and synthetic TiO_2 preparation is described later.

2.4.2 Preparation of TiO_2/CdS System:

Nano-scale CdS particles were deposited onto commercial TiO_2 particles by Chemical Bath Deposition (CBD) following literature procedures[6-11] A specific amount of commercial rutile titanium dioxide (10 g) were suspended in distilled water (30 ml) in a container, Scheme (2.3). To the reaction container 5.0 ml aqueous solution of $CdCl_2$ (1.0 M) were added. Then NH_4Cl (10.0 ml, 1.0 M) was added. The mixture was made basic by adding MH_4OH (15 mL, 1.0 M) while firmly Stoppered with continued mixing. A solution of thiourea (5.0 ml, 1.0 M) was added as a source for sulfur. The mixture was thermo-stated for 60 min at 85°C with continuous stirring. The reddish solid particles of TiO_2/CdS were then isolated by filtration, washed with distilled water and dried in air followed by drying in a furnace at 120°C for 1 hr to evaporate excess water. The CdS uptake content in the final TiO_2/CdS system was calculated to be 3.2 % by mass. Part of the TiO_2/CdS solid was annealed at 400°C under nitrogen bubbling for 3 hrs., the visual inspection of the prepared catalyst is shown in Figure (2.4).

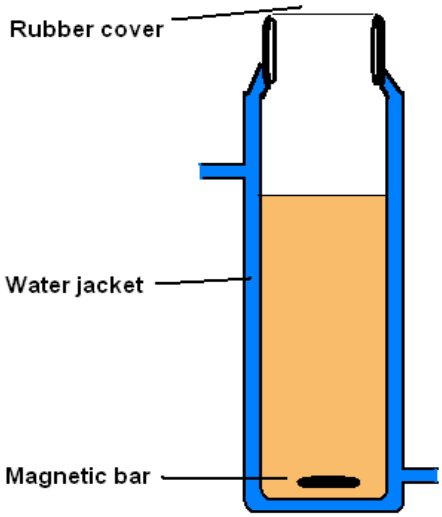

Scheme 2.3: Chemical Bath Deposition container.

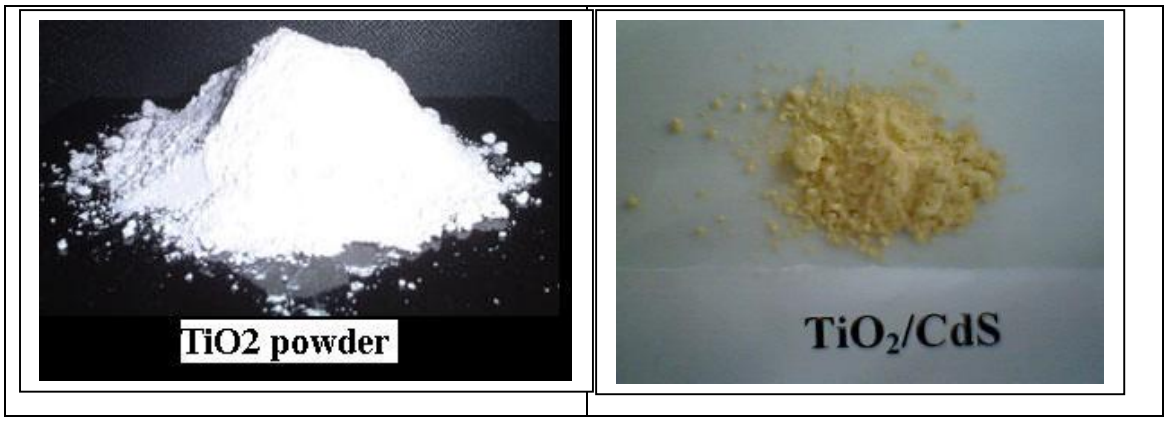

(a) **(b)**

Figure 2.4: The visual inspection of the a) Commercial rutile TiO_2 and b) the prepared TiO_2/CdS catalyst.

2.4.3 Preparation of Sand/TiO_2/CdS System:

The preparation was a two-step process, starting first with Sand/TiO_2 preparation, then with CdS deposition. The Sand/TiO_2 system was prepared by pyrolysis of $TiCl_{3(aq)}$ onto sand surface. The Rutile TiO_2 particle was

laboratory prepared following literature preparation [12-13]. Natural sea shore sand particles were cleaned by acidification with conc. HCl and HNO_3 solutions successively. The solid sand particles were then filtered and washed several times with water before drying and sieving, with the fraction 100-50 mesh taken (particle Diameter 150-300 micron.).

The sand (50.0 g) was then placed inside a 500 ml round bottomed flask. Distilled water (100 ml) was added to the flask together with 3.0 g solid NaOH. The mixture was stirred mechanically and thermo-stated at 60°C. To the mixture was added 50.0 mL of $TiCl_3$ solution (~10% by mass) drop wise. Stirring was continued for 6 h, keeping the pH above 3.0 by gradual addition of NaOH. The white color mixture was then continuously stirred for additional 8 h before leaving overnight [12-13]. The aqueous layer was pipetted out to avoid loss of the ultra-fine unsupported titanium dioxide particles forming at the surface. More water was added and the mixture was allowed to settle overnight before pipetting. This procedure was repeated many times to completely remove sodium and chloride ions. Removal of chloride ions was ensured by testing the aqueous phase with $AgNO_3$ solutions, which showed negative test for chloride ions. The wet solid was dried by heating under continuous stirring. The dried solid was isolated and further dried at 130°C for 60 min, in an oven, before calcination at 350°C for 4 h and slow cooling. To obtain the starting Sand/TiO_2 system only, the resulting gross solid mixture was sieved at 50 mesh to remove unsupported TiO_2 fine powder. The TiO_2 content in the Sand/TiO_2 was measured gravimetrically to be 5%. Based on literature, the TiO_2 particles are of the

more stable Rutile type [14-15]. Calcination at 400°C does not convert the Rutile into Anatase TiO_2 [16]. The Sand/TiO_2 particles were then used to prepare the Sand/TiO_2/CdS system by CBD method, the visual inspection of the prepared catalyst is shown in Figure (2.5).

Annealing of TiO_2/CdS and Sand/TiO_2/CdS systems was performed, by heating at 400°C for 3 h, in a tube furnace under nitrogen. Both pre-annealed and non-annealed Sand/TiO_2/CdS systems were used in catalytic experiments. Unless otherwise stated, the pre-annealed systems were used.

Figure 2.5: The visual inspection of prepared Sand/TiO_2/CdS catalyst.

The mass percent for CdS in the final Sand/TiO_2/CdS solid was analyzed and found to be 0.41%. This was achieved by complete dissolution of CdS (onto measured amounts of the solid) in concentrated HCl solution, yielding Cd^{2+} ions, which were in turn measured by voltametry, as mentioned before. For recovery/reuse experiments, Sand/TiO_2/CdS samples with higher CdS uptake (1.9%) were also prepared.

2.5 Characterization of TiO_2/CdS Catalysis Systems:

Solid state UV-Visible electron absorption spectra, photoluminescence emission spectra, XRD diffraction and SEM analysis have been measured for the prepared **TiO_2/CdS** catalyst systems.

2.5.1 UV-Visible Spectral Characterization:

The prepared catalyst was characterized using UV-Visible Spectrophotometry. The spectra were scanned on dispersed small amount of fine solid catalyst particles in toluene. The suspension was transferred to a quartz analysis cell. Figure (2.6) shows the spectra for both pre-annealed (A) and non-annealed (B) samples of CBD prepared CdS. The pre-annealed CdS showed absorbance edge at ~560 nm while non-annealed system showed absorbance edge at ~530 nm. The spectra are consistent with literature [17-23].

UV-Visible spectra were also measured for TiO_2/CdS system. The spectra are presented in Figure (2.7). Spectrum (A), for pre-annealed TiO_2/CdS, showed absorbance maximum at ~550 nm due to CdS and absorbance edged at ~400 nm due to TiO_2. Spectrum (B), for non-annealed TiO_2/CdS, showed absorbance maximum at ~530 nm for CdS and absorbance edge at ~400 nm for TiO_2.

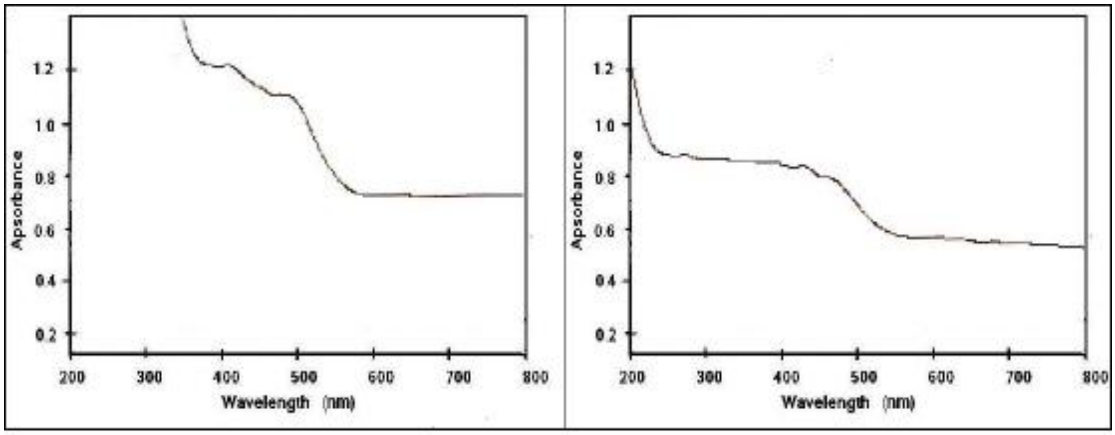

(a) (b)

Figure 2.6: Solid state electronic absorption spectra measured for CdS dispersed colloidal in toluene for (a) pre-annealed and (b) non-annealed.

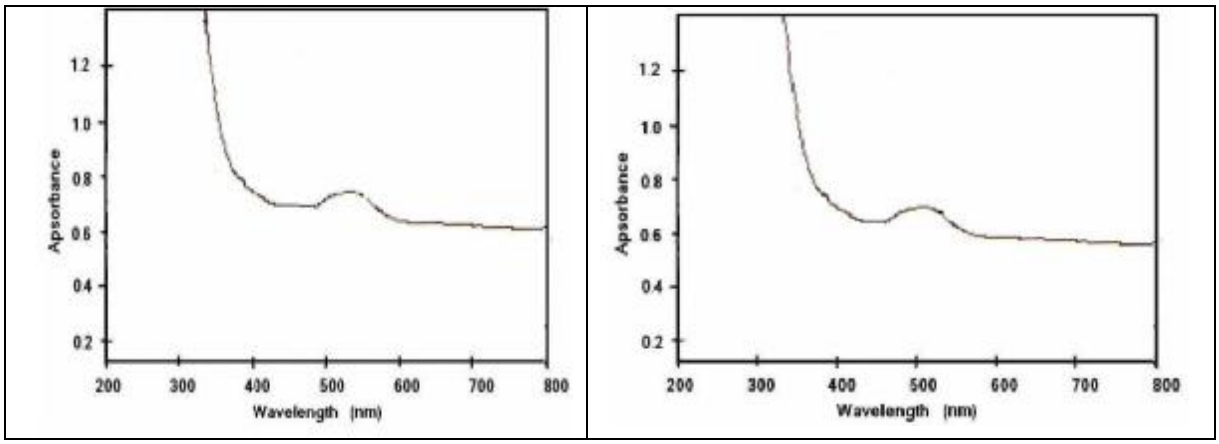

(a) **(b)**

Figure 2.7: Solid state electronic absorption spectra measured for TiO_2/CdS dispersed colloidal in toluene, for (a) pre-annealed and (b) non-annealed.

2.5.2 Photoluminescence Spectra:

Catalyst systems were characterized using Fluorescence spectra. The presented spectra were then correlated with literatures spectra. A small amount of the catalyst powder was dispersed in ethanol, and placed in the analysis quartz cell. The sample was excited at a proposed wavelength.

Emission spectrum was then measured to determine the characteristic emission wavelength.

2.5.2.1 TiO_2 Photoluminescence:

Photoluminescence emission spectrum was studied for both the commercial and the prepared rutile TiO_2. The excitation wavelength was done using 270 nm. The emission peaks were at ~400 nm for the commercial rutile TiO_2 (Figure 2.8a) and ~410 nm for synthesized TiO_2 (Figure 2.8b**)** as described earlier [24-25].

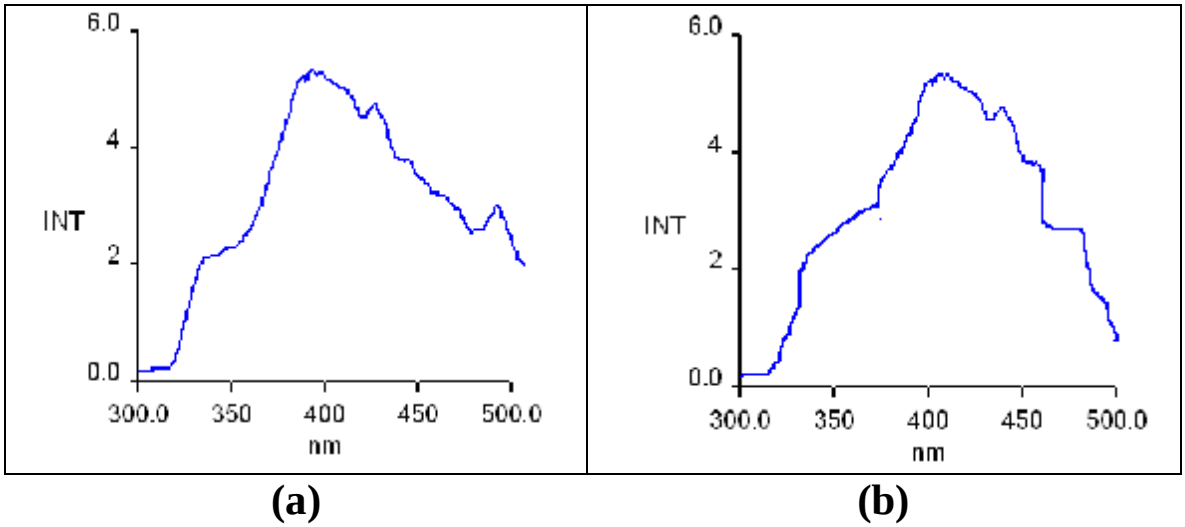

(a) **(b)**

Figure 2.8: Photoluminescence spectra measured for Rutile TiO_2 a) commercial b) synthetic.

2.5.2.2 CdS Photoluminescence:

Figure (2.9) shows the photoluminescence emission spectra for CBD prepared CdS, The pre-annealed CdS showed emission wavelength ~ 590 nm, and the non-annealed CdS showed emission at 580 nm, both samples were excited at 220 nm [17, 26-27].

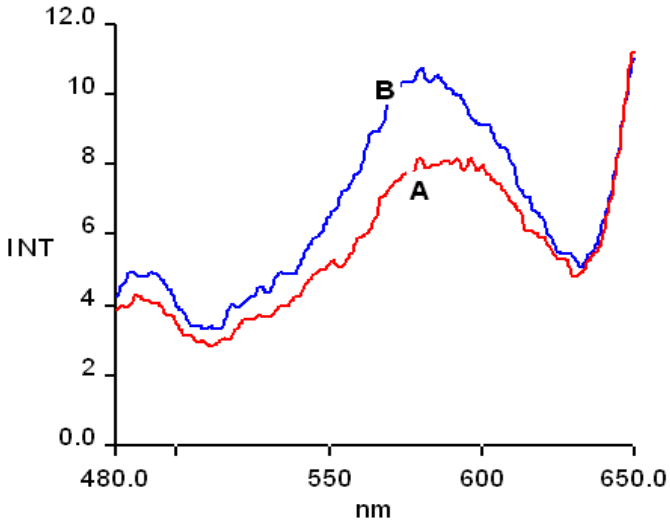

Figure 2.9: Photoluminescence spectrum of prepared CdS A) pre-annealed B) non-annealed

2.5.2.3 TiO_2/CdS Photoluminescence:

The photoluminescence emission spectra for both pre-annealed and non-annealed TiO_2/CdS systems were studied. The emission spectra are presented in Figure (2.10). The excitation wave length for both systems was 220 nm. Curve (A) shows an emission spectrum for pre-annealed TiO_2/CdS system, with an intense emission maximum at wavelength 580 nm and a lower emission at 530 nm. Curve (B) shows an emission spectrum for non-annealed TiO_2/CdS system, with an intense emission maximum at 530 nm and a lower emission at 580 nm.

A wider scan range emission spectrum for non-annealed TiO_2/CdS spectrum is presented in Figure (2.11). The system was excited at 270 nm, and shows an intense emission at ~ 415 nm, which is attributed to TiO_2 rutile emission. Another intense emission at ~ 543, due to CdS is also observed.

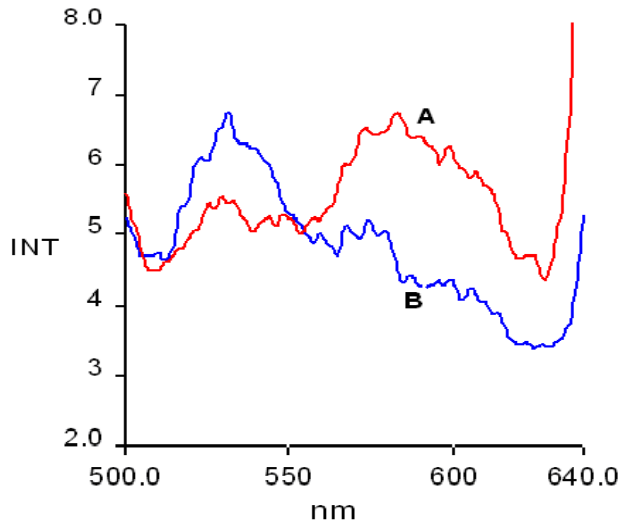

Figure 2.10: Photoluminescence spectra measured for TiO_2/CdS A) pre-annealed B) non-annealed.

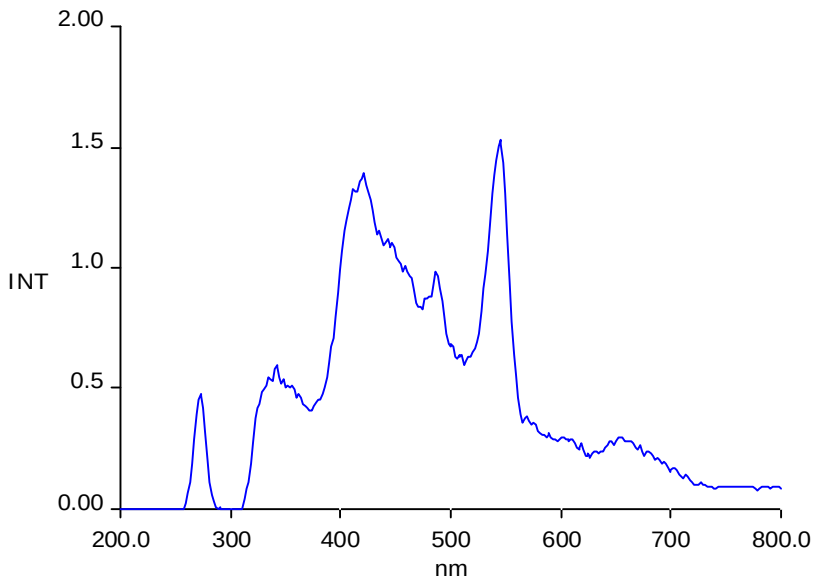

Figure 2.11: Photoluminescence spectrum of non-annealed prepared TiO_2/CdS.

Photoluminescence emission spectrum for pre-annealed TiO_2/CdS, showing two distinguished emission maxima at ~ 410 nm (for TiO_2) and ~ 570 nm (for CdS), (Figure 2.12).

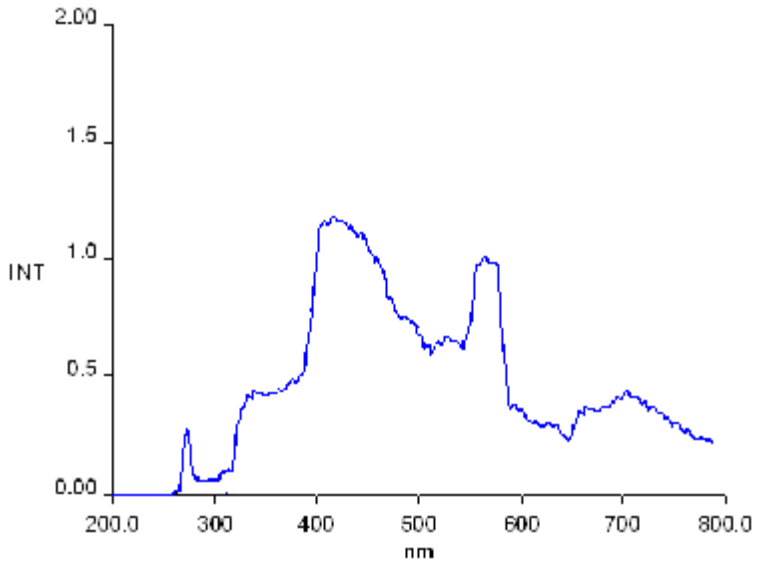

Figure 2.12: Photoluminescence spectrum of pre-annealed prepared TiO_2/CdS.

5.5.3 X-ray Diffraction (XRD):

XRD patterns were measured for CdS powder and for TiO_2/CdS system. The measurements were carried out in the ICMCB laboratories, Bordeax University, using a Philips XRD X'PERT PRO diffractometer with Cu Kα ($\lambda_{1.5418Å}$) as a source. The XRD lines were identified by comparing the measured diffraction patterns to JCPDS data-base cards.

Despite the relatively low uptake of CdS onto TiO_2 in TiO_2/CdS, at thin sub-monolayer coverage level, the XRD pattern showed noticeable peaks for the supported CdS system at 2θ values of 26.7 (002), 44.1 (110) and 54.9^o (004), (Figure 2.13). Due to small intensity of the CdS peaks, compared to those of TiO_2, no conclusive calculation of particle size for the supported CdS could be made. Therefore, CdS particle sizes were calculated from XRD diffraction patterns measured for CdS powders prepared in a similar manner to supported CdS particles, (Figure 2.14). Particle size was calculated using the Scherrer equation:

$$D = (0.9\lambda)/(b\cos\theta)$$

Where **D** is the average crystallite diameter (nm), **λ** is the X-ray wavelength (nm), **b** is the full width at half maximum (FWHM) of the peak corrected for instrumental broadening (rad.) and **θ** is the Braggs' angle (deg.) [32]. The calculated CdS particle diameters for non-annealed and pre-annealed CdS powders were 17 and 20 nm respectively. The values are consistent with literature values [33]. Little crystallite growth by annealing at 350°C is observed from measured particle sizes.

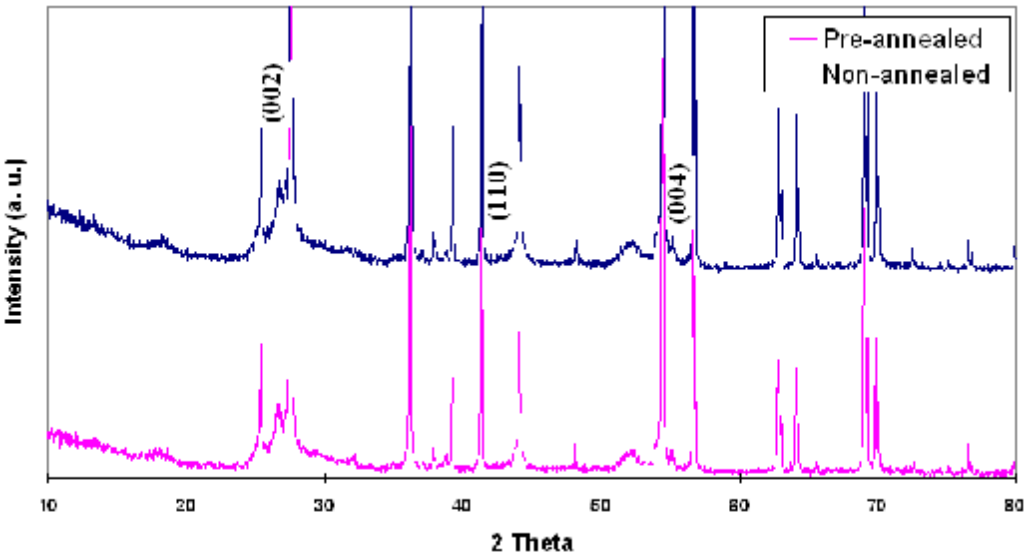

Figure 2.13: X-ray diffraction patterns for TiO_2/CdS powder (lower) pattern present pre-annealed and (Upper) pattern present non-annealed.

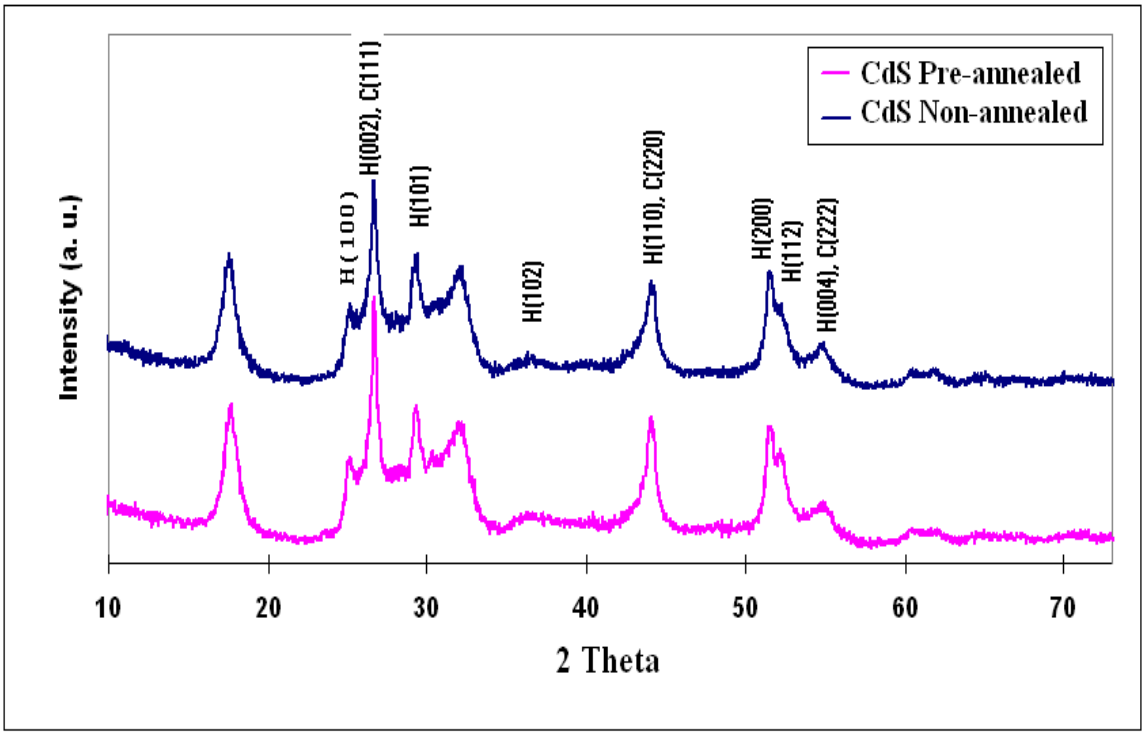

Figure 2.14: X-ray diffraction patterns for CdS powder (lower) pattern present pre-annealed and (Upper) pattern present non-annealed.

The X-ray patterns show both Hexagonal and cubic crystal types for CdS, (Figure 2.14).

CdS Type	Peak position (2θ) deg.	FWHM Rad.	D=(0.9λ)/(FWHM *COSθ*) λ = 0.154 nm
Non-annealed	26.7	0.008381	17.0 nm
Pre-Annealed	26.7	0.0071587	19.9 nm

2.5.4 Scanning Electron Microscopy (SEM):

Field emission scanning electron microscopic/energy dispersive spectroscopic (FE-SEM/EDS) studies were conducted on a Jeol microscope, (Model JSM-6700F). SEM scanning was performed to

investigate the surface morphology of the TiO_2/CdS particles. Surface morphology of the non-annealed CdS over TiO_2 particles is depicted in Figure (2.15). SEM image shows that the CdS exists as a monolayer of spheres with comparable sizes at the nanoscale. The nanoparticles are attached to the TiO_2 particle surfaces. The estimated CdS nanoparticles size is less than ~20 nm. Figure (2.16) shows SEM micrographs for the pre-annealed TiO_2/CdS, and also shows the sintering of slightly fused CdS nanoparticles. Figures (2.15) and (2.16) show that sintering between neighboring CdS particles occurred by annealing. This is evident from size 1µm scale pictures.

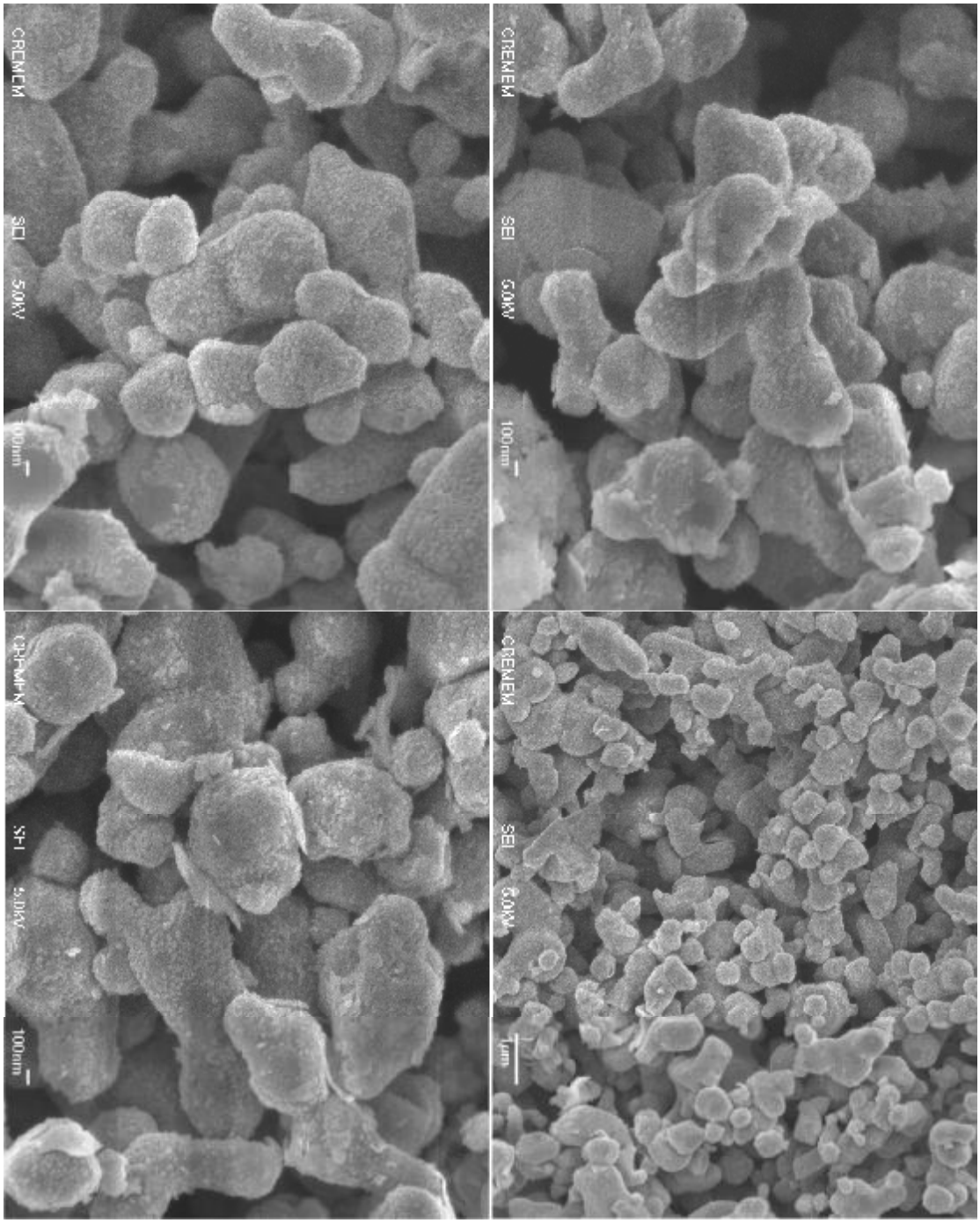

Figure 2.15: SEM images for non-annealed TiO_2/CdS.

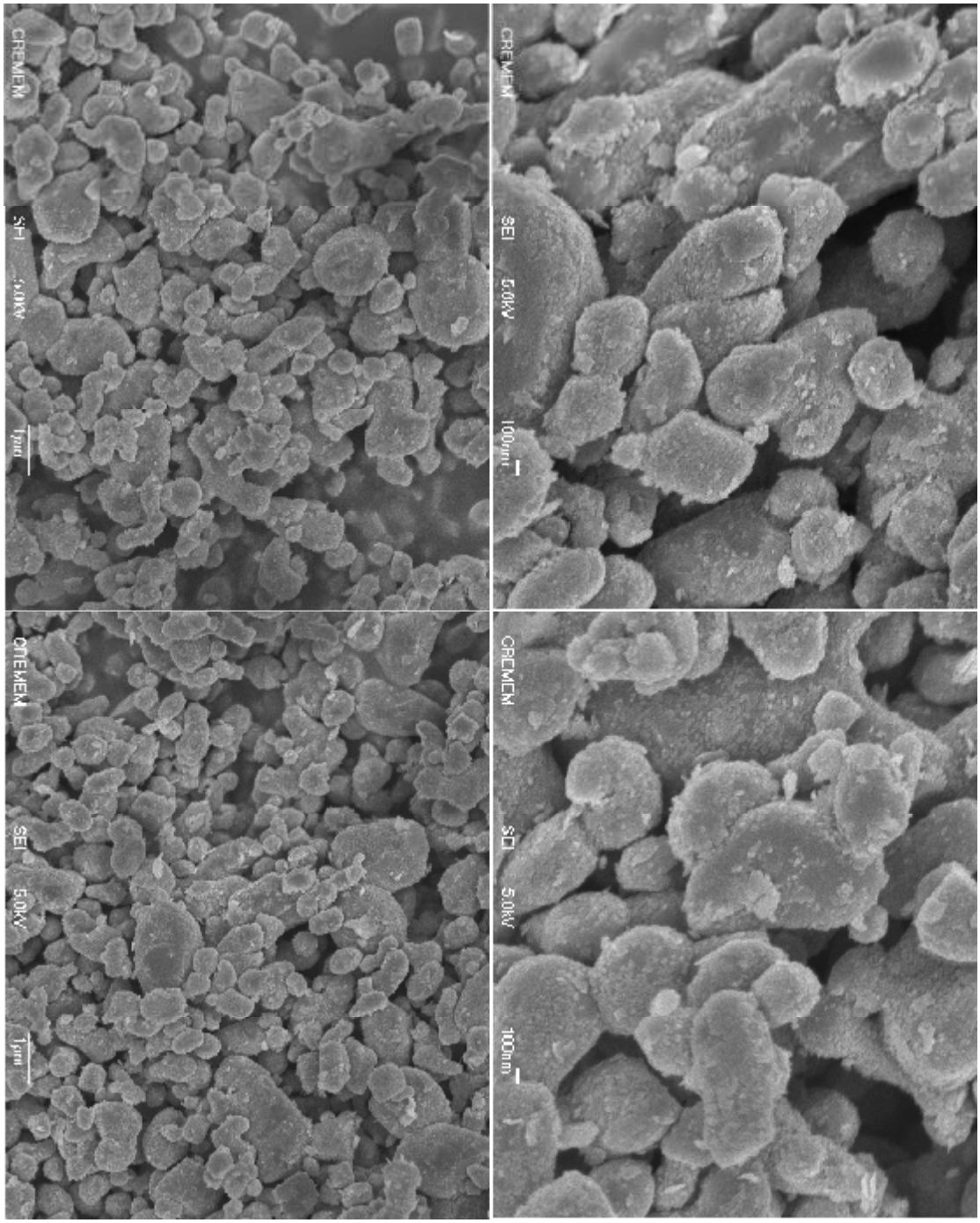

Figure 2.16: SEM images for pre-annealed TiO_2/CdS

2.6 Photo-Degradation Control Experiments:

The first control experiment was conducted using of the proposed catalyst system with the contaminant solution. The mixture was conducted under continuous stirring in dark. The purpose was to determine if there is any contaminant loss in absence of light. There was no noticeable contaminant loss in the dark in case of TiO_2 or TiO_2/CdS systems. A noticeable adsorption of contaminant was observed when using AC in dark, as expected from adsorption of contaminant on activated carbon AC. In other control experiments, the contaminant solution (known concentration) was exposed to irradiation in the absence of catalyst. This was to know if the contaminant undergoes photolysis in absence of catalyst. Control experiments were also conducted using a UV light filter (400 nm and shorter waves eliminated) placed between the solar simulator and the reaction mixture. This was to prevent UV radiation to reach the reaction mixture under study.

2.7 Cadmium Ions Voltametric analysis:

CdS uptake values in TiO_2/CdS and in Sand/TiO_2 systems were experimentally measured as mentioned above.

2.8 Analysis of Photo-degradation Remaining Reactant:

Complete mineralization of organic contaminants into CO_2, H_2O, and other minerals, under solar simulator light, can be assumed based on earlier reports, especially for Methyl Orange [14]. Figure (2.17) shows the UV-visible spectrum for Methyl Orange. Figure (2.18) shows the UV-visible

spectrum for Phenazopyridine. The molecules in the pH range 4.1–9.5 is characterized by a band in the range 485–465nm in the visible region attributed to azo form (λ_{max}) and the band in the range 200 - 300 nm is due to the presence of benzene rings in Methyl Orange. Complete mineralization of either contaminant after reaction completion was confirmed by the absence of 430 nm absorption for Phenazopyridine, (Figure 2.17), and absence of 480 nm absorption for Methyl Orange, (Figure 2.18). The absence of any benzene derivatives was also confirmed by the absence of any absorption bands characteristics for phenyl group at 200 nm or longer, as observed from absorption spectra after reaction completion. Voltametric determination of $\mathbf{SO_4^{-2}}$ and $\mathbf{S_2O_3^{-}}$were performed during Methyl Orange photo-degradation experiments. Both $\mathbf{SO_4^{-2}}$ and $\mathbf{S_2O_3^{-2}}$ were observed during the photo-degradation experiment, (Figure 2.19). Voltametric determination of $\mathbf{NO_3^{-}}$ was performed in Phenazopyridine remaining analysis. Gradual increasing in $\mathbf{NO_3^{-}}$ concentration was observed through the photo-degradation process, (Figure 2.20). Such observation indicates complete mineralization of Methyl Orange and Phenazopyridine contaminants under photo-degradation conditions here.

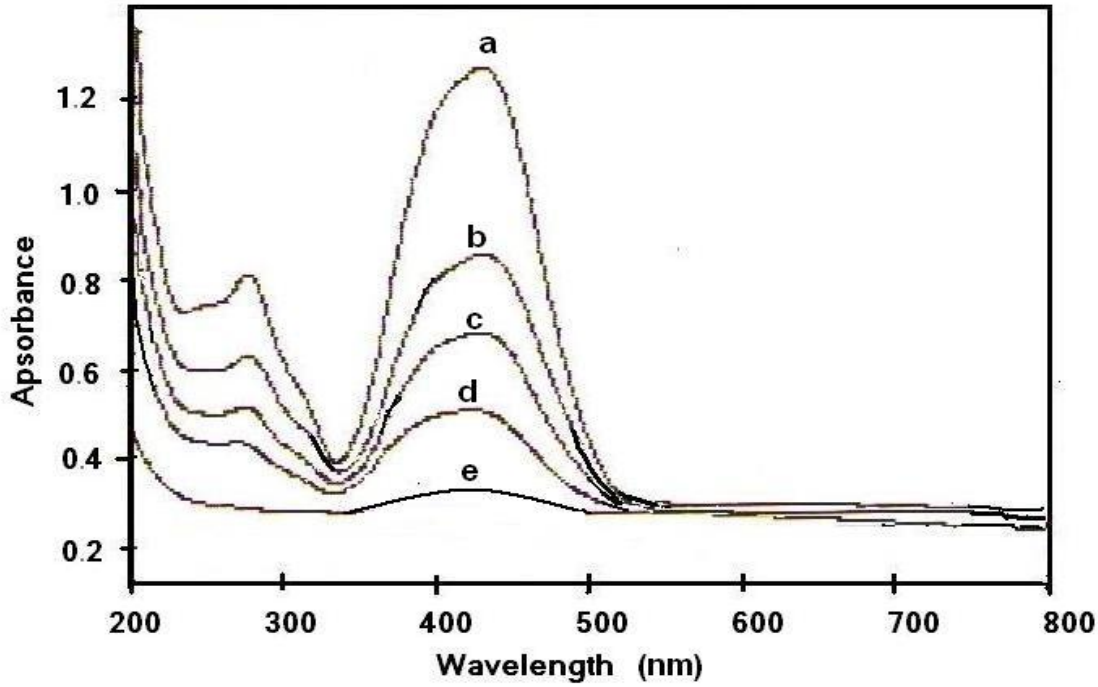

Figure 2.17: UV-Vis spectra measured for Phenazopyridine through the photo-degradation process with time, the sample were taken periodically every 10 min (a-e).

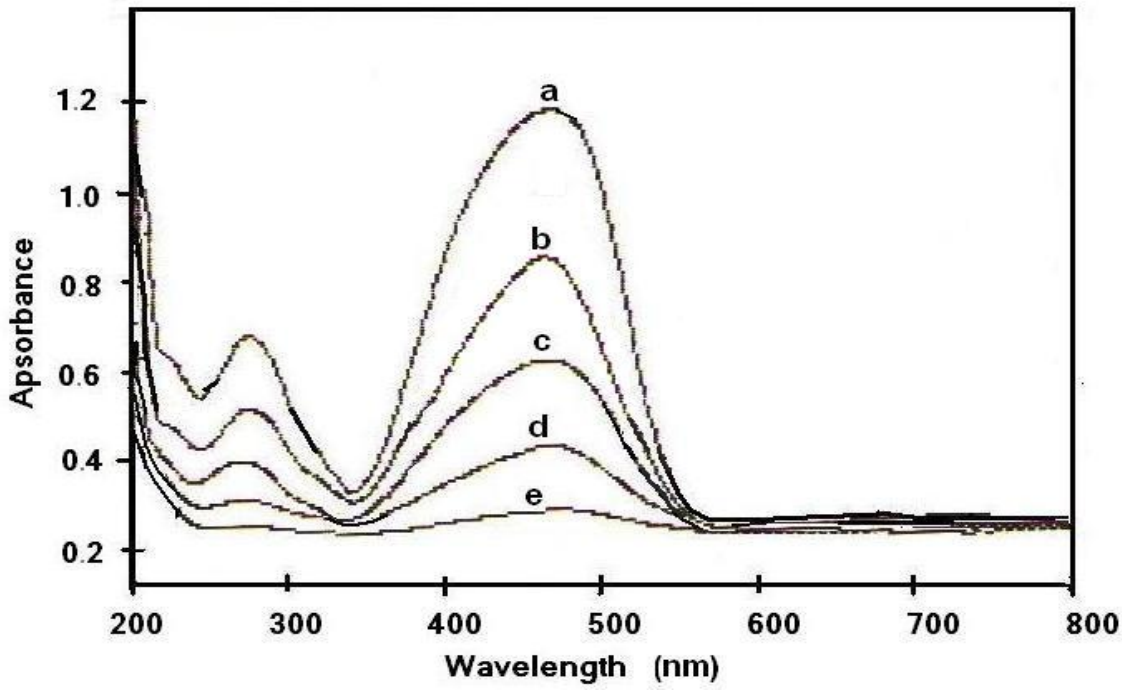

Figure 2.18: UV-Vis spectra measured for Methyl Orange through the photo-degradation process with time, the sample were taken periodically every 10 min (a-e).

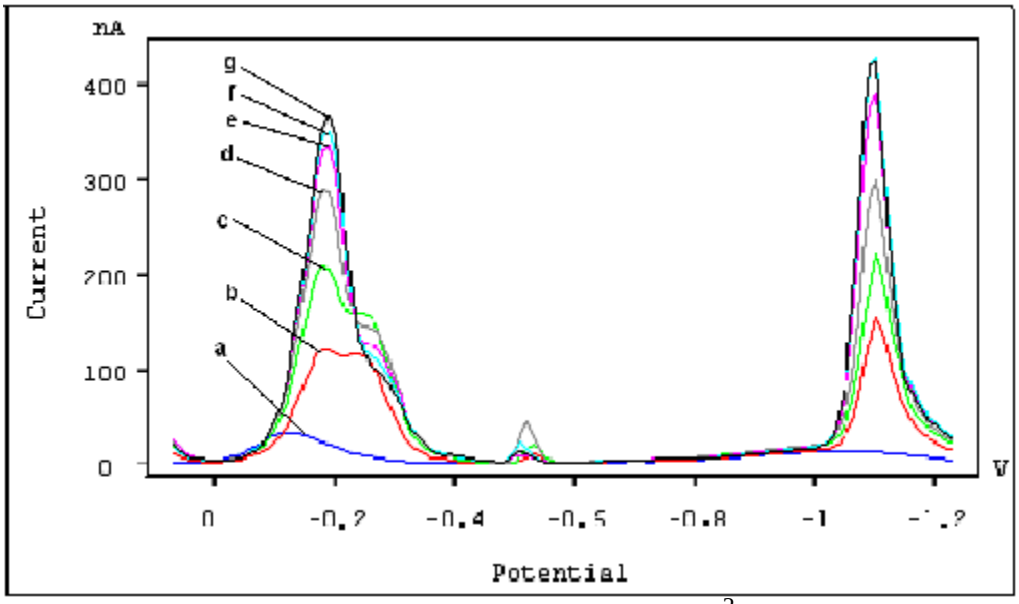

Figure 2.19: Voltametric determination of $S_2O_3^{2-}$ at (~-0.2V and SO_4^{2-} at (~-1.1V) during photo-degradation experiment of Methyl Orange with time, the sample were taken periodically every 10 min. (a-g).

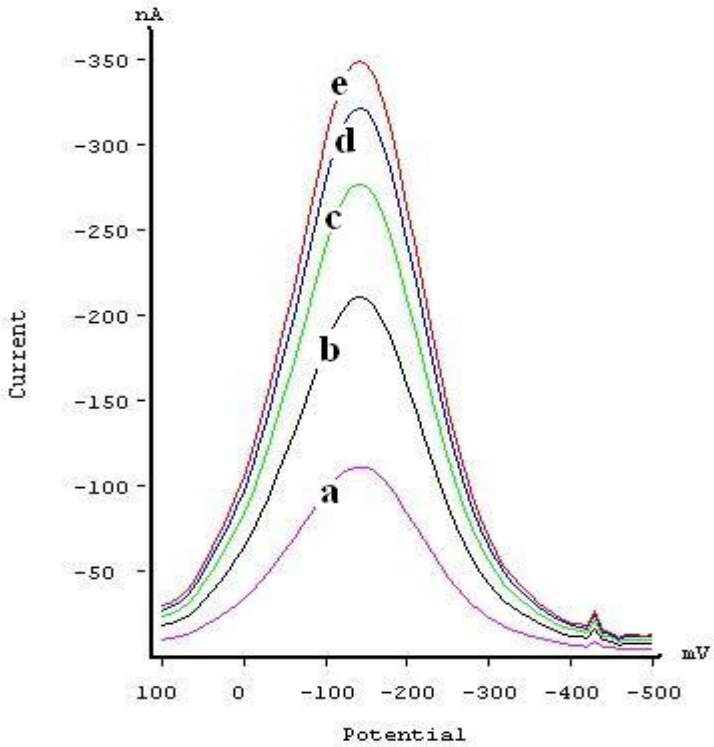

Figure 2.20: Voltametric determination of NO_3^- during photo-degradation experiment of Phenazopyridine with time, the sample were taken periodically every 10 min (a-e).

References:

1. H. S. Hilal, L. Z. Majjad, N. Zaatar and A. El-Hamouz, Dye-effect in TiO_2 catalyzed contaminant photo-degradation: Sensitization vs. charge-transfer formalism, *Solid State Sci.*, **9** (2007) 9-15.

2. A. L. Linsbigler, G. Lu and J. T. Yates, Photocatalysis on TiO_2 surfaces: Principles, mechanisms, and selected results, *Chem. Rev.*, **95 (**1995) 735-758.

3. K. Tanaka, M. F. V. Capule and T. Hisanaga, Effect of crystallinity of TiO_2 on its photocatalytic action, *Chem. Phys. Lett.*, **187 (**1991) 73-76.

4. Thermo Oriel: 500W Xenon/Mercury (Xenon) ARC Lamp Power Supply Model 68911.

5. X. Sun, N. Peyghambarian, and A. R. Kost, Large blueshift of the band gap of GaAsSb/AlSb quantum wells with ion implantation, *Appl. Phys. Lett.*, **86** (2005) 1-3.

6. Y. Bessekhouad, D. Robert, J.V. Weber, Bi_2S_3/TiO_2 and CdS/TiO_2 heterojunctions as an available configuration for photocatalytic degradation of organic pollutant, *J. Photochem. Photobiol. A*, ***163*** (2004) 569–580.

7. O. Vigil-Galán, A. Morales-Acevedo, F. Cruz-Gandarilla, M.G. Jiménez-Escamilla, Characterization of CBD–CdS layers with different S/Cd ratios in the chemical bath and their relation with the efficiency of CdS/CdTe Solar Cells, *Thin Solid Films*, **515** (2007) 6085–6088.

8. J.N. Ximello-Quiebras, G. Contreras-Puente, J. Aguilar-Hernandez, G. Santana-Rodriguez, A. A.-C Readigos,. Physical Properties of chemical bath deposited CdS thin films, *Sol. Energ. Mat. Sol. C.*, **82** (2004) 263–268.

9. P. Roy, S. K. Srivastava, A new approach towards the growth of cadmium sulphide thin film by CBD method and its characterization, *Mater. Chem. Phys.*, **95** (2006) 235–241.

10. K.V. Zinoviev, O. Zelaya-Angel, Influence of low temperature thermal annealing on the dark resistivity of chemical bath deposited CdS films, *Mater. Chem. Phys.*, **70** (2001) 100–102.

11. F. Chen, W. Jie, Growth and photoluminescence properties of CdS solid solution semiconductor, *Cryst. Res. Technol.*, **42** (2007) 1082–1086.

12. S. Cassaignon, M. Koelsch and J. Jolivet, From $TiCl_3$ to TiO_2 nanoparticles (anatase, brookite and rutile): Thermohydrolysis and oxidation in aqueous medium, *J. Phys. Chem. Solids*, **68** (2007) 695-700.

13. F. Pedraza, A. Vazquez**,** Obtention of TiO_2 rutile at room temperature through direct Oxidation of $TiCl_3$, *J. Phys. Chem. Solids*, **60** (1999) 445-448.

14. L. F. Pedraza, A . Vazquez, Obtention of TiO_2 rutile at room temperature through direct oxidation of $TiCl_3$, *J. Phys. Chem. Solids*, **60** (1999) 445-448.

15. X. Huanga, C. Pana, Large-scale synthesis of single-crystalline rutile TiO_2 nanorods via a one-step solution route, *J. Cryst. Growth*, **306** (2007) 117–122.

16. S. Cassaignon, M. Koelsch , J.-P. Jolivet, Soft synthesis conditions of original shaped TiO_2 nanoparticles from $TiCl_3$, *Chimie de la Matiere Condensee de Paris UPMC (CMCP-UPMC), 4 place jussieu, Paris 75252, France* , (2007).

17. M. Sima, I. Enculescu, V. Ghiordanescu, L. Mihut, Absorption and Photoluminescence properties of $CdS:Mn^{2+}:Cu^{+}$ Nanostructures, *J. Optoelectron. Adv. M.*, **7** (2005) 1949–1955.

18. Y. Bessekhouad, D. Robert, J.V. Weber, Bi_2S_3/TiO_2 and CdS/TiO_2 heterojunctions as an available configuration for photocatalytic degradation of organic pollutant, *J. Photochem. Photobiol. A*, **163** (2004) 569–580.

19. O. Vigil-Galán, A. Morales-Acevedo, F. Cruz-Gandarilla, Jiménez-M.G. Escamilla, Characterization of CBD–CdS layers with different S/Cd ratios in the chemical bath and their relation with the efficiency of CdS/CdTe Solar Cells, *Thin Solid Films*, **515** (2007) 6085–6088.

20. J.N. Ximello-Quiebras, G. Contreras-Puente, J. Aguilar-Hernandez, G. Santana-Rodriguez, A. A.-C. Readigos, Physical Properties of chemical bath deposited CdS thin films, *Sol. Energ. Mat. Sol. C.*, **82** (2004) 263–268.

21. P. Roy, S. K. Srivastava, A new approach towards the growth of cadmium sulphide thin film by CBD method and its characterization, *Mater. Chem. Phys.*, **95 (**2006) 235–241.

22. K.V. Zinoviev, O. Zelaya-Angel, Influence of low temperature thermal annealing on the dark resistivity of chemical bath deposited CdS films, *Mat. Chem. Phys.*, **70** (2001) 100–102.

23. F. Chen, W. Jie, Growth and photoluminescence properties of CdS solid solution semiconductor, *Cryst. Res. Technol*. **42** (2007) 1082-1086.

24. R. Palomino-Merino, J. Torres-Kauffman, R. Lozada-Morales, O. Portillo-Moreno, M. García-Rochaand O. Zelaya-Angel**,** Photoluminescence of Rhodamine 6G-doped amorphous TiO_2 thin films grown by sol–gel, *Vacuum*,**81** (2007) 1480-1483**.**

25. Z. Qing-nan, L. Chun-ling, L. Bao-shun, Z. Xiu-jian, UV-Vis and Photoluminescent Spectra of TiO_2 Films, *J. Wuhan Univ. Technol.*, **18** (2003) 36-39.

26. 29] M. V. Artemyev, L. I. Gurinovich, A. P. Stupak, S. V. Gaponenko, Luminescence of CdS Nanoparticles Doped with Mn, *Physica Status Solidi A*, **224** (2001) 191–194.

27. B. Ullrich, R. Schroeder, W. Graupner, H. Sakai, The influence of self-absorption on the photoluminescence of thin film CdS demonstrated by two-photon absorption, *Opt. Express*, **9** (2001) 116-120.

28. K. Manickathai, S. Kaswanathan, M. Alagar, Synthesis and characterization of CdO and CdS nanoparticles, *Indian J. Pure Ap. Phy.*, **46** (2008) 561-564.

29. N. J. Cherepy, G. P. Smestad, M. Gra1tzel, and J. Z. Zhang, Ultrafast Electron Injection: Implications for a Photoelectrochemical Cell Utilizing an Anthocyanin Dye-Sensitized TiO_2 Nanocrystalline Electrode**,** *J. Phys. Chem. B,* **101 (**1997**)** 9342-9351.

CHAPTER 3

PHOTO-DEGRADATION OF METHYL ORANGE [MO] USING TiO_2/CdS

3.1 Introduction:

The highly positive potential of TiO_2 valence band edge, makes it a very powerful oxidizing agent which practically photo-degrades any water organic contaminant. Despite this advantage, TiO_2 has a relatively large band gap, 3.2 eV, which demands radiations with 390 nm and shorter. Since oncoming solar light has longer wavelengths, the use of TiO_2 in large scale water purification applications by solar light will be limited. For this purpose, research has been active to sensitize TiO_2 to visible regions. Different types of dyes, with band gap values ~1.5-2.5 eV, and conduction band edges less positive than that of TiO_2, have been suggested. One example of such sensitizers is CdS which is typically deposited as small particles onto TiO_2 particle surface.

Scheme (3.1) summarizes the concept of TiO_2 sensitization by CdS. The Scheme shows that TiO_2 demands UV light to excite the electrons from the valence band to the conduction band of TiO_2 itself. In CdS sensitized TiO_2, the CdS particle itself is excited in the visible region (CdS band gab ~ 2.2 eV). As mentioned earlier, in Chapter one, the electrons are excited from the valence band to the conduction band of the CdS itself leaving positive holes (**h**$^+$) in its valance band, followed by transfer of the excited electron of CdS conduction band to the TiO_2 conduction band. Thus TiO_2 activity

enhancement, by CdS semiconductor in the visible region, is attributed to sensitization.

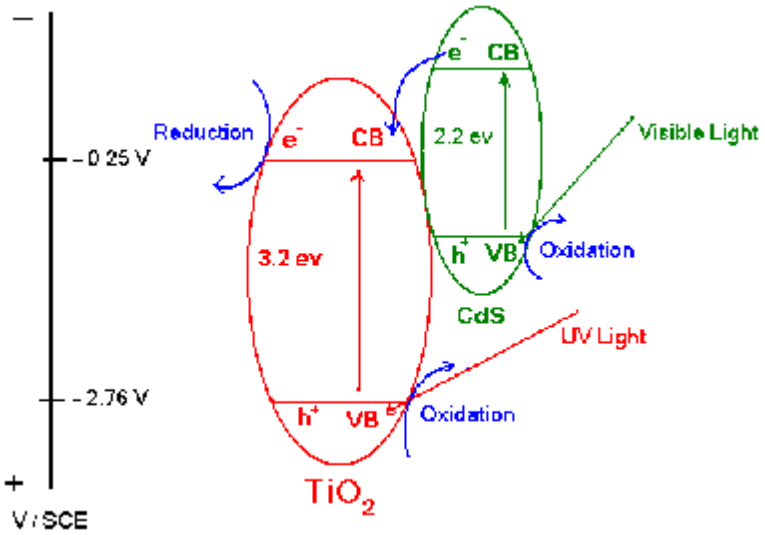

Scheme 3.1: Comparison between sensitized and naked TiO_2 excitation processes.

TiO_2 sensitization with CdS is still being heavily investigated in photo-degradation studies [3-4]. Many reports described using the TiO_2/CdS system in photo-degradation of water contaminants, but few referred to the hazards associated with CdS stability and Cd^{2+} ion leaching out to solution [4-5] and/or techniques to eliminate such difficulties. The other technical difficulty of recovering TiO_2/CdS system from solutions after reaction completion has not also been seriously targeted by literature. Separating small TiO_2, particles from water after use, is also difficult due to their hydrophilic nature [6] and needs to be achieved by economic techniques.

For these reasons, TiO_2/CdS system has been revisited here to assess the potential value of the CdS sensitized TiO_2. Taking into account the toxic

effects of Cd^{2+} ions, it is intended to investigate the sensitizing power of CdS together with its tendency to degrade under photo-degradation conditions [7].

Supporting TiO_2 onto insoluble solid surfaces has been widely suggested for photo-degradation study. In addition to many other solid supports, Sand has been widely described for such purposes [8- 16].

Supported TiO_2 systems are widely studied [4]. Other than photo-electrochemical solar cells, in which dye-sensitized TiO_2 systems were supported onto conducting thin films [17], only very few reports described supporting the combined dye-sensitized TiO_2 systems in degradation experiments [18]. We hereby wish to see if using solid supports, such as sand, may help in TiO_2/CdS system recovery from reaction mixtures after reaction completion. Moreover, we wish to see if sand particles may reduce the tendency of CdS to leach out. Sand was chosen here because it is widely abundant in natural waters, such as lakes, and it may thus interact with dye-sensitized TiO_2 particles suggested for use as contaminant photo-degradation catalysts. This study will shed more light on the future feasibility of using CdS as a potential sensitizer for supported and unsupported TiO_2 in water purification with solar light.

3.2 Experimental:

3.2.1 Catalyst Systems (TiO_2/CdS & Sand/TiO_2/CdS) Preparation:

CdS was deposited onto commercial TiO_2 particles by Chemical Bath Deposition (CBD) techniques as described earlier [19-24]. TiO_2 was also

deposited on Sand particles by hydrolysis method, which has been mentioned a above. The final prepared Sand/TiO_2 particles were used to prepare Sand/TiO_2/CdS system by a chemical bath deposition CBD. The deposition procedure was described before, Chapter two. The percent of CdS in the solid TiO_2/CdS system was found to be 3.2% by mass. In Sand/TiO_2/CdS system the CdS uptake was 0.41% by mass. For recovery/reuse experiments, special Sand/TiO_2/CdS samples with higher CdS uptake (1.9% by mass) was prepared.

3.2.2 Catalytic Experiments:

Catalytic experiments were conducted in magnetically stirred thermostated aqueous solutions of known concentrations of contaminant and catalyst. The pH was controlled by addition of NaOH or HCl solutions. Direct irradiation (with intensities 0.0032 W/cm^2 in case of UV, wavelengths shorter than 400 nm, and 0.0212 W/cm^2 for visible) was conducted by exposing the reaction mixture to incident irradiation directly coming out from the source lamp (placed above the reaction mixture). The reaction mixture was exposed to air under continuous stirring. The reaction was conducted in a 100 mL glass beaker, jacketed with controlled temperature water bath. The reaction vessel walls were covered from outside with reflecting aluminum foil.

Known amounts of contaminant solution, together with added acid or base, were placed inside the reaction vessel. The catalyst was then added with continuous stirring in the dark. The reaction mixture was then allowed to

stand for a few minutes before analyzing the contaminant concentration. This was to check if contaminant loss occurred by adsorption onto solid system. Details of control experiment are described later. Reaction time was then recorded the moment direct irradiation was started. The reaction progress was followed up by syringing out small aliquots, from the reaction mixture, at different time intervals. Each aliquot was then immediately centrifuged (500 rounds/s for 5 min), and the liquid phase was pipetted out for electronic absorption analysis, at 480 nm, for methyl orange. The aqueous phase was analyzed, for dissolved Cd^{2+} ions, by voltametry as described in Chapter two. The reaction rate was measured based on measuring remaining contaminant concentration with time. Catalyst efficiency and kinetics were studied based on initial rate, turnover number (contaminant reacted moles per TiO_2 moles) and quantum yield (contaminant reacted molecules per incident photon). Complete mineralization of methyl orange into carbon dioxide, ammonia (or nitrate) and sulphate, under UV and/or visible light, was confirmed by further analysis of the final reaction mixture, and also assumed based on earlier reports [26].

Reuse experiments were conducted using recovered catalyst, by filtration, after reaction completion. The recovered catalyst system was treated like the fresh catalyst samples, as described above.

3.3 Results and Discussions:

The three TiO_2, TiO_2/CdS and Sand/TiO_2/CdS systems were used as catalysts in photo-degradation of methyl orange, under UV and visible radiations. Comparative study between such three catalyst systems was performed in order to assess the feasibility of CdS as a future sensitizer. For this reason, the efficiency of CdS sensitizer was studied in terms of reaction rates, values of turnover number and values of quantum yield. The tendency of CdS to leach out from TiO_2 surface was also investigated under different conditions. The ability of Sand support to prevent Cd^{2+} ion leaching was investigated. Sand/TiO_2/CdS catalyst recovery and reuse was also studied.

The effects of catalyst types, pH, temperature, catalyst concentration and contaminant concentration were all studied. Unless otherwise stated, all TiO_2/CdS and Sand/TiO_2/CdS systems were annealed and cooled prior to catalytic use.

3.3.1 Control Experiments:

Control experiments, conducted under irradiation in the absence of catalyst systems, showed no loss of contaminant concentration. Experiments conducted using different catalyst systems in the dark showed no significant contaminant loss. This indicates that the contaminant loss under irradiation experiments is due to photo-degradation.

3.3.2 UV Irradiation Experiments*:*

Despite the limitations of UV degradation of contaminants, as discussed above, a number of UV degradation experiments were conducted here for comparison purposes and to assess the sensitizing effect of CdS dye thereafter. Aqueous solutions, pre-contaminated with methyl orange, were irradiated with UV light using the three different systems: TiO_2, TiO_2/CdS and Sand/TiO_2/CdS. The contaminant concentration decreased with reaction time due to photo-degradation, as shown in (Figure 3.1). Among the three different catalyst systems, the naked TiO_2 was the most efficient one, with quantum yield value 0.00264 (reacted molecule per incident UV photon). Figure (3.1) shows that the catalyst efficiency varied in the order: TiO_2 > TiO_2/CdS > Sand/TiO_2/CdS. The estimated turnover number (and quantum yield) values for different systems were 0.001167 (0.002562), 0.001105 (0.00243) and 0.000807 (0.00177), respectively. Small turnover number and quantum yield values are expected in photo-degradation studies [27].

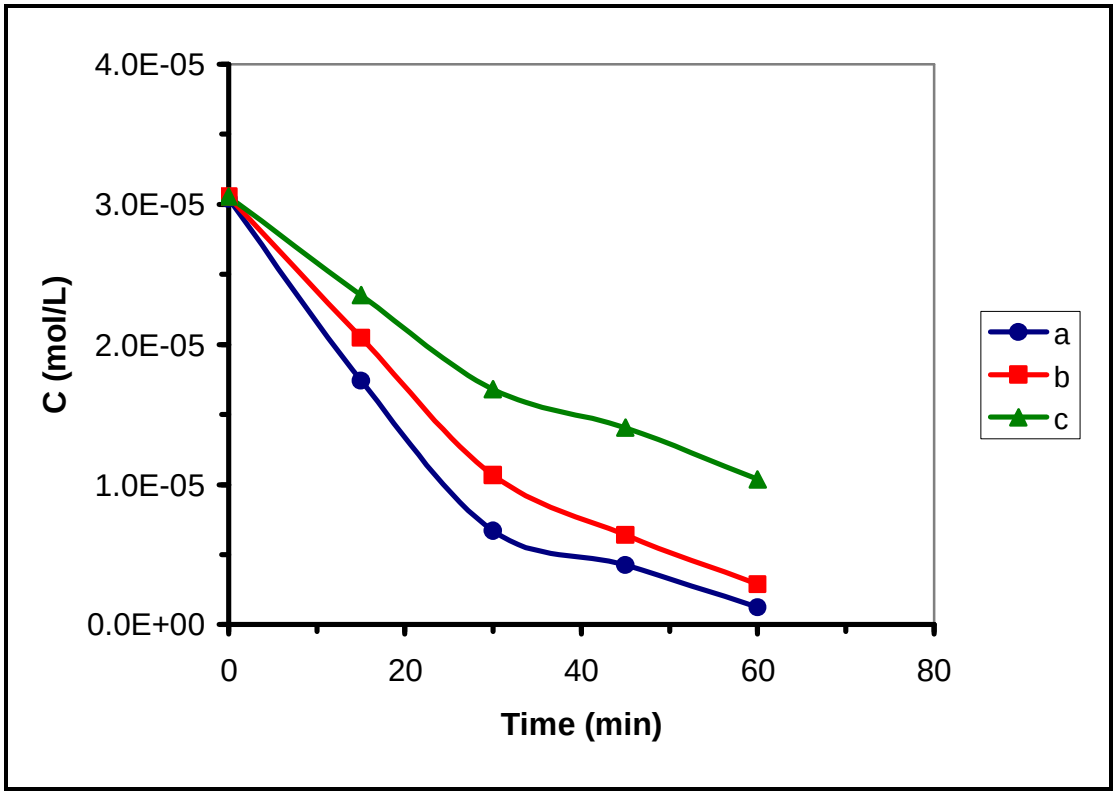

Figure 3.1: Effect of type of catalyst on methyl orange degradation. All experiments were conducted under UV (0.0032 W/cm^2) at 25°C in a neutral 50 mL mixture, using **a**) 0.1g naked TiO_2, **b**) 0.1 g TiO_2/CdS, **c**) 2.0g Sand/TiO_2/CdS (contains 0.1g TiO_2). Turnover number (and quantum yield) values were: 0.001167 and (0.002562) 0.001105 (0.00243) and 0.000807 (0.00177) respectively.

Since irradiation is in the UV region, there was no need for dyes to interfere with TiO_2 excitation. With its 3.2 eV band gap TiO_2 demands radiation of wavelengths ~390 nm or shorter (UV). The naked TiO_2 is thus effectively excited and shows relatively high efficiency in the UV range. The inhibition effect of CdS is attributed to blocking UV radiations away from the TiO_2 surface. Such activity lowering by CdS is not unexpected. Sand particles do additional shielding of radiations and prevent them from reaching TiO_2 surface. In case of Sand/TiO_2/CdS surface, it is assumed that particles on the upper side of reaction mixture only are effectively exposed

to UV light. This should lower overall efficiency of the supported catalyst. Presumably, the overall efficiency is lower when less TiO_2 surface is exposed to irradiation and reaction mixture. This has been evidenced by studying effect of concentration of naked TiO_2 on the rate of the UV degradation.

3.3.2.1 Effect of Loaded TiO_2:

Figure (3.2) shows that the initial reaction rate slightly increased with higher TiO_2 amounts. The order, of UV degradation reaction of methyl orange, was only 0.1315 with respect to naked TiO_2 catalyst. The fact that the order is less than a unity supports the idea of screening effect, since higher TiO_2 concentrations screen more irradiation. The facts that higher concentrations of TiO_2 increase the rate, and such effect is not first order, support the idea of screening effect in case of Sand/TiO_2/CdS systems. Values of turnover number per hour (and quantum yield) for the naked TiO_2 UV reactions with different amounts (0.05, 0.10 and 0.20 g) were calculated as: 0.00259 (0.00284), 0.00164 (0.003594) and 0.0008126 (0.00357) respectively. Despite the increase in rate, the decrease in values of turnover number and quantum yield, with increasing catalyst amount, is a direct evidence of screening effect by naked TiO_2. Thus, shielding of TiO_2 surface from UV source, by support and/or dye, would further lower its overall catalyst efficiency.

Moreover, the CdS particles may also lower the mass-transfer rate, to and from TiO_2 surface. This would lower the overall catalytic efficiency of TiO_2 particles in UV degradation of methyl orange.

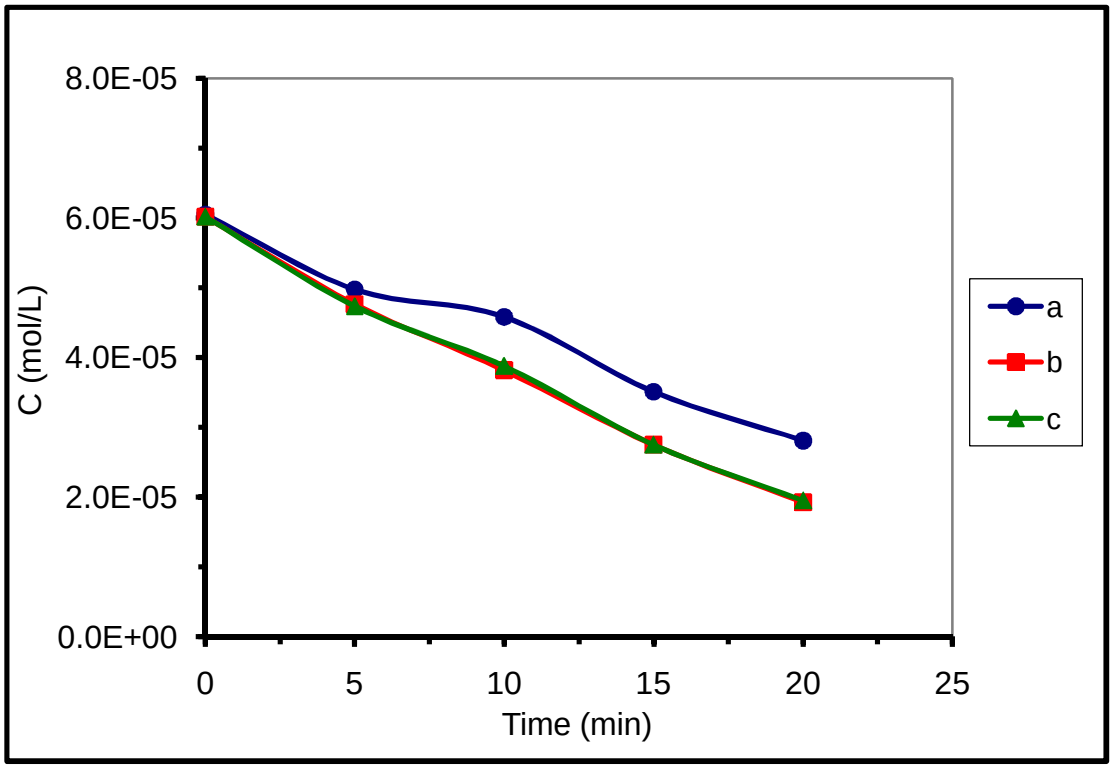

Figure 3.2: Effect of naked TiO_2 catalyst nominal amount on photo-degradation of methyl orange (neutral 50 ml, 20 ppm) at room temperature under UV (0.0032 W/cm^2) . Catalyst amount: **a**) 0.05 g **b**) 0.1 g **c**) 0.2g. Turnover number (and quantum yield) values are: 0.00259 (0.00284) , 0.00164 (0.003594) and 0.0008126 (0.00357) respectively.

3.3.2.2 Effect of Temperature:

Effect of temperature on reaction rate was investigated. Figure (3.3) shows that UV degradation of methyl orange is only slightly enhanced by increasing temperature.

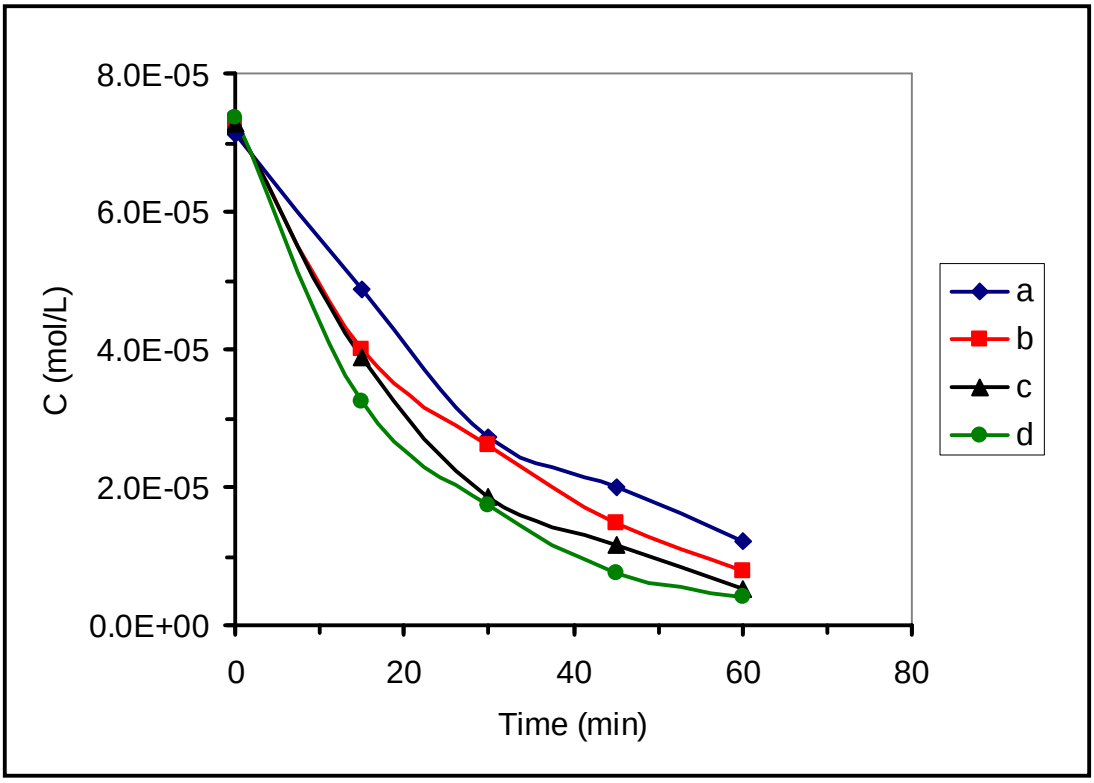

Figure 3.3: Effect of Temperature on photo-degradation of methyl orange (neutral 50 ml suspension, 25 ppm) using 0.1 g TiO_2 under UV (0.0032 W/cm^2). Reaction temperatures are: **a**) 25°C, **b**) 50°C, **c**) 70°C, **d**) 90°C.

A low value of activation energy (E_{act} = 7.86 KJ/mol) for the reaction process, was observed. Unlike thermal catalytic reactions, where the ln(rate) is linearly related to inverse Kelvin temperature by Arrhenius equation, photo-degradation reactions are known to be insensitive to temperature [2]. Energy provided by heating is relatively small, *viz* heating to 60°C (333 K) provides only a fraction of an electron volt, which is far less than needed to excite the high-band gap TiO_2. Moreover, at higher temperatures, contaminant molecules are more desorbed away from TiO_2 surface, which lowers the reaction rate [25]. Higher temperatures are also

responsible for removal of oxygen from the reaction mixture [18] which is necessary for contaminant oxidation.

3.3.2.3 Effect of Contaminant Concentration:

The effect of methyl orange concentration on reaction rate was studied. The initial rate was not affected with increasing contaminant concentration. Values of turnover number (and quantum yield), did not show significant dependence on contaminant concentration, Figure (3.4). More discussion on contaminant concentration effect is presented below.

3.3.3 Solar Simulator Experiments:

As stated earlier, photo-degradation experiments conducted in visible region are potentially more useful than in the UV region, since the former is more abundant in solar energy. However, in order to function effectively in the visible, TiO_2 needs sensitization. CdS has a suitable band gap (~2.1 eV, 590 nm), and its conduction band bottom edge is suitably higher than the valence band upper edge for TiO_2 [17]. Despite the hazardous nature of CdS, it is still being widely described by other workers as an efficient sensitizer for TiO_2 in photo-degradation studies [3-5]. Thus it is worth to revisit such a sensitizer and to see if its efficiency can be enhanced by further modification. Due to its hazardous nature, CdS needs to be carefully considered as a sensitizer [5].

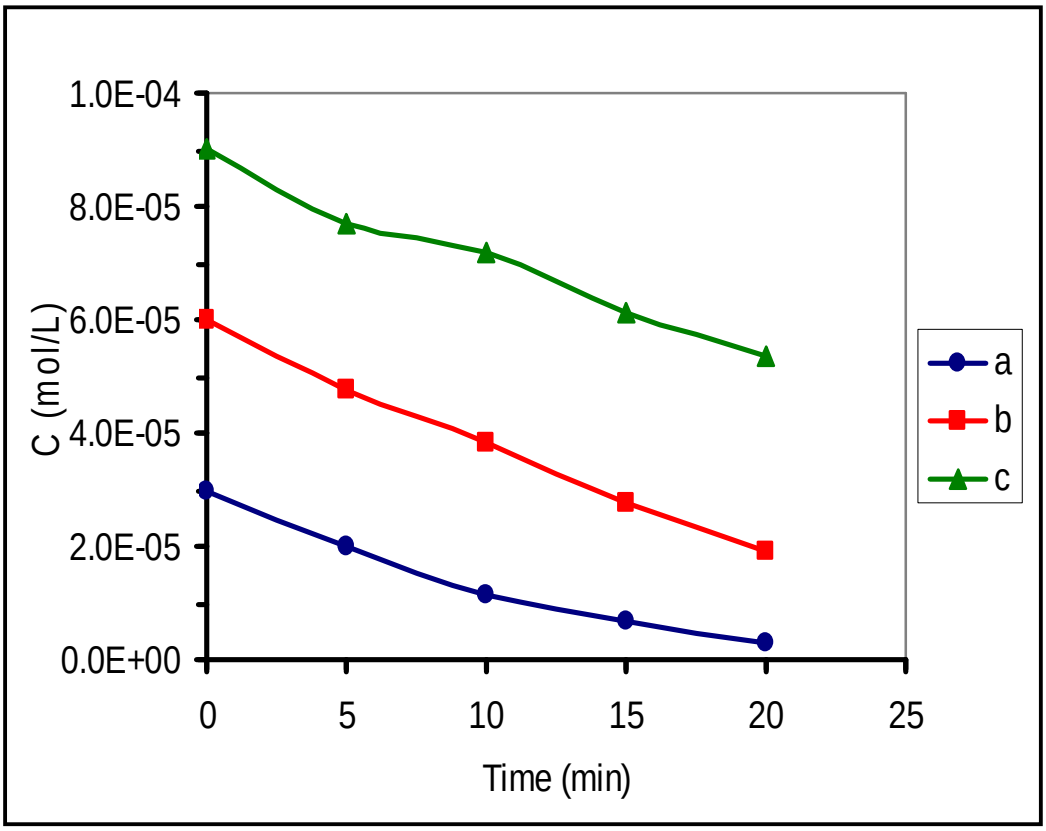

Figure 3.4: Effect of methyl orange concentration on rate of photo-degradation with 0.1 g TiO_2 under UV (0.0032 W/cm^2) in 50 ml neutral suspension at room temperature. Contaminant concentrations are: **a**) 10 ppm **b**) 20 ppm **c**) 30 ppm. Values of turnover number (and quantum yield) are: 0.001075 (0.00236), 0.00165 (0.00362) and 0.00147 (0.00322).

Therefore, it is necessary to study its tendency to leach out hazardous soluble Cd^{2+} ions. Furthermore, it is necessary to assess possible techniques to prevent such possible leaching out processes by using solid support for TiO_2/CdS systems such as the abundant Sand. In the visible irradiation experiments, different systems were studied as catalysts for degradation of methyl orange.

3.3.3.1 CdS as TiO_2 Sensitizer Under Solar Simulator Radiation:

Three different catalyst systems were examined in degradation of Methyl Orange under solar simulator radiation. Unlike the case with UV region experiments, the catalyst efficiency varied in the order: TiO_2/CdS > Sand/TiO_2/CdS > naked TiO_2. This was based on reaction rates, turnover number and quantum yield, (Figure 3.5). The TiO_2/CdS system was the most efficient one with quantum yield 0.00094. The fact, that CdS lowered TiO_2 efficiency in UV and enhanced it in the visible, is direct evidence in favor of sensitization by CdS. This is in accordance with earlier literature [1-7]. The Sand/TiO_2/CdS system showed lower efficiency than TiO_2/CdS system, which is attributed to the ability of Sand particles to screen the catalyst sites away from incident light, as discussed above. However, the efficiency lowering due to Sand support should not be considered a shortcoming, since the Sand/TiO_2/CdS systems were far easier to isolate and recover from the mixture after reaction completion, as discussed below. Moreover, the Sand/TiO_2/CdS system showed higher (about two fold) efficiency than the naked TiO_2 system itself, indicating a sensitization effect.

The fact that Sand/TiO_2 showed lower efficiency than naked TiO_2, Figure (3.5 a & c) in the visible indicates a screening effect by Sand. Moreover, it excludes any activation by the Sand itself. This is another indication that sensitization is only by CdS in the Sand/TiO_2/CdS systems.

Despite its relatively low catalytic efficiency, TiO_2 still shows some activity by irradiation with the solar simulator, causing about 20% degradation of methyl orange within 60 min. This is due to availability of a

minor tail, with 400 nm and shorter, within the visible light coming out of solar simulator lamps. The fact, that the Quantum yield for naked TiO_2 in UV (0.002) is much higher than under solar simulator light (0.000095), indicates the inefficiency of TiO_2 in visible regions. When a cut-off filter (removing 400 nm and shorter wavelengths) was placed between the solar simulator and the reaction mixture, the naked TiO_2 and Sand/TiO_2 showed no catalytic activities. The TiO_2/CdS and Sand/TiO_2/CdS systems functioned with the cut-off filter. This is direct evidence in favor of CdS sensitization.

The ability of TiO_2 to degrade methyl orange under solar simulator radiation, due to the UV tail, may be inhibited by Sand and mud particles commonly present in natural waters. The results show that Sand particles screen the TiO_2 from the minor UV tails. This limits the use of naked TiO_2 on large scale water purification. Sensitization is thus needed for water purification with TiO_2.

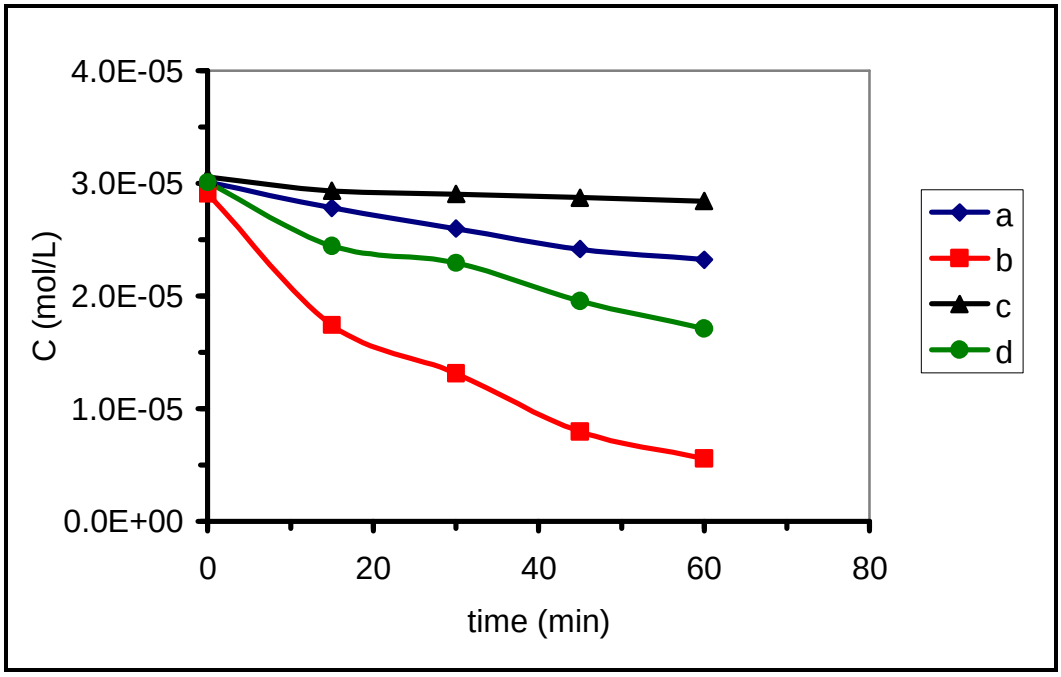

Figure 3.5: Effect of catalyst type on photo-degradation rate of methyl orange (neutral suspension, 50.0 ml suspension, 10.0 ppm) under solar simulator radiation (0.0212 W/cm^2) at room temperature. Nominal catalyst amounts are: **a**) 0.1g TiO_2, **b**) 0.1 g TiO_2/CdS, **c**) 2.0 g Sand/TiO_2, **d**) 2.0g Sand/TiO_2/CdS (contains about 0.1g TiO_2). Turnover number (and quantum yield) values are: 0.000275 (9.11649X10^{-5}), 0.000941 (31.21104X10^{-5}), 0.0000856(2.83978X10^{-5}) and 0.000519 (17.22446X10^{-5}) respectively.

3.3.3.2 Effect of Catalyst Concentration*:*

As Sand shows lowering of reaction rate due to screening, as discussed above, the catalyst concentration effect on reaction rate was studied for the TiO_2/CdS system only. Figure (3.6) shows the effect of TiO_2 nominal concentration on rate of degradation of methyl orange. Values of initial rates show a first order with respect to the TiO_2/CdS nominal concentration. Values of turnover number and quantum yield indicate that the efficiency is not lowered by increasing catalyst amount.

No systematic kinetic data could be observed for Sand/TiO_2/CdS system, due to the screening effect of Sand, as described earlier. These results are consistent with earlier reports [2].

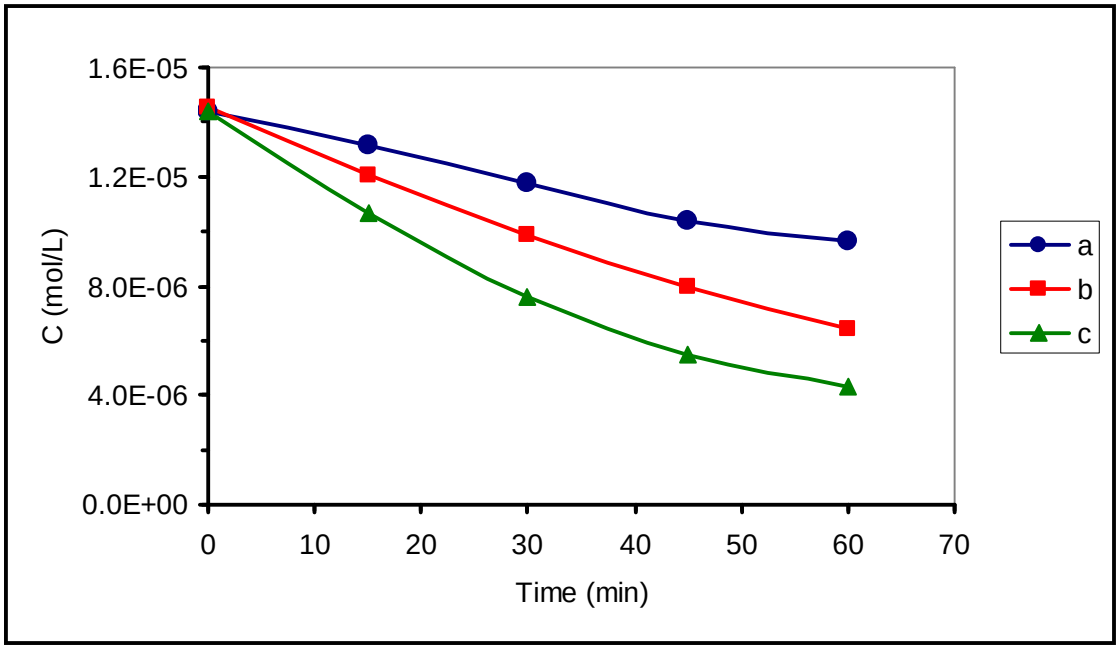

Figure 3.6: Effect of TiO_2/CdS catalyst amount on photo-degradation of methyl orange (neutral suspension, 50 ml of 5 ppm methyl orange), under solar simulator (0.0212 W/cm^2) at room temperature using TiO_2/CdS a) 0.05 g **b**) 0.1 g **c**) 0.15. Turnover number (and quantum number) values are: 0.00038 (6.284 X 10^{-5}), 0.000324 (1.074 X10^{-4}) and 0.000271 (1.346 X10^{-4}) respectively.

3.3.3.3 Contaminant Concentration Effect:

The effect of Methyl Orange contaminant concentration on rate of reaction was studied. The reaction rate was slower as the contaminant concentration

was increased, (Figure 3.7). This is not unexpected. Literature showed that photo-degradation is independent of the contaminant concentration, and in some cases, the rate is lowered with increased initial concentration [2]. Different explanations are proposed, all of which rely on the adsorption of contaminant molecules on the solid surface in a Langmuire Hinshelwood model.

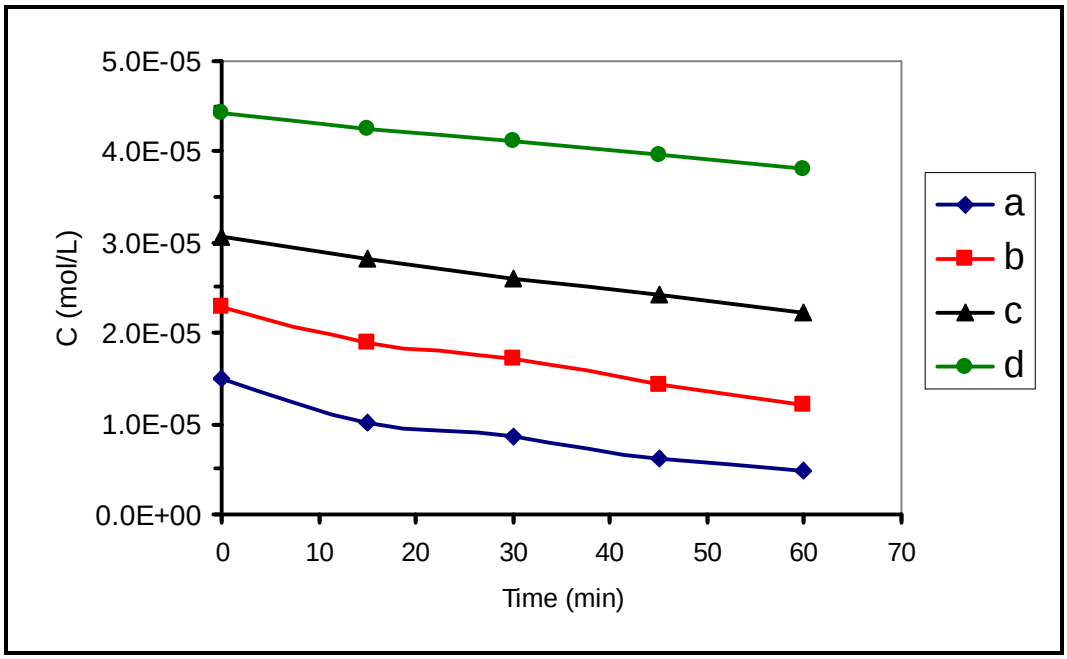

Figure 3.7: Effect of methyl orange concentration on rate of degradation using TiO_2/CdS (0.1 g) in 70 ml neutral suspension at room temperature under solar simulator (0.0212 W/cm^2). Methyl orange concentrations are: **a**) 5 ppm **b**)7.5 ppm **c**) 10 ppm **d**) 15 ppm. Turnover number (and quantum yield) values are: 0.000565 (0.000134), 0.000599(0.000142), 0.000465 (0.00011) and 0.000342(0.000081), respectively.

One acceptable explanation is the fact that at higher contaminant concentration, the contaminant molecules may compete with other adsorbed species (O_2 or $OH^{\bullet}$) and inhibit degradation [2, 18], other

explanation is the poor penetration of visible light into decreased transparency of the concentrated dyes solution [45-48].

3.3.3.4 Temperature Effect*:*

Photo-decomposition of methyl orange, in the visible range, was studied at different temperatures. Similar to UV results, the visible photo-degradation was not much affected by the reaction temperature, as shown in Figure (3.8). The value for activation energy was immeasurably small. The discussion to these findings follows that presented earlier for UV systems.

3.3.3.5 Effect of pH:

The efficiency of Sand/TiO_2/CdS system in photo-degradation of methyl orange, with solar simulator light, was investigated at different pH values, Figure (3.9). In basic solutions the reaction rates, the turnover number and the quantum yield values, were higher than in neutral or acidic solutions. The efficiency of naked TiO_2 is known to increase in acidic media [2]. Sulphonated TiO_2 surfaces are known to have enhanced surface acidity and to be more efficient photo-degradation catalytic activity [28-30]. The presence of OH groups may also enhance TiO_2 efficiency in photo-degradation reactions [2].

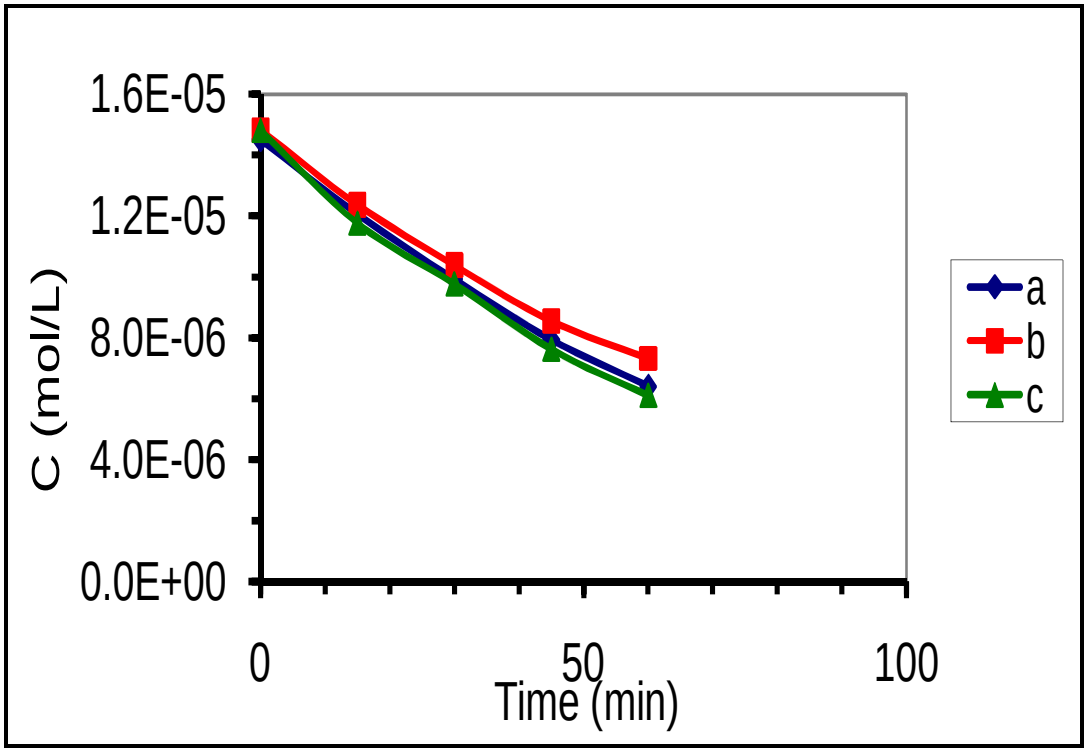

Figure 3.8: Temperature effect on photo-degradation rate of methyl orange (neutral suspension, 50 ml, 5 ppm) under solar simulator using TiO_2/CdS (0.1 g), at different temperatures: **a**) 30°C **b**) 45°C **c**) 60°C.

The Sand/TiO_2/CdS system showed higher catalytic efficiency in more basic media with higher pH value. This is possibly due to the tendency of CdS to leach out of the TiO_2 surface. In this study, it has been found that CdS decomposes into soluble Cd^{2+} ions under irradiation conditions. Such tendency is higher in more acidic conditions, and this is more pronounced for the Sand/TiO_2/CdS system, as will be shown later.

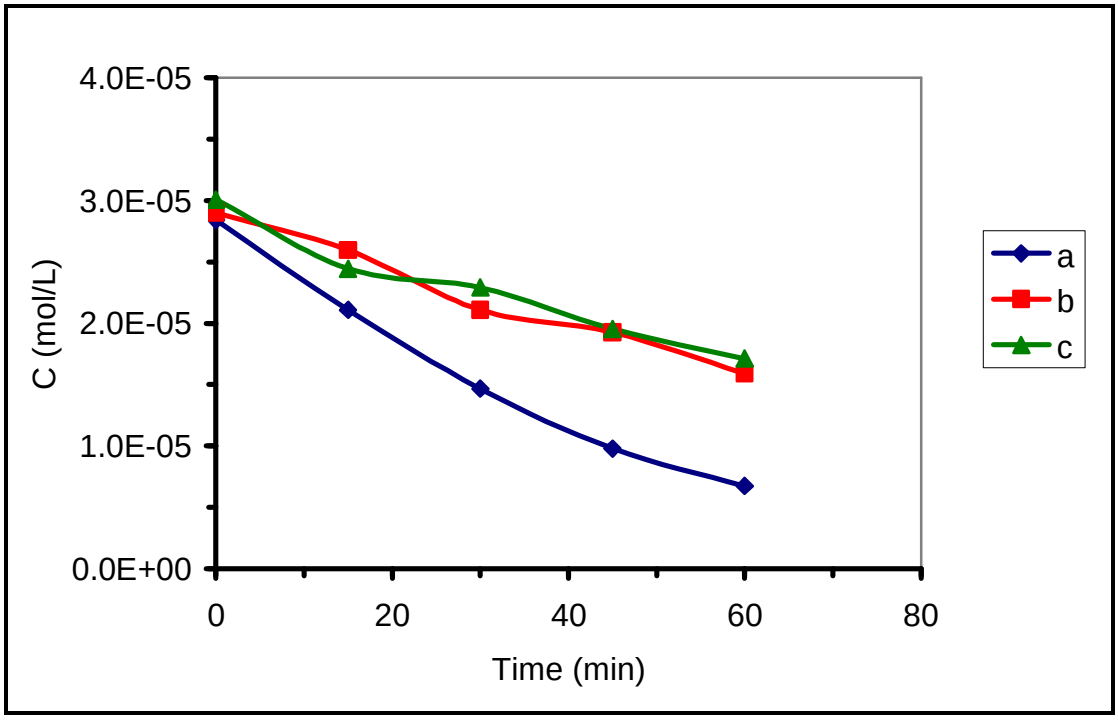

Figure 3.9: Effect of pH on photo-degradation rate of methyl orange (50 ml, 10 ppm) using Sand/TiO_2/CdS (2.0 g) at room temperature. Values of pH are: **a**) 9.5 **b**) 4 **c**) 7.8 . Turnover number (and quantum yield) values are: 0.000868 (0.000288), 0.0005255 (0.000174) and 0.00051936 (0.0001723) respectively.

The catalytic efficiency lowering, in neutral and acidic media, is a shortcoming for Sand/TiO_2/CdS and TiO_2/CdS systems. Since natural waters commonly have pH values close to 7, the lowered efficiency of such catalytic systems limits their use for large scale natural water purification, as discussed below.

3.3.4 Leaching Out Experiments (Catalyst Stability):

Despite the ability of CdS to successfully sensitize TiO_2 surfaces in photo-degradation of methyl orange, the tendency of CdS to decompose into hazardous Cd^{2+} ions has been investigated under different conditions. The ability of Sand support to prevent such tendency has also been investigated.

Concentrations of aqueous Cd^{2+} ions, leaching out during visible photo-degradation reaction experiments, have been measured with time using voltametry. Effect of different parameters, on tendency of Cd^{2+} ions to leach out from TiO_2/CdS and Sand/TiO_2/CdS systems, was studied. Since no noticeable effect of temperature was observed, leaching experiments were conducted at room temperature unless otherwise stated. Figures (3.10) through Figures (3.13) summarize the results.

3.3.4.1 TiO_2/CdS System:

In case of TiO_2/CdS systems, used in methyl orange degradation experiments with visible light, the Cd^{2+} ion leaching tendency was slightly affected with solution pH value. Acidic and neutral solutions showed similar concentrations of Cd^{2+} ions, as shown in Figures 3.10 and 3.11, while basic solutions exhibited lower Cd^{2+} ions. Annealing the TiO_2/CdS systems showed only little stabilizing effect on the TiO_2/CdS system. Again the acidic systems showed slightly higher Cd^{2+} concentrations than basic systems. The percent of CdS decomposition after 50 min. are found to be 100%, 90% and 100% respectively for acidic, basic and neutral solutions.

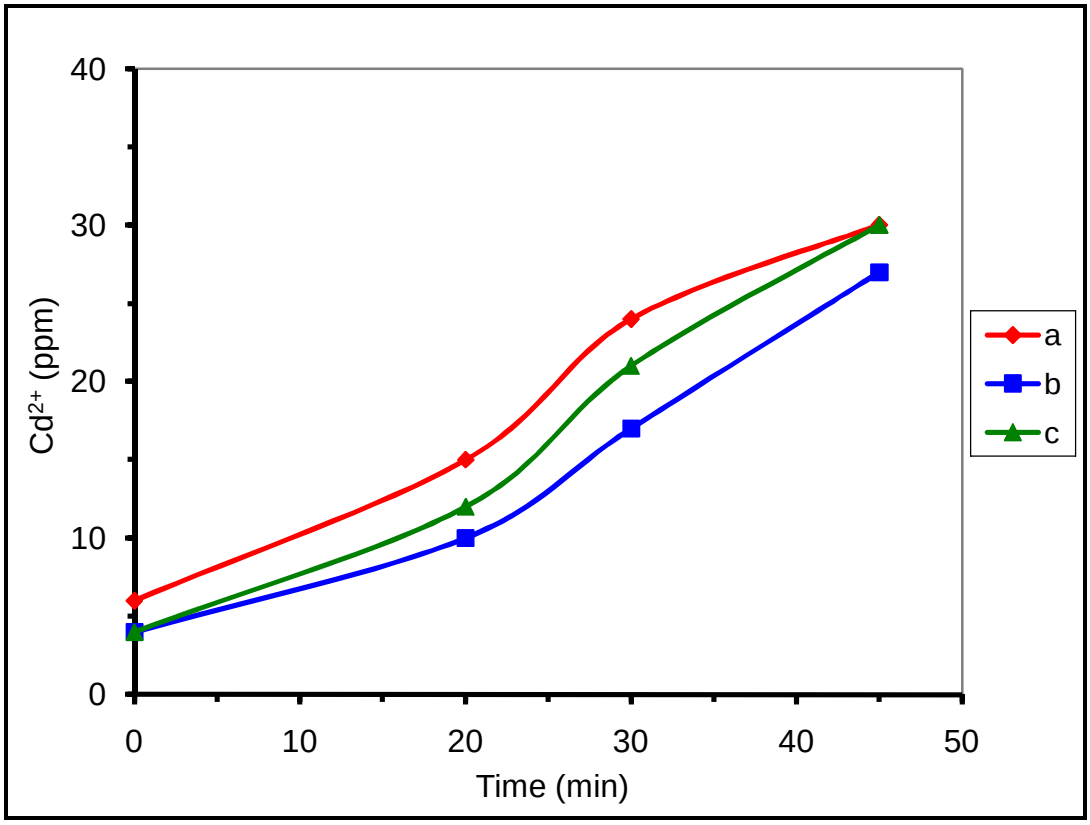

Figure 3.10: Reaction profiles showing Cd^{2+} ion concentrations leaching out of non-annealed TiO_2/CdS (0.1 g) under methyl orange degradation conditions (solar simulator 0.0212 W/cm^2, room temperature, in 70 ml suspension of 5 ppm methyl orange) at different pH values: **a**) 3.5 **b**) 9 **c**) neutral. Values of leaching out percentage for Cd^{2+} are: 100%, 90% and 100% respectively.

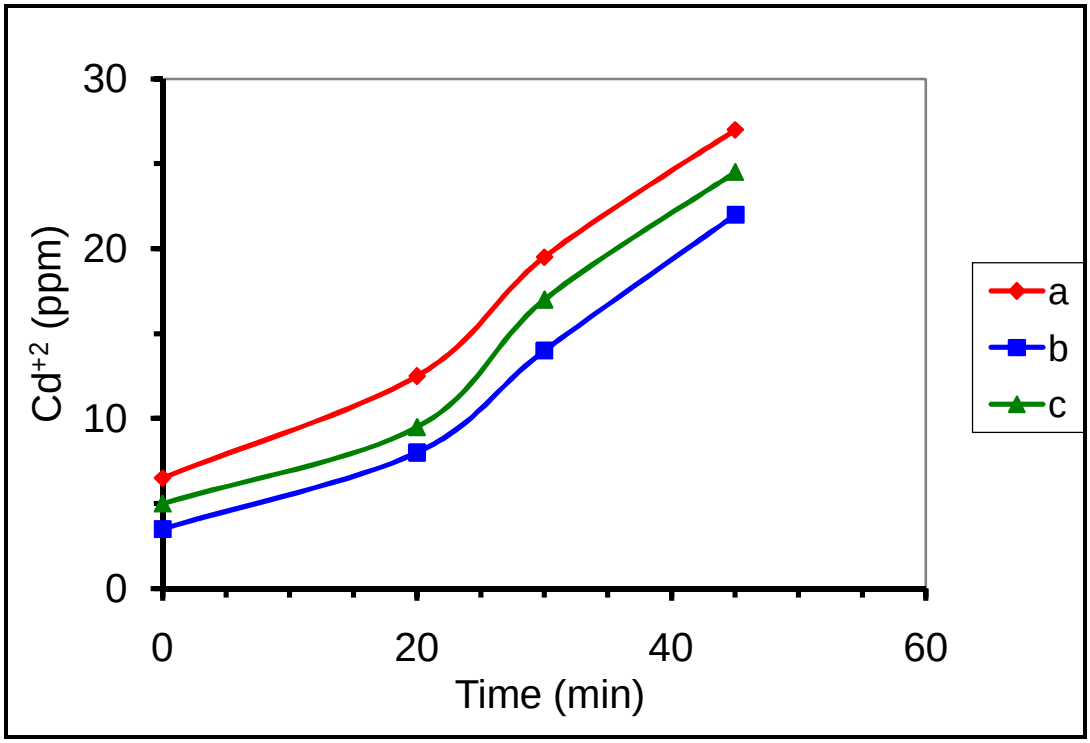

Figure 3.11: Reaction profiles showing Cd^{2+} ion concentrations leaching out of pre-annealed TiO_2/CdS (0.1 g) under methyl orange degradation conditions (solar simulator 0.0212 W/cm^2, room temperature, in 70 ml suspension of 5 ppm methyl orange) at different pH values: **a**) 3.5 **b**) 9 **c**) neutral. Percentage values of Cd^{2+} leaching out are: 90%, 73% and 82%, respectively.

3.3.4.2 Sand/TiO_2/CdS System:

In case of Sand/TiO_2/Cds systems, Figures (3.12) and (3.13), a slightly different behavior was observed. At lower pH values, CdS showed high tendency to decompose, reaching up to 90% decomposition within 50 min. This was exhibited in both pre-annealed and non-annealed Sand/TiO_2/CdS systems. Under neutral conditions, significantly less decomposition was observed, reaching only up to 30% in cases of pre-annealed and non-annealed systems. In basic media, the tendency of decomposition was less than 10% within 50 min.

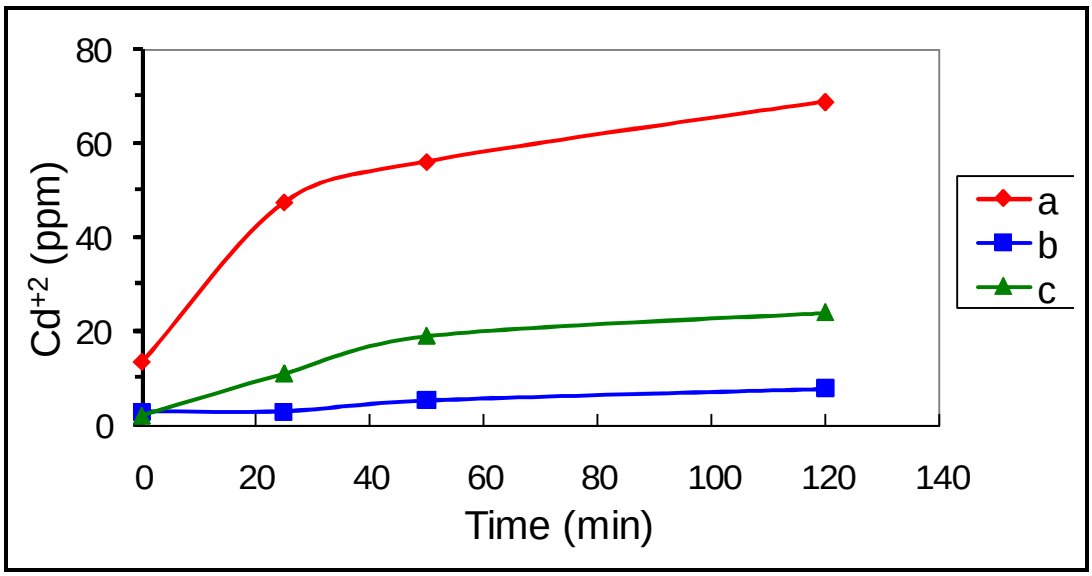

Figure 3.12: Reaction profiles showing Cd^{2+} ion concentrations leaching out of non-annealed Sand/TiO_2/CdS (1.0 g) under methyl orange degradation conditions (solar simulator 0.0212 W/cm^2, room temperature, in 70 ml suspension of 5 ppm methyl orange) at different pH values: **a**) 3.5, **b**) 9, and **c**) neutral. Values of leaching out percentage for Cd^{2+} are: 77%, and 9% and 24%, respectively.

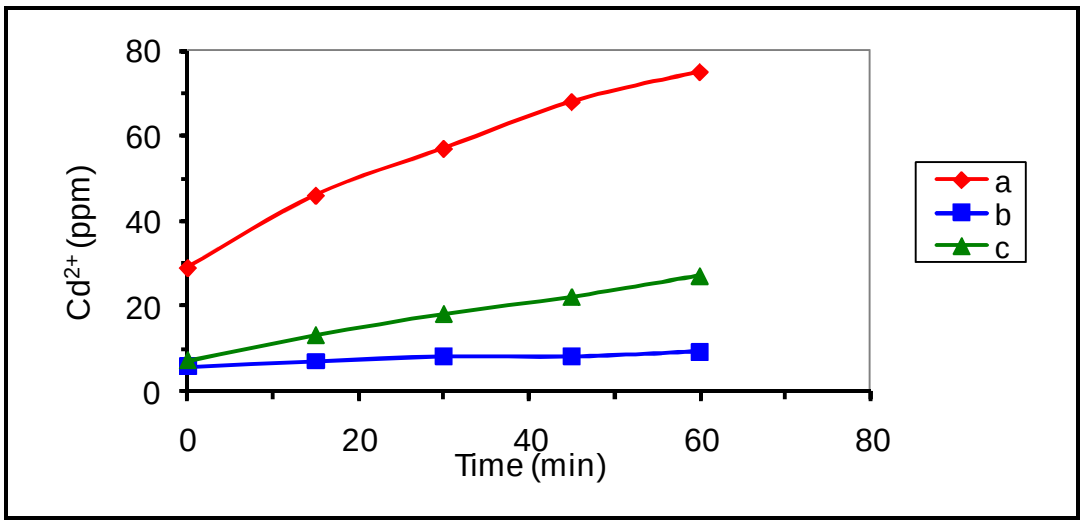

Figure 3.13: Reaction profiles showing Cd^{2+} ion concentrations leaching out of pre-annealed Sand/TiO_2/CdS (1.0 g) under methyl orange degradation conditions (solar simulator 0.0212 W/cm^2, room temperature, in 70 ml suspension of 5 ppm methyl orange) at different pH values: **a**) 3.5, **b**)9 and **c**)neutral. Values of leaching out percentage for Cd^{2+} are: **a**) 83% **b**) 11% **c**) 31%, respectively.

Annealing the Sand/TiO_2/CdS systems did not significantly lower the leaching tendency, as shown in Figures (3.12-3.13). With and without annealing, the Sand/TiO_2/CdS systems showed some relatively high stability in basic media compared to acidic and neutral media. Despite this, Sand/TiO_2/CdS system should be avoided in water purification due to the hazardous nature of Cd^{2+} ions. The concentration of Cd^{2+} ions (~10 ppm) leaching out of Sand/TiO_2/CdS system in basic media, evidently with least leaching tendency among the used systems, is still higher than the phyto-toxic threshold limits for Cd^{2+} ions (0.005 mg/L, $5X10^{-2}$ ppm) in agricultural waters [31]. This imposes a limitation on applicability of the widely ongoing current studies of CdS-sensitized TiO_2 systems.

3.3.5 Catalyst Reuse Experiments:

Supporting TiO_2 particles onto insoluble supports has been widely reported in literature [2, 4, 7-16, 18, 32-45]. However, only a few reports are known for supporting the combined TiO_2/Dye degradation catalysts onto insoluble supports, as discussed on Chapter one [18]. TiO_2 is hydrophilic in nature, and is commonly used as fine particles with nano- or micro-scale size. This makes it difficult to isolate by simple techniques such as filtration or decantation. Supporting TiO_2/CdS onto Sand is one possible solution for such technical difficulties. As stated earlier, Sand is a cheap widely abundant stuff in natural lakes. Therefore, any TiO_2 systems added to natural waters will interact with Sand particles. Therefore, it is necessary to study Sand as support for TiO_2/CdS systems. Despite the tendency of CdS

to leach out from Sand/TiO_2/CdS systems, as described above, Sand support has the added value of making the catalyst system recoverable for further reuse.

Due to the tendency of CdS to leach out, Sand/TiO_2/CdS catalyst recovery and reuse study could not be performed, since complete CdS leaching out occurred within one hour, (vide infra). Therefore, special Sand/TiO_2/CdS samples, with higher CdS uptakes (1.93% by mass) were prepared for recovery/reuse purposes. Figure (3.14) shows data on rates of methyl orange degradation, in neutral solutions at room temperature, under visible radiation, using a fresh, first recovery and second recovery samples of Sand/TiO_2/CdS samples. The catalyst partly looses its efficiency on reuse. This is due to the tendency of CdS to leach out of the catalyst system under photo-degradation conditions, as described above. Figure (3.14) shows about 30% efficiency loss, for the Sand/TiO_2/CdS system, in the third use.

The results indicate that the support could not completely prevent CdS leaching out, but 70% efficiency still remains after third use. Sand surface seems to be a good candidate for future sensitized TiO_2 surfaces with dyes more safe than CdS. Work is underway here to utilize Sand as support for TiO_2 surfaces sensitized with safe natural dyes, as alternatives for CdS systems.

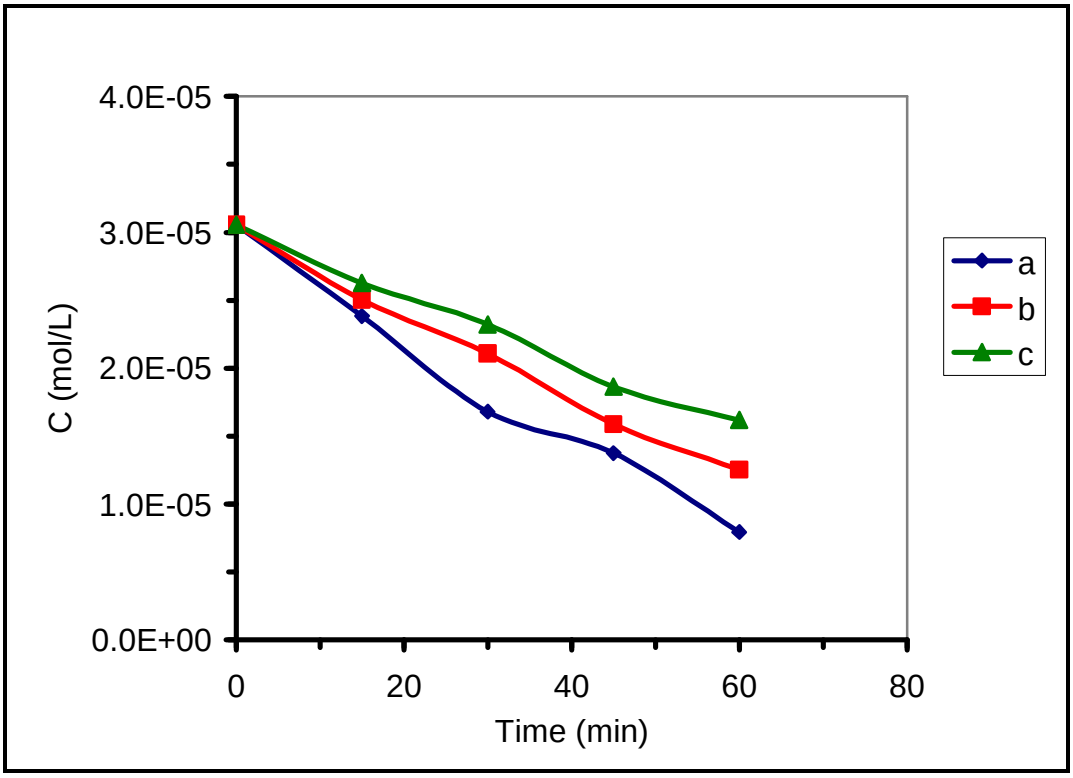

Figure 3.14: Effect of Sand/TiO_2/CdS (1.0 g, containing 1.9% mass CdS) catalyst recovery and reuse on photo-degradation rate of methyl orange (neutral 50 ml suspension, 10 ppm) at room temperature. **a**) Fresh sample, **b**) 2nd use and **c**) 3rd use.

3.4 Conclusion:

CdS effectively sensitizes TiO_2 to visible region in degradation of organic contaminants such as methyl orange. However, its tendency to degrade into soluble Cd^{2+} ions limits its applicability in water purification with solar light. The Sand support partially limited the Cd^{2+} ions leaching out only under basic condition. Moreover the support made recovery of the sensitized catalyst easier, giving relatively high efficiency reusable system. To avoid the hazardous nature of CdS system, more work is needed to completely prevent its leaching out, or better replacing it with safer dyes.

References:

1. J.-M. Herrmann[a], C. Duchamp[a], M. Karkmaz[a], B. T. Hoai[a], H. Lachheb[a], E. Puzenat,[a] C. Guillard, Environmental green chemistry as defined by photocatalysis, *J. Hazard. Mater.*, **145** (2007) 624-629

.

2. Y. Bessekhouad, N. Chaoui, M. Trzpit, N. Ghazzal, D. Robert, J.V. Weber, UV–vis versus visible degradation of Acid Orange II in a coupled CdS/TiO_2 semiconductors suspension, *J. Photochem. Photobiol. A*, **183** (2006) 218–224.

3. D. Robert, Photosensitization of TiO_2 by M_xO_y and M_xS_y nanoparticles for heterogeneous photocatalysis applications, *Catal. Today.*, **122** (2007) 20–26.

4. Y. Bessekhouad, N. Chaoui, M. Trzpit, N. Ghazzal, D. Robert, J.V. Weber, UV–vis versus visible degradation of Acid Orange II in a coupled CdS/TiO_2 semiconductors suspension, *J. Photochem. Photobiol. A*, **183** (2006) 218–224.

5. N. Sakai, R. Wang, A. Fujishima, T. Watanabe, K. Hashimoto, Effect of ultrasonic treatment on highly hydrophilic TiO_2 surfaces, *Langmuir*, **14** (1998) 5918 -5920.

6. H. Greijer[a, b], L. Karlson[b], S.-E. Lindquist,[a] A. Hagfeldt, Environmental aspects of electricity generation from a nanocrystalline dye sensitized solar cell system, *Renew. Energ.*, **23** (2001) 27-39.

7. P. Pizarro, C. Guillard, N. Perol, J.-M. Herrmann, Photocatalytic degradation of imazapyr in water: Comparison of activities of different supported and unsupported TiO_2-based catalysts, *Catal. Today.*, **101** (2005) 211-218.

8. M. C. Hidalgo, D. Bahnemann, Highly photoactive supported TiO_2 prepared by thermal hydrolysis of $TiOSO_4$: Optimisation of the method and comparison with other synthetic routes, *Appl. Catal. B: Environ.*, **61 (**2005) 259-266.

9. M.J. Lo`pez-Munˇoz, R. Grieken, J. Aguado, J. Marugan, Role of the support on the activity of -supported TiO_2 photocatalysts: Structure of the TiO_2/SBA-15 photocatalysts, *Catal. Today.*, **101 (**2005) 227-234.

10. M. Hirano, K. Ota, Preparation of photoactive anatase-type TiO_2/Sand gel by direct loading anatase-type TiO_2 nanoparticles in

acidic aqueous solutions by thermal hydrolysis, *J. Mater. Sci.*, **39** (2004) 1841-1844.

11. J Aguado, R Grieken, M.-J. Lo`pez-Munˇoz, J. Maruga´n, Removal of cyanides in wastewater by supported TiO_2-based photocatalysts, *Catal. Today.*, **75** (2002) 95-102.

12. J. N. Najm, V. L. Snoeyink, M. T. Suidan, C.H. Lee, Z. Richard, *J. Am. Water Works Ass.*, **82** (1990) 65-72.

13. P. Periyat, K.V. Baiju, P. Mukundan, P. K. Pillai, K. G. K. Warrier, High temperature stable mesoporous anatase TiO_2 photocatalyst achieved by addition, *Appl. Catal. A: Gen.*, **349** (2008) 13-19.

14. J. Marugán. R. v. Grieken, A. E. Cassano and O. M. Alfano, Intrinsic kinetic modeling with explicit radiation absorption effects of the photocatalytic oxidation of cyanide with TiO_2 and Sand-supported TiO_2 suspensions, *Appl. Catal. B: Environ.*, **85** (2008) 48-60.

15. Lee, J.W.; Othman, M.R.; Eom, Y.; Lee, T.G.; Kim, W.S.; Kim, J. "The effects of sonification and TiO_2 deposition on the micro-characteristics of the thermally treated SiO_2/TiO_2 spherical core–shell particles for photo-catalysis of methyl orange", *Micropor. Mesopor. Mat.*, **116** (2008) 561-568.

16. M. Grätzel, Photoelectrochemical cells, *Nature*. **414** (2001) 338-344.

17. H.S. Hilal, L.Z. Majjad, N. Zaatar, A.El-Hamouz, Dye-effect in TiO_2 catalyzed contaminant photo-degradation: Sensitization vs. charge-transfer formalism, *Solid State Sci.*, **9** (2007) 9-15.

18. Y. Bessekhouad, D. Robert, J.V. Weber, Bi_2S_3/TiO_2 and CdS/TiO_2 heterojunctions as an available configuration for photocatalytic degradation of organic pollutant, *J. Photochem. Photobiol. A*, **163** (2004) 569–580.

19. O. Vigil-Galán, A. Morales-Acevedo, F. Cruz-Gandarilla, M.G. Jiménez-Escamilla, Characterization of CBD–CdS layers with different S/Cd ratios in the chemical bath and their relation with the

efficiency of CdS/CdTe Solar Cells, *Thin Solid Films*, **515** (2007) 6085–6088.

20. J.N. Ximello-Quiebras, G. Contreras-Puente, J. Aguilar-Hernandez, G. Santana-Rodriguez, A. A.-C. Readigos, Physical Properties of chemical bath deposited CdS thin films, *Sol. Energ. Mat. Sol. C.* ***, 82*** (2004) 263–268.

21. P. Roy, S. K. Srivastava, A new approach towards the growth of cadmium sulphide thin film by CBD method and its characterization, *Mater. Chem. Phys.*, **95** (2006) 235–241.

22. K.V. Zinoviev, O. Zelaya-Angel, Influence of low temperature thermal annealing on the dark resistivity of chemical bath deposited CdS films, *Mater. Chem. Phys.*, **70** (2001) 100–102.

23. F. Chen, W. Jie, Growth and photoluminescence properties of CdS solid solution semiconductor, *Cryst. Res. Technol.*, **42** (2007) 1082 – 1086.

24. J. M. Hermann, Heterogeneous photocatalysis: fundamentals and applications to the removal of various types of aqueous pollutants, *Catal. Today*, **53** (1999) 115-129.

25. N. Guettai, H. A. Amar, Photocatalytic oxidation of methyl orange in presence of titanium dioxide in aqueous suspension. Part I: Parametric study, *Desalination*, **185** (2005) 427-437.

26. H. Hiroaki, H, Ayako, U. Mamoru, O. Kunihiko, H. Hiroshi , Determination of the photo-degradation quantum yield of organic dyes in the film state, *Nippon Kagakkai Koen Yokoshu.*, **83** (2003) 747.

27. D.S. Muggli, L. Ding, Photocatalytic performance of sulfated TiO_2 and Degussa P-25 TiO_2 during oxidation of organics, *Appl. Catal. B: Environ.*, **32** (2001) 181-194.

28. P.B. Amama, K. Itoh, M. Murabayashi, Gas-phase photocatalytic degradation of trichloroethylene on pretreated TiO_2, *Appl. Catal. B: Environ.*, **37** (2002) 321-330.

29. M.M. Lewandowski, D.F. Ollis, Halide acid pretreatments of photocatalysts for oxidation of aromatic air contaminants: rate enhancement, rate inhibition, and a thermodynamic rationale, *J. Catal.* **217** (2003) 38-46.

30. Toxic chemicals hazard of irrigation water *http://www.lenntech.com/irrigation/toxic-ions-hazard-of-irrigation-water.htm* , accessed Aug. 13th, (2008).

31. A. Bhattacharyya, S. Kawi, M. B. Ray, Photocatalytic degradation of orange II by TiO_2 catalysts supported on adsorbents, *Catal. today*, **98** (2004) 431-439.

32. Y. Jiang[a, b], Y. Sun[a,], H. Liu[a, b], F. Zhu,[b] H. Yin, Solar photocatalytic decolorization of C.I. Basic Blue 41 in an aqueous suspension of TiO_2–ZnO, *Dyes Pigments*, **78** (2008) 77-83.

33. Y. Li, X. Li, J. Li, J. Yin, Photocatalytic degradation of methyl orange by TiO_2-coated activated carbon and kinetic study, *Water Res.*, **40** (2006) 1119–1126.

34. J. Matos, J. Laine, J. Herrmann, Synergy effect in the photocatalytic degradation of phenol on a suspended mixture titania and activated carbon, *Appl. Catal. B: Environ.* **18** (1998) 281-291.

35. D. Chatterjee, S. Dasgupta, N.N. Rao, Visible light assisted photo-degradation of halocarbons on the dye modified TiO_2 surface using visible light, *Sol. Energ. Mat. Sol. C.*, **90** (2006) 1013-1020.

36. A. C.H., S.C. Lee, Combination effect of activated carbon with TiO2 for the photo-degradation of binary pollutants at typical indoor air level, *J. Photochem. Photobiol. A*, **161** (2004) 131-140.

37. J. Aran˜a, J.M. Don˜a-Rodrı´guez, E.T. Rendo´n, I. Garriga, C. Cabo, O. Gonza´lez-Dı´az, J.A. Herrera-Melia´n, J. Pe´rez-Pen˜a, G. Colo´n, J.A. Navı´o, TiO_2 activation by using activated carbon as a support, Part I. Surface characterisation and decantability study, *Appl. Catal. B: Environ.*, **44** (2003) 161-172.

38. J. Marugan, R.V. Grieken, O. M. Alfano, A.E. Cassano, Optical and physicochemical properties of Sand-supported TiO_2 photocatalysts, *Aiche J.*, **52** (2006) 2832-2843.

39. M. Nazir, J. Takasaki, H. Kumazawa, Photocatalytic degradation of gaseous ammonia and trichloroethylene over TiO2 ultrafine powder deposited on activated carbon particles, *Chem. Eng. Comm.*, **190** (2003) 322-333.

40. T. Y. Kim, Y.-H. Lee, K.-H. Park, S. J. Kim, S. Y. Cho, A study of photocatalysis of TiO_2 coated onto chitosan beads and activated carbon, *Res. Chem. Intermediat*, **31** (2005) 343–358.

41. S.-X. Liu, C.-L. SunPreparation and performance of photocatalytic regenerationable activated carbon prepared via sol-gel TiO_2, *J. Environ. Sci.*, **18** (2006) 557-561.

42. A. Jaroenworaluck, W. Sunsaneeyametha, N. Kosachan, R. Stevens, Characteristics of Sand-coated TiO_2 and its UV absorption for sunscreen cosmetic applications, *Surf. Interface Anal.*, **38** (2005) 473-477.

43. M.S. Vohra, K. Tanaka, Photocatalytic degradation of aqueous pollutants using Sand-modified TiO_2, *Water Res*. **37** (2003) 3992-3996.

44. C.-F. Chi, Y.-L. Lee, H.-S. Weng, A CdS-modified TiO_2 nanocrystalline photoanode for efficient hydrogen generation by visible light, *Nanotechnology*. **19** (2008) 125704 (5pp).

45. K. Dutta, S. Mukhopadhyay, S. Bhattacharjee, B. Chaudhuri, Chemical oxidation of methylene blue using Fenton-like reactions *J. Hazard. Mater.*, **84** (2001) 57–71.

46. L. Gomathi Devi, S. Girish Kumar, K. Mohan Reddy, C. Munikrishnappa, Photo degradation of Methyl Orange an azo dye by Advanced Fenton Processusing zero valent metallic iron: Influence of various reactionparameters and its degradation mechanism, *J. Hazard. Mater.*, **164** (2009) 459–467.

47. B. Neppolian, H.C. Choi, S. Sakthivel, B. Arabindoo, V. Murugesan, Solar UV-indiced photocatalytic degradation of hthree commercial textile dyes, *J. Hazard. Mater.*, **89** (2002) 303.

48. R.J. Davis, J.L. Gainer, G.O. Neal, I.W, Wu, Photocatalytic decolorization of wastewater dyes, *water Environ. Res.*, **66** (1994) 50.

CHAPTER 4

PHOTO-DEGRADATION OF PHENAZOPYRIDINE USING TiO_2/CdS

4.1 Introduction:

The main goal of his work is to assess the feasibility of using CdS as sensitizer for TiO_2 in light-driven organic compound degradation. A medically active compound, Phenazopyridine hydrochloride, was used here as a model for future safe degradation of water contaminants. This report focuses on the environmental drawbacks of using **TiO_2/CdS** systems in large scale future purification processes. The tendency of CdS to leach out Cd^{2+} ions was investigated. Techniques to prevent such leaching were investigated. Effect of annealing **TiO_2/CdS** on leaching out process was investigated. Supporting system **TiO_2/CdS** onto sand was also studied. The feasibility of these techniques to prevent leaching out Cd^{2+} ions, and consequently to enhance future perspectives of CdS sensitizers at large scale purification strategies, is discussed here.

The TiO_2/CdS, has been earlier studied from different angles, such as synthetic methods, characterization, photo-catalytic efficiency, and kinetics. Little concern about the hazardous nature of **TiO_2/CdS** and its prevention was mentioned in literature [8-12, 17], although the tendency of CdS to degrade into toxic Cd^{2+} ions and SO_4^{2-} (or elemental sulfur) under light is known [13].

4.2 Experimental:

4.2.1 Materials:

Acquisition, preparation and characterization of Rutile TiO_2 powder, TiO_2/CdS, and Sand/TiO_2/CdS were described earlier in Chapter 3. The

contaminant Phenazopyridine hydrochloride was kindly donated by Birzeit-Palestine Pharmaceutical Company in a pure form

4.2.2 Equipment:

Contaminant (Phenazopyridine) concentrations were spectrophotometrically measured on a Shimadzu UV-1601 spectrophotometer at wavelength 430 nm. Pre-constructed calibration curves were used.

To analyze dissolved Cd^{2+} ions, anodic stripping differential pulse voltametry was conducted using a dropping mercury electrode (MDE150) on a PC controlled Polarograph (POL150). Details of operation conditions were earlier described in Chapters 2 and 3.

Solar simulator irradiation was conducted using a model 45064 - 50 W Xe solar simulator lamp (Leybold Didactic Ltd.). Exact lamp specifications are described in special manuals as shown in Chapter two [27-33].

4.2.3 Catalytic Experiments:

Catalytic experiments were conducted in magnetically stirred thermostated aqueous solutions. Procedures (which were applied in photodegradtion of Methyl Orange) are applied here for photo-degradation of Phenazopyridine. The aqueous phase was also analyzed for dissolved Cd^{2+} ions, by voltametry as described above. The reaction rate was measured based on analyzing remaining contaminant concentration with time. Turnover number and quantum yield were also calculated and used for

efficiency comparison. Complete mineralization of organic contaminants into carbon dioxide, and other compounds, under visible light, can be assumed based on earlier reports [34], Voltametric and UV/visible spectral analysis confirmed complete mineralization. This was evident by the absence of 430 nm absorption band after reaction cessation. Complete mineralization was also evident from the absence of any benzene derivatives. This was confirmed by absence of any absorption band characteristic for phenyl group at 200 nm or longer, as observed from UV-Visible absorption spectra. The gradual increase in NO_3^- ions with reaction time in the treated solution confirmed complete mineralization of the contaminant, as observed from voltametric analysis.

Recovery and reuse experiments were conducted using recovered catalyst, by filtration, after reaction completion. The recovered catalyst system was re-used like the fresh catalyst samples, as described before.

4.3 Results and Discussions:

The three systems **TiO_2**, **TiO_2/CdS** and **Sand/TiO_2/CdS**, were used as catalysts in photo-degradation of Phenazopyridine, under solar simulator radiations. Comparative study between such three catalyst systems was performed in order to assess the feasibility of CdS as a future sensitizer. For this purpose, the efficiency of CdS sensitizer was studied in terms of reaction rates, values of turnover number and values of quantum yield. The relatively low turnover number values are due to small fractions of surface active sites, *viz*. most sites are in the bulk. The tendency of CdS to leach

out of TiO_2 surface was also investigated under different conditions. Effect of annealing of **TiO_2/CdS** on its stability to degradation was studied. The ability of Sand support to prevent Cd^{2+} ion leaching out was investigated, with and without annealing. Recovery and reuse of catalyst was also studied.

4.3.1 Control Experiments:

Control experiments, conducted under irradiation in the absence of catalyst systems, showed no loss of contaminant concentration. Experiments conducted using different catalyst systems in the dark showed no significant contaminant loss, which indicates that the loss under irradiation experiments is due to photo-degradation. The visible light was responsible for the degradation. When a cut-off filter (removing 400 nm and shorter wavelengths) was placed between the solar simulator and the reaction mixture, the naked **TiO_2** and **Sand/TiO_2** showed no catalytic activities. The **TiO_2/CdS** and **Sand/TiO_2/CdS** systems functioned with the cut-off filter. This is direct evidence in favor of CdS sensitization.

4.3.2 Studied Factors:

The effects of type of catalyst, pH, temperature, catalyst concentration and contaminant concentration were all studied. Unless otherwise stated, **TiO_2/CdS** and **Sand/TiO_2/CdS** were pre-annealed and cooled.

***Effect of CdS as Sensitizer*:**

The naked TiO_2 powders failed to effectively catalyze the degradation of Phenazopyridine in the visible radiation. The slight loss of Phenazopyridine using TiO_2 and sand/TiO_2 is due to small UV fraction in the solar simulator Xe lamp simulator spectrum. This was confirmed when a cut-off filter was used. With complete removal of waves shorter than 400 nm, no degradation occurred by the naked TiO_2 systems. The sensitized system TiO_2/CdS showed significantly higher efficiency, as shown in Figure (4.1). This indicates the sensitizing effect of CdS in degradation of Phenazopyridine. This is understandable since TiO_2 can not be excited by visible radiation and needs shorter wavelengths. On the other hand, CdS (2.2 eV) can be readily excited in the visible region.

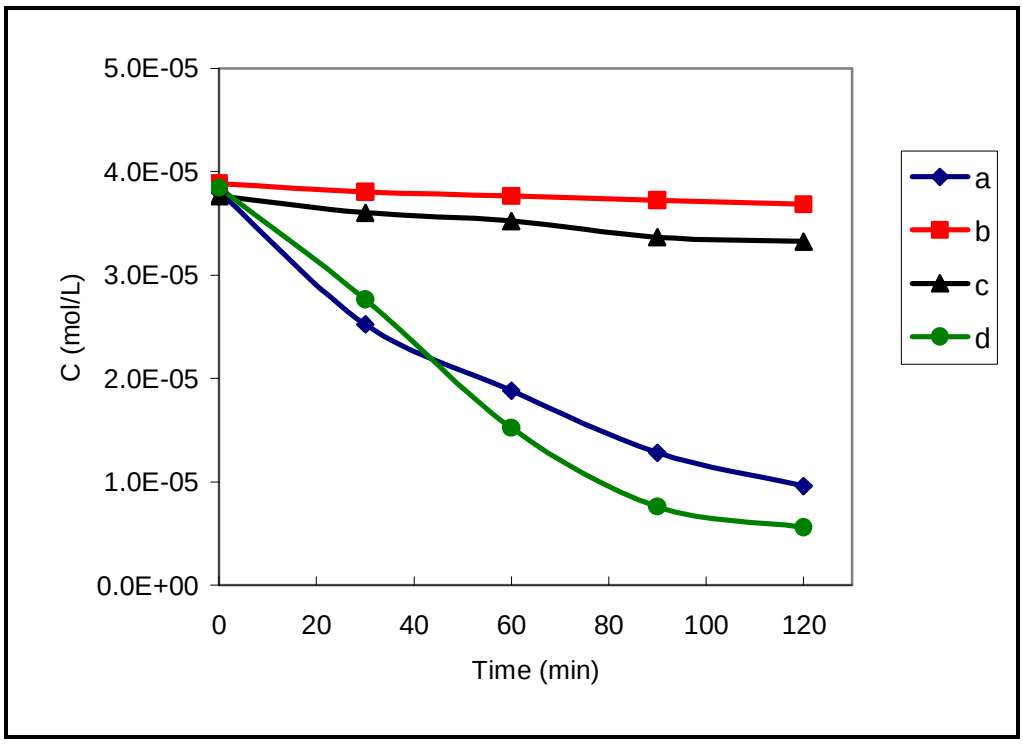

Figure 4.1: Effect of catalyst type on photo-degradation rate of Phenazopyridine (neutral suspension, 50.0 ml suspension, 10.0 ppm) under solar simulator radiation (0.0212 W/cm^2) at room temperature. Nominal catalyst amounts are: **a**) 2.0 g Sand/TiO_2/CdS (contains ~0.1g TiO_2/CdS),

b) 2.0 g Sand/TiO_2 (contains ~0.1 g TiO_2) **c**) 0.1g TiO_2, **d**) 0.1g TiO_2/CdS. Turnover number (and quantum yield) values are: 0.00077 ($2.55X10^{-4}$); 0.000048 ($1.59X10^{-5}$); 0.0000944 ($3.13X10^{-5}$) and 0.000929 ($3.08X10^{-4}$) respectively.

In the absence of sensitizers, excitation of TiO_2 occurs in the UV region, whereas the sensitizer is excited in the visible. The suggested mechanism for CdS sensitization TiO_2 under visible light has been discussed before in Scheme (3.1).

Supporting naked TiO_2 onto sand failed to enhance its efficiency, as shown in Figure (4.1). Sand also failed to enhance the catalytic efficiency of TiO_2/CdS. The Sand/TiO_2/CdS system was slightly less efficient than TiO_2/CdS. This is presumably due to the role of the support to screen the catalyst active sites away from incident light. On the other hand, the support made recovery of the catalyst system easy by simple filtration. Thus, the **Sand/TiO_2/CdS** system has an edge over other catalyst systems in being easy to recover.

4.3.3 Kinetic Study:

Kinetic study on system TiO_2/CdS was conducted. The kinetics resembled earlier results of solar driven degradation processes [3, 17]. Based on initial rate calculations, Figure (4.2) indicates that the order of the reaction rate was 0.5 with respect to nominal concentration of TiO_2/CdS. The non-linear dependence of rate on nominal catalyst concentration is presumably due to the tendency of solid catalyst particles to screen incident light. Similar observations are reported [3, 17]. Turnover number values, measured after

60 min, showed systematic decrease as catalyst concentration was increased, within the experimental conditions. This is another evidence of light screening effect. Quantum yield values, measured after 60 minutes, slightly increased with higher concentrations.

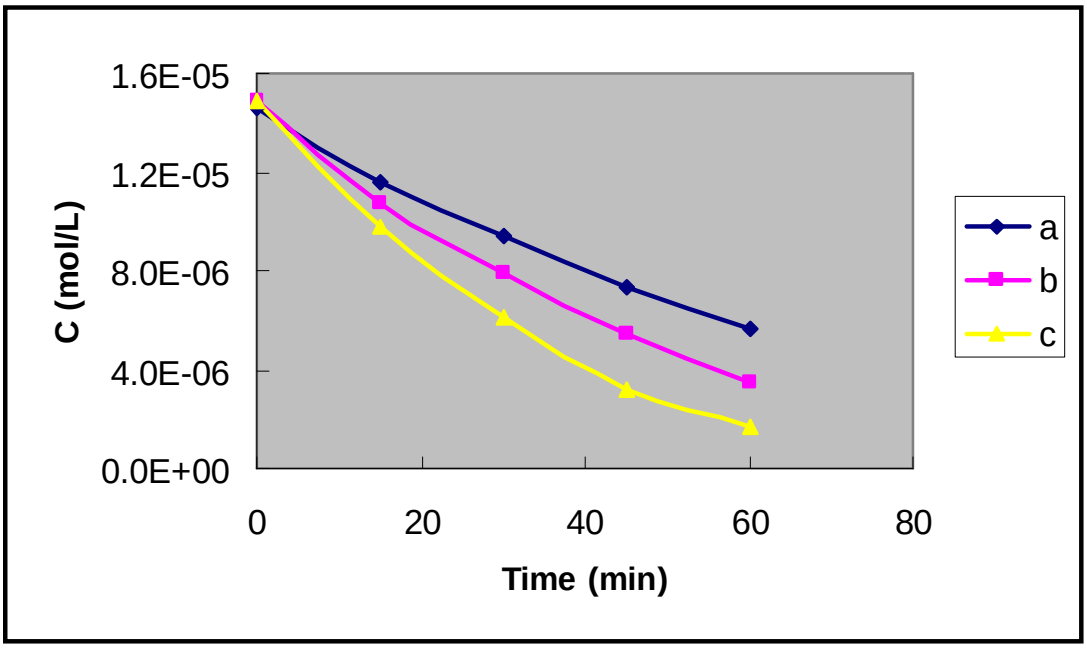

Figure 4.2: Effect of TiO_2/CdS nominal amount on photo-degradation of Phenazopyridine (neutral suspension, 50 ml of 5 ppm Phenazopyridine), under solar simulator (0.0212 W/cm^2) at room temperature using TiO_2/CdS a) 0.05 g **b**) 0.1 g **c**) 0.15 g. Turnover number (and quantum number) values are: 0.000711 (11.74 X 10^{-5}), 0.000456 (15.11 X10^{-5}) and 0.000353(17.54X10^{-5}) respectively. n = 0.51

4.3.3.1 Effect of Contaminant Concentration:

Effect of contaminant concentration or reaction rate was studied, as shown in Figure (4.3). The reaction was slower with higher contaminant concentrations. Turnover number and quantum yield values were decreased with higher concentrations. These behaviors are not unexpected. Literature showed that photo-degradation is independent of the contaminant

concentration, and in some cases, the rate is lowered with increased initial concentration [3]. Different explanations are proposed, all of which rely on the adsorption of contaminant molecules on the solid surface in a Langmuire Hinshelwood model. One acceptable explanation is the fact that at higher contaminant concentration, the contaminant molecules may compete with the adsorbed intermediates and inhibit degradation [3, 14], other explanation is the poor penetration of visible light into lowered transparency concentrated dye solution, as discussed in Chapter three.

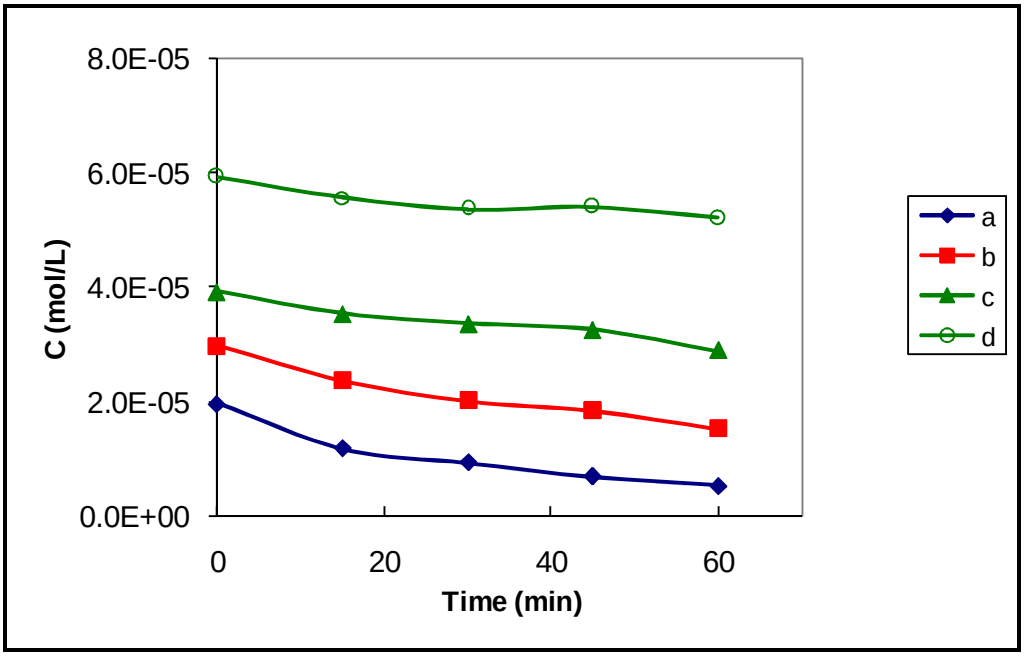

Figure 4.3: Effect of Phenazopyridine concentration or rate of degradation using TiO_2/CdS (0.1 g) in 50 ml neutral suspension at room temperature under solar simulator (0.0212 W/cm^2). Phenazopyridine concentrations are: a) 5 ppm b)7.5 ppm c) 10 ppm d) 15 ppm. Turnover number (and quantum yield) values are: 0.000577 (0.000191), 0.000577(0.000191), 0.000418 (0.000138) and 0.0002884 (0.0000956), respectively.

4.3.3.2 Effect of Temperature:

The effect of temperature on photo-degradation rate was studied at 30, 45 and 66 C^o, the photo-degradation curves are presented in Figure (4.4). The reaction rate was not affected by temperature, as shown in Figure (4.4). The activation energy was less than 4 kJ/mol. This behavior resembles earlier results for different contaminant degradation systems [17]. The independence of reaction rate of temperature is well justified in literature [3, 14, 33].

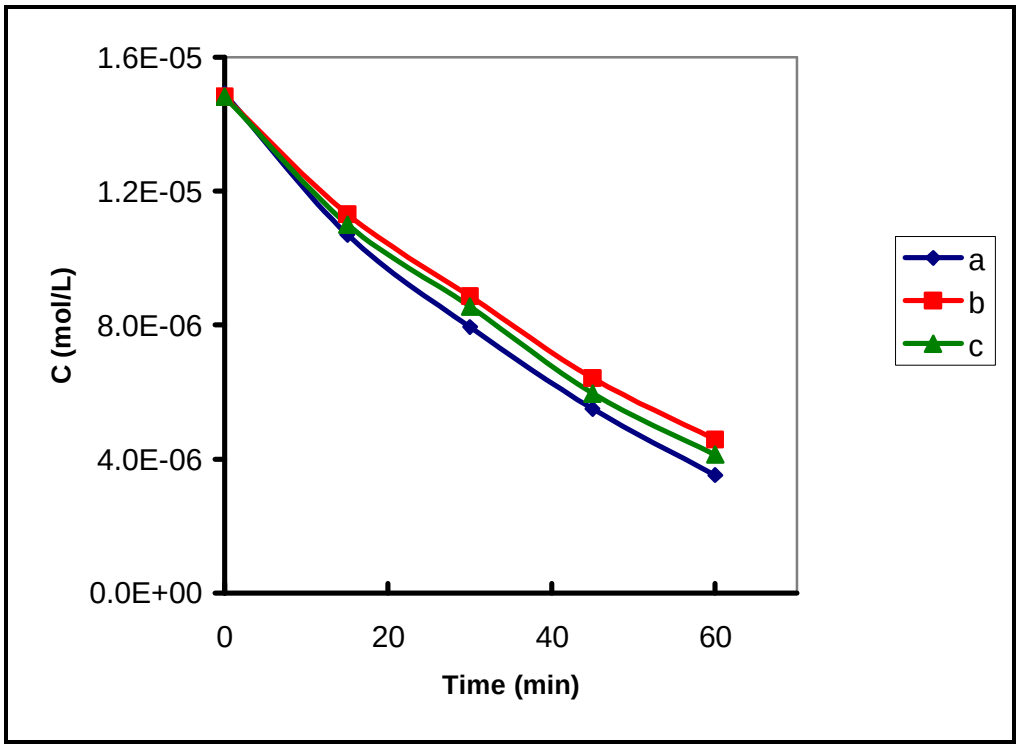

Figure 4.4: Temperature effect on photo-degradation rate of Phenazopyridine (neutral suspension, 50 ml, 5 ppm) under solar simulator using TiO_2/CdS (0.1 g), at different temperatures: **a**) 30°C **b**) 45°C **c**) 60°C.

4.3.3.3 Effect of pH:

Effect of pH on reaction rate was investigated, the photo-degration rate was studied at different pH values, it was studied at pH 4, 7,8 and 9.5. Figure (4.5) shows that the activity was relatively not much affected with pH changes within the range 4-9, with slightly higher activity observed at pH 9. The fact that higher pH gave higher efficiency could partly be explained by lower leaching tendency of CdS from TiO_2/CdS, as will be discussed later, also the presence of OH^- may be a source of $OH^\bullet$ formation which is a photo-degradation route.

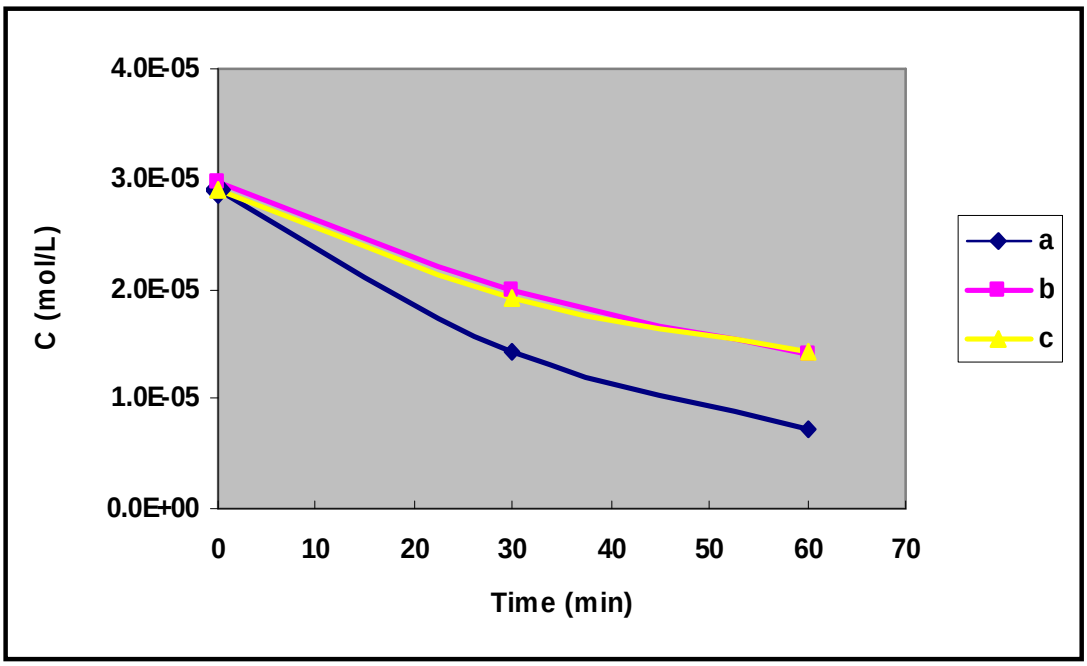

Figure 4.5: Effect of pH on photo-degradation rate of Phenazopyridine (50 ml, 10 ppm) using Sand/TiO_2/CdS (2.0 g) at room temperature. Values of pH are: **a**) 9.5 **b**) 4 **c**) 7.8 . Turnover number (and quantum yield) values are: 0.000868 (0.000287), 0.000623 (0.0002066) and 0.0005865 (0.0001945) respectively.

4.3.4 Leaching out Studies:

The tendency of system TiO_2/CdS to leach out Cd^{2+} ions under photo-degradation of Phenazopyridine in the visible region was studied at different pH values. Figure 4.6 shows that Cd^{2+} continued to leach off compound TiO_2/CdS**,** with time. Such results were confirmed by voltametry. Leaching out occurred at different pH values, but slightly lower at higher pH. This is consistent with the higher catalyst efficiency at higher pH discussed above. This is consistent with increasing CdS solubility at lower pH values due to resultant H_2S that escapes away as dictated by ***leChatelier's principle***.

CdS leaching out is a serious concern. Firstly, because catalytic activity is lowered as a result of leaching, *viz*. the CdS is removed and less TiO_2 sensitization occurs. Secondly, the Cd^{2+} ions are hazardous in nature and are good examples of hazardous materials in water. Therefore, the wisdom behind using CdS sensitizers for water purification is questionable. Research is still being conducted on CdS-sensitized TiO_2 for water purification [4, 6-12; 33-42]. It should be noted herein that unless such leaching out is completely prevented; the whole TiO_2/CdS based water purification processes should be terminated. Unfortunately, very little efforts, if any, have been made to prevent such leaching tendency.

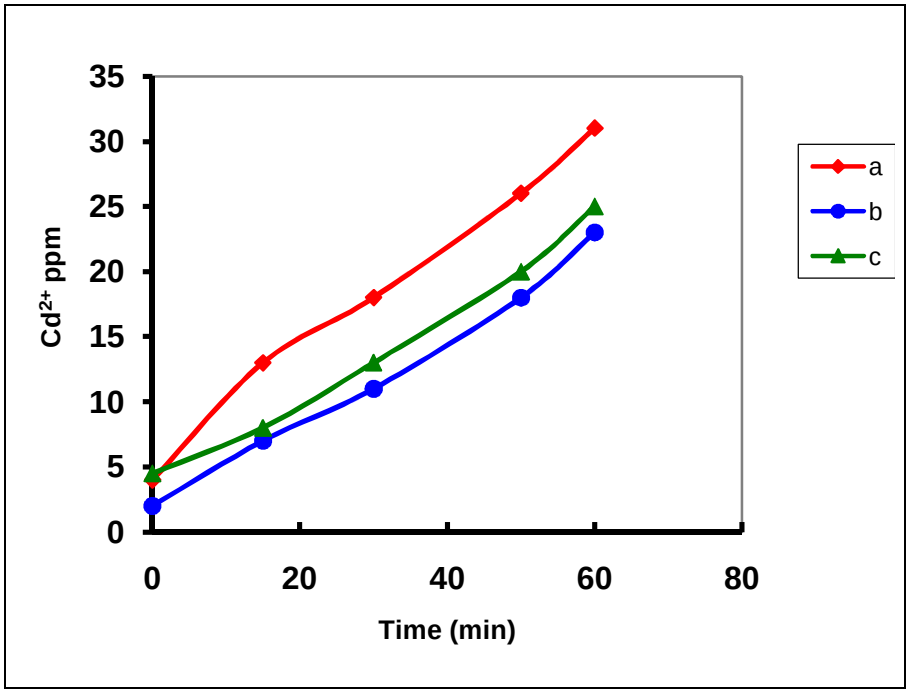

Figure 4.6: Reaction profiles showing Cd^{2+} ion concentrations leaching out of non-annealed TiO_2/CdS (0.1 g) under Phenazopyridine degradation conditions under solar simulator (0.0212 W/cm^2, room temperature, in 70 ml suspension of 5 ppm contaminant) at different pH values: **a**) 3.5 **b**) 9 **c**) neutral. Percentage values of Cd^{2+} leaching out are: 89, 66% and 71% respectively.

Pre-annealing of TiO_2/CdS did not prevent leaching out. Figure 4.7 shows that Cd^{2+} ions continued to leach out of pre-annealed TiO_2/CdS under photo-degradation of Phenazopyridine. Leaching out occurred at different pH values. This indicates that pre-annealing, which is commonly practiced in CdS-sensitization strategies, is not a solution for Cd^{2+} leaching out.

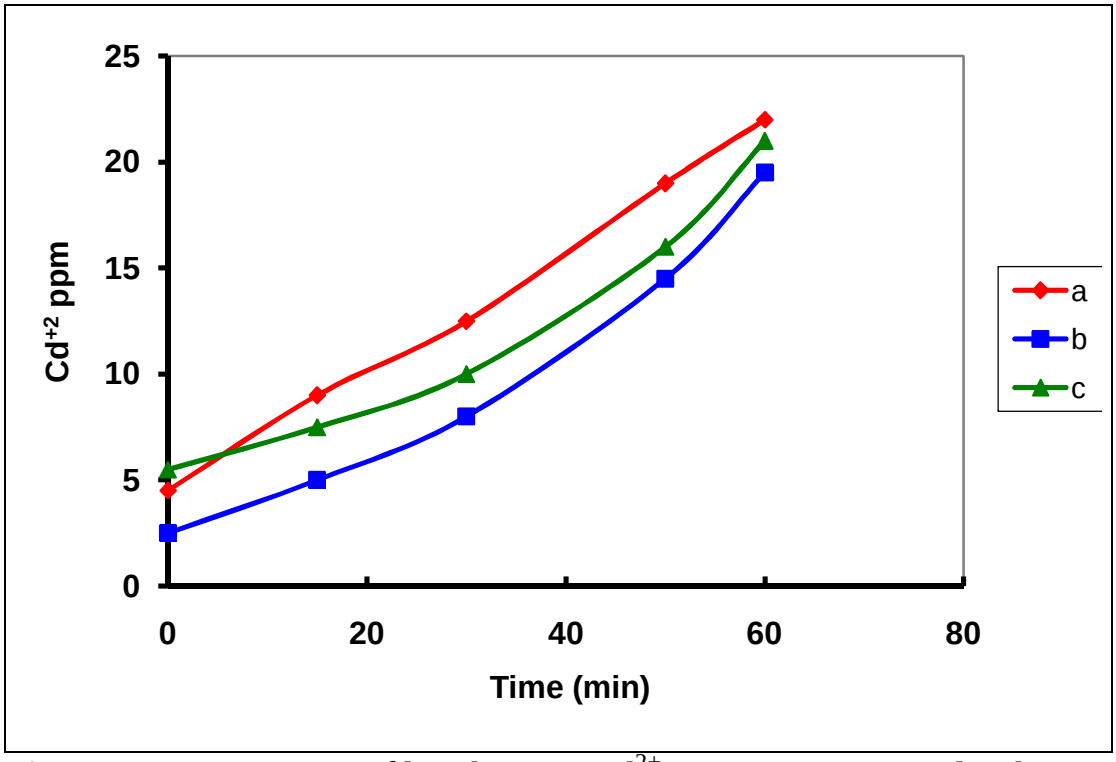

Figure 4.7: Reaction profiles showing Cd^{2+} ion concentrations leaching out of pre-annealed TiO_2/CdS (0.1 g) under Phenazopyridine degradation conditions under solar simulator (0.0212 W/cm^2, room temperature, in 70 ml suspension of 5 ppm Phenazopyridine) at different pH values: a) 3.5 b) 9 c) neutral. Percentage values of Cd^{2+} leaching out are: 63 %, 56 % and 60 %, respectively.

To prevent Cd^{2+} ion leaching, the system TiO_2/CdS was supported onto stable solid sand support, to yield Sand/TiO_2/CdS. The Cd^{2+} ions continued to leach out of Sand/TiO_2/CdS under degradation conditions at different pH values, as shown in Figure (4.8). Annealing the system Sand/TiO_2/CdS did not make a significant difference and the Cd^{2+} ions continued to leach out, as shown in Figure (4.9).

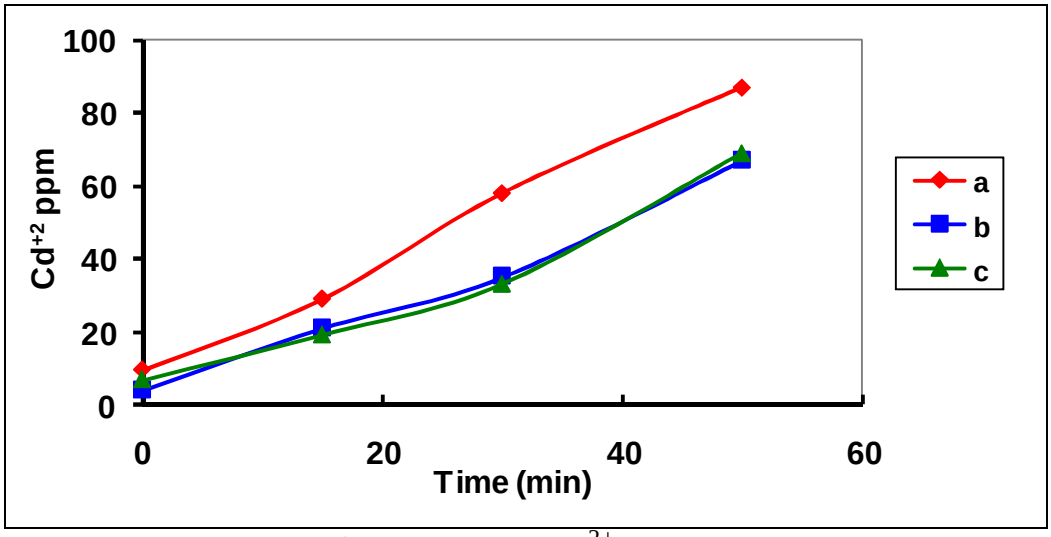

Figure 4.8: Reaction profiles showing Cd^{2+} ion concentrations leaching out of non-annealed Sand/TiO_2/CdS (1.0 g) under Methyl Orange degradation conditions under solar simulator (0.0212 W/cm^2, room temperature, in 70 ml suspension of 5 ppm Methyl Orange) at different pH values: **a**) 3.5, **b**) 9, and **c**) neutral. Values of leaching out percentage for Cd^{2+} are: 97 %, and 74% and 77 %, respectively.

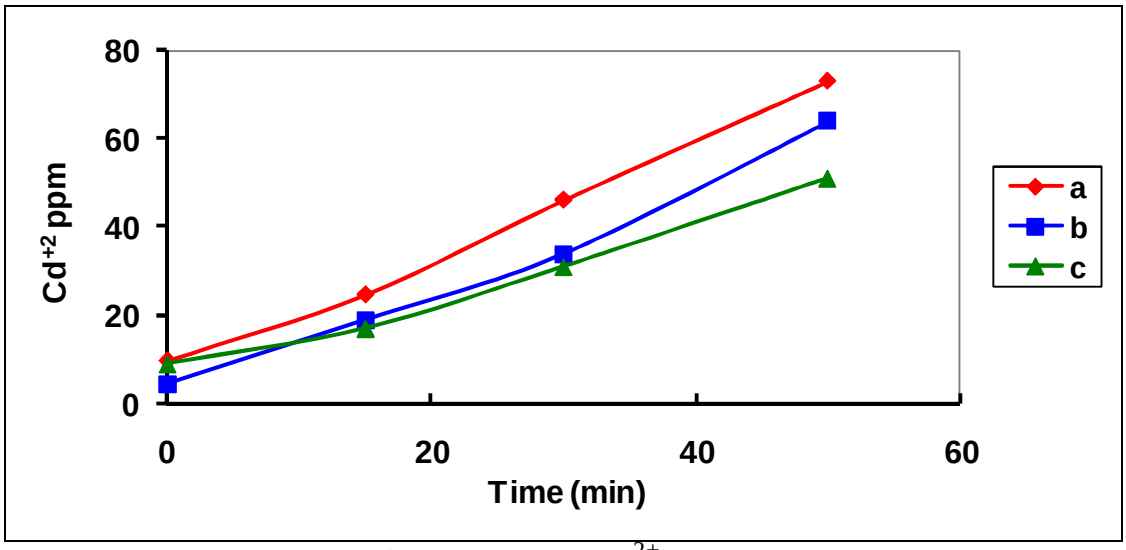

Figure 4.9: Reaction profiles showing Cd^{2+} ion concentrations leaching out of pre-annealed Sand/TiO_2/CdS (1.0 g) under Phenazopyridine degradation conditions under solar simulator (0.0212 W/cm^2, room temperature, in 70 ml suspension of 5 ppm Phenazopyridine) at different pH values: **a**) 3.5, **b**) 9 and **c**) neutral. Values of leaching out percentage for Cd^{2+} are: **a**) 81 % **b**) 71% **c**) 57 %, respectively.

4.3.5 Recovery and Reuse Studies:

The results indicate that sand support is not able to prevent Cd^{2+} ion leaching. This is a serious matter to consider. Despite that, the sand support made it easier to recover the catalyst system, for re-use purposes, by simple filtration. Such a process is not feasible for the system TiO_2/CdS, which demanded more complicated centrifugation processes. Supporting naked TiO_2 particles onto insoluble supports has been widely reported in literature [3, 8, 13-14, 17, 43-66]. However, only a few reports are known for supporting the combined TiO_2/Dye degradation catalysts onto insoluble supports [14, 17].

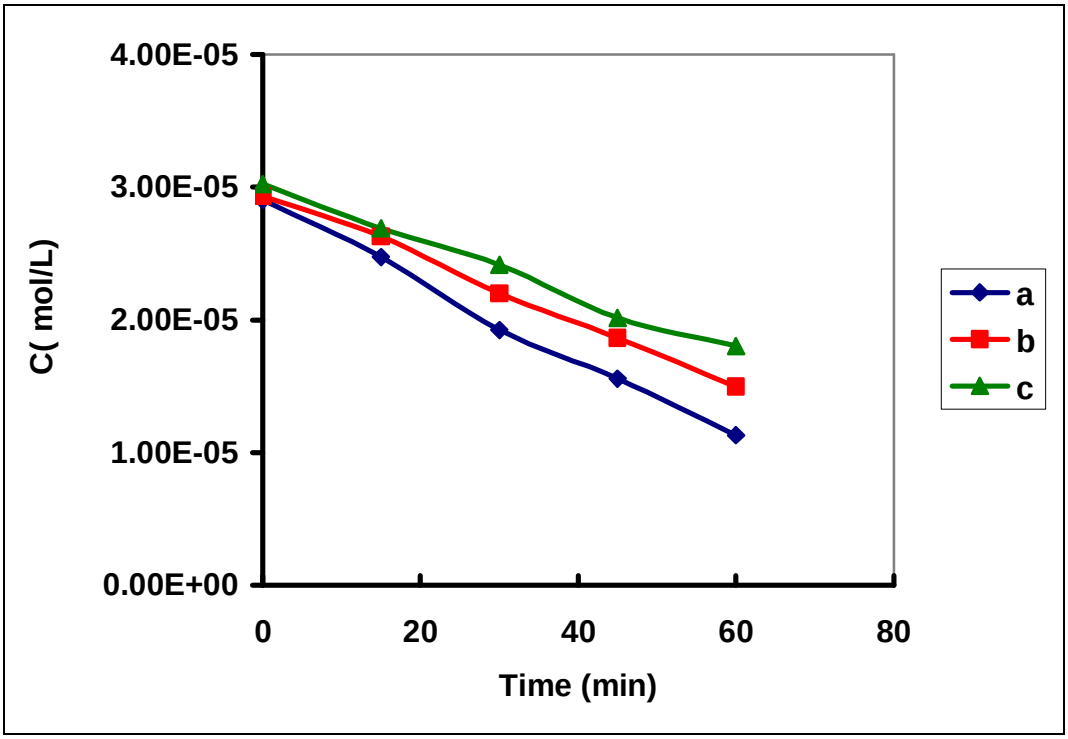

Figure 4.10: Effect of Sand/TiO_2/CdS (1.0 g, containing 1.9% mass CdS) catalyst recovery and reuse on photo-degradation rate of Phenazopyridine (neutral 50 ml suspension, 10 ppm) at room temperature. **a**) Fresh sample, **b**) 2nd use and **c**) 3rd use.

While keeping an eye on leaching out tendency, special samples of Sand/TiO_2/CdS, with high CdS content were prepared. The samples were used in photo-degradation of Phenazopyridine under visible light using neutral solutions. After reaction cessation, the catalyst system was recovered easily by simple filtration. Figure (4.10) shows that the system loses it efficiency on reuse. Despite the high concentrations of CdS used, its high tendency to leach out causes efficiency lowering on re-use.

4.4 Conclusion:

Despite the ability of CdS to sensitize TiO_2 efficiently in Phenazopyridine degradation under visible light, it decomposes readily and leaches out hazardous Cd^{2+} ions in water. Annealing the TiO_2/CdS system did not prevent leaching out. The supported Sand/TiO_2/CdS catalyst system has the advantage of being easy to recover, but the sand support failed to completely prevent Cd^{2+} ion leaching out. Unless the tendency of CdS to leach out Cd^{2+} ions is completely prevented, its application as sensitizer should be avoided.

References:

1. O. Carp, C. L. Huisman and A. Reller, Photoinduced reactivity of titanium dioxide, *Prog. Solid State Ch.,* **32** (2004) 33–177.

2. S. K. Kansal, M. Singh and D. Sud, Studies on photo-degradation of two commercial dyes in aqueous phase using different photocatalysts, *J. Hazard. Mater*., **141** (2007) 581–590.

3. Y. Bessekhouad, D. Robert and J. V. Weber, Bi_2S_3/TiO_2 and CdS/TiO_2 heterojunctions as an available configuration for photocatalytic degradation of organic pollutant, *J. Photochem. Photobiol. A*, **163** (2004) 569–580.

4. Y. Bessekhouad, N. Chaoui, M. Trzpit, N. Ghazzal, D. Robert and J.V. Weber, UV–vis versus visible degradation of Acid Orange II in a coupled CdS/TiO_2 semiconductors suspension, *J. Photochem. Photobiol. A*, **183** (2006) 218–224.

5. D. Robert, Photosensitization of TiO_2 by M_xO_y and M_xS_y nanoparticles for heterogeneous photocatalysis applications, *Catal. Today*, **122** (2007) 20–26.

6. H. Fuji, M. Ohtaki, K. Eguchi and H.Arai,; *J. Mol. Catal. A: Chem.,* **129** (1998) 61–68.

7. N. Serpone, P. Marathamuthu, P. Pichat, Pelizzetti, E. and H. Hidaka,; *J. Photochem. Photobiol. A,* **85** (1995) 247.

8. **X.** Hanling, **L.** Jianwei, **G.** Lingmei, Photocatalytic degradation of methyl thionine chloride in aqueous solution over nanometer (CdS/TiO_2)/MCM-41, *J. Wuhan Univ. Technol,* **21** (2006) 19-23.

9. P. Reeves[†],; R. Ohlhausen[†], D. Sloan[†], K. Pamplin[†], T. Scoggins[†], C. Clark[†], B. Hutchinson and[‡] D. Green , Photocatalytic destruction of organic dyes in aqueous TiO_2 suspensions using concentrated simulated and natural solar energy, *Sol. Energy*, **48 (**1992) 413-420.

10. H. Greijer[a, b], L. Karlson[b], S.-E. Lindquist and[a] A. Hagfeldt, Environmental aspects of electricity generation from a nanocrystalline dye sensitized solar cell system, *Renew Energ.*, **23 (**2001) 27-39.

11. H. S. Hilal, L. Z. Majjad, N. Zaatar and A. El-Hamouz, Dye-effect in TiO_2 catalyzed contaminant photo-degradation: Sensitization vs. charge-transfer formalism, *Solid State Sci.*, **9** (2007) 9-15.

12. A. H. Zyoud and H. S. Hilal, Sand-supported CdS-sensitized TiO_2 particles in photo-driven water purification: Assessment of efficiency, stability and recovery future perspectives; *a chapter in a book "Water Purification", Novascience, Newyork, in Press*, (2009).

13. S. Cassaignon, M. Koelsch, J.-P. Jolivet, From $TiCl_3$ to TiO_2 nanoparticles (anatase, brookite and rutile): Thermohydrolysis and oxidation in aqueous medium, *J. Phys. Chem. Solids*, **68** (2007) 695-700**.**

14. X. Huanga and C. Pana, Large-scale synthesis of single-crystalline rutile TiO_2 nanorods via a one-step solution route, *J. Cryst. Growth*, **306** (2007) 117–122.

15. Z. Ambrus, N. Balázs, T. Alapi, G. Wittmann, P. Sipos, A. Dombi, K. Mogyorósi, Synthesis, structure and photocatalytic properties of Fe(III)-doped TiO_2 prepared from $TiCl_3$, *Appl. Catal. B: Environ.*, **81** (2008) 27-37.

16. H.O. Finklea, in: H. O. Finklea (Ed.), Semiconductors Electrodes, *Elsevier, Amsterdam*, (1988) 44-47.

17. D. Shoemaker, C. Garland and J. Nibler, Experiments in Physical Chemistry, 5th edition, *Mc Graw-Hill, Inc., N.Y.*, (1989).

18. H.S. Hilal, L.Z. Majjad, N. Zaatar and A. El-Hamouz1, Dye-effect in TiO_2 catalyzed contaminant photo-degradation: Sensitization vs. charge-transfer formalism, *Solid State Sci.*, **9** (2007) 9-1.

19. The Book of Photon Tools, Oriel Instruments, *Stratford, CT, USA*, pp. 44, 50 (Manual).

20. Thermo Oriel: 500 W Xenon/Mercury (Xenon) ARC Lamp Power *Supply Model 68911* (Manual).

21. B. J. Clark, T. Frost and M. A. Russell, U.V. Spectroscopy, *Chapman & Hall, London*, (1993) 18-21.

22. S. S. Nath, D. Chakdar, G. Gope and D. K. Avasthi, Characterization of CdS and ZnS quantum dots prepared via a chemical method on SBR latex, *J. nanotech.*, **4** (2008).

23. J. M. Hermann, Heterogeneous photocatalysis: fundamentals and applications to the removal of various types of aqueous pollutants, *Catal. Today*, **53** (1999) 115-129.

24. N. Guettai, H. A. Amar, Photocatalytic oxidation of Methyl Orange in presence of titanium dioxide in aqueous suspension. Part I: Parametric study, *Desalination and the Environment. Conference, Santa Margherita Ligure , ITALIE* (22/05/2005) , **185** (2005) 427-437.

25. L. GE, M. XU and H. FANG, Photo-catalytic degradation of Methyl Orange and formaldehyde by Ag/$InVO_4$-TiO_2 thin films under visible-light irradiation, *J. Mol. Catal. A: Chem.*, **258** (2006) 68-76.

26. Y. Xu, Z. Chen, Photo-oxidation of Chlorophenols and Methyl Orange with Visible Light in the Presence of Copper Phthalocyaninesulfonate, *Chem. Lett.* **32** (2003) 592-593.

27. S. Xu, W. Shangguan, J. Yuan, J.Shi and M.Chen; Preparations and photocatalytic degradation of Methyl Orange in water on magnetically separable $Bi_{12}TiO_{20}$ supported on nickel ferrite, *Sci. Technol. Adv. Mat.* **8** (2007) 40–46.

28. C. Huang, D. H. Chen and K. Li, Photocatalytic oxidation of butyraldehyde over titania in air: by-product identification and reaction pathways, *Chem. Eng. Commun.*, **190** (2003) 373-392.

29. L. Spanhel, H. Weller, A. Henglein, Photochemistry of Semiconductor Colloids: Electron Injection from Illuminated CdS into Attached TiO_2 and ZnO Particles, *J. Am. Chem. Soc*. **109** (1987) 6632 – 6635.

30. M. G. Kang, H. E. Han and K. J. Kim, Enhanced photodecomposition of 4-chloro- phenol in aqueous solution by deposition of CdS on TiO_2, *J. Photochem. Photobiol. A*, **125** (1999) 119.

31. Sesha S Srinivasan, Jeremy Wade, Elias K Stefanakos, Visible Light Photocatalysis via Nano-Composite CdS/TiO_2 Materials, *J. Nanomat.*, **2006** (2006) 24.

32. M. A. Jhonsi, A. Kathiravan, R. Renganathan, Interaction between certain porphyrins and CdS colloids: A steady state and time resolved fluorescence quenching study, *Spectrochim. Acta A,* **71** (2008) 1507-1511**.**

33. P. Pizarro, C. Guillard, N. Perol and J. M. Herrmann,. Photocatalytic degradation of imazapyr in water: Comparison of activities of different supported and unsupported TiO_2-based catalysts, *Catal. Today,* **101**.(2005) 211-218.

34. M. C. Hidalgo and D. Bahnemann, Highly photoactive supported TiO_2 prepared by thermal hydrolysis of $TiOSO_4$: Optimisation of the method and comparison with other synthetic routes, *Appl. Catal. B, Environ.*, **61** (2005) 259-266.

35. M. J. Lo`pez-Munˇoz, R Grieken, J. Aguado and J. Marugan, Role of the support on the activity of -supported TiO_2 photocatalysts: Structure of the TiO_2/SBA-15 photocatalysts, *Catal. Today*. **101** (2005) 227.

36. M. Hirano and K.Ota, Preparation of photoactive anatase-type TiO_2/Sand gel by direct loading anatase-type TiO_2 nanoparticles in acidic aqueous solutions by thermal hydrolysis, *J. Mater. Sci.*, **39** (2004) 1841.

37. M. Hirano, K. Ota, M. Inagaki and H. Iwata, Hydrothermal Synthesis of TiO_2/SiO_2 Composite Nanoparticles and Their Photocatalytic Performances, *J. Ceram. Soc. Jpn.*, **112** (2004) 143-148.

38. J. Aguado, R. Grieken and M. J. Lo`pez-Munˇoz, Maruga´n, Removal of cyanides in wastewater by supported TiO_2-based photocatalysts, *Catal. Today,* **75** (2002) 95-102.

39. J. N. Najm, V. L. Snoeyink, M. T. Suidan, C. H. Lee and Z. Richard, Effect of Particle Size and Background Organics on the

Adsorption Efficiency of PAC, *J. Am. Water. Works Ass.* **82** (1990) 65-72.

40. P. Periyat, K. V. Baiju, P. Mukundan, P. K. Pillai and K. G. K. Warrier, High temperature stable mesoporous anatase TiO_2 photocatalyst achieved by addition, *App. Catal. A: Gen.*, **349** (2008) 13-19.

41. J. Marugán, R.Grieken, A. E. Cassano and O. M. Alfano, Scaling-up of slurry reactors for the photocatalytic oxidation of cyanide with TiO_2 and Sand-supported TiO_2 suspensions, *Catal. Today*, **144** (2009) 87-93.

42. J. W. Lee, M. R. Othman, Y. Eom, T. G. Lee, W. S. Kim and J. Kim, The effects of sonification and TiO_2 deposition on the micro-characteristics of the thermally treated SiO_2/TiO_2 spherical core–shell particles for photo-catalysis of Methyl Orange, *Micropor. Mesopor. Mat.*, **116** (2008) 561-568.

43. A. Bhattacharyya, S. Kawi and M. B. Ray, Photocatalytic degradation of orange II by TiO_2 catalysts supported on adsorbents, *Catal. Today*, **98** (2004) 431-439.

44. Y. Jiang[a, b], Y. Sun[a, ,], H. Liu[a, b], F. Zhu and H. Yin, Solar photocatalytic decolorization of C.I. Basic Blue 41 in an aqueous suspension of TiO_2–ZnO, *Dyes and Pigments*, **78** (2008) 77-83.

45. Y. Li, X. Li, J. Li and J. Yin, Photocatalytic degradation of Methyl Orange by TiO_2-coated activated carbon and kinetic study, *Water Res.*, **40** (2006) 1119–1126.

46. J. Matos, J. Laine and J. Herrmann, Synergy effect in the photocatalytic degradation of phenol on a suspended mixture titania and activated carbon, *Appl. Catal. B: Environ.* **18** (1998) 281-291.

47. D. Chatterjee, S. Dasgupta and N.N.Rao, Visible light assisted photo-degradation of halocarbons on the dye modified TiO_2 surface using visible light, *Sol. Energ. Mat. Sol. C.*, **90** (2006) 1013-1020.

48. C. H. Ao and S. C. Lee, Combination effect of activated carbon with TiO_2 for the photo-degradation of binary pollutants at typical indoor air level, *J. Photochem. Photobiol. A*, **161** (2004) 131-140.

49. J. Aran˜a, J. M. Don˜a-Rodrı´guez, E. T. Rendo´n, C. Garriga i Cabo, O. Gonza´lez-Dı´az, J. A. Herrera-Melia´n, J. Pe´rez-Pen˜a, G. Colo´n and J. A. Navı´o, TiO_2 activation by using activated carbon as a support, Part I. Surface characterisation and decantability study, *Appl. Catal. B: Environ.*, **44** (2003) 161-172.

50. J. Marugan, R. van Grieken, O. M.Alfano and A. E. Cassano , Optical and physicochemical properties of Sand-supported TiO_2 photocatalysts, *AIChE J.*, **52** (2006) 2832-2843.

51. M. Nazir, J. Takasaki and H. Kumazawa, Photocatalytic degradation of gaseous ammonia and trichloroethylene over TiO_2 ultrafine powders deposited on activated carbon particles, *Chem. Eng. Commun.*, **190** (2003) 322-333

52. T. Y. Kim, Y.-H. Lee, K.-H. Park, S. J. Kim and S. Y. Cho, A study of photocatalysis of TiO_2 coated onto chitosan beads and activated carbon, *Res. Chem. Intermediat*, **31** (2005) 343–358.

53. S.-X. Liu and C.-L. Sun, Preparation and performance of photocatalytic regenerationable activated carbon prepared via sol-gel TiO_2, *J. Environ. Sci.* **18** (2006) 557-561.

54. A. Jaroenworaluck, W. Sunsaneeyametha, N. Kosachan and R. Stevens, Characteristics of Sand-coated TiO_2 and its UV absorption for sunscreen cosmetic applications; *Surf. Interface Anal.*, **38** (2006) 473-477.

55. M. S. Vohra and K. Tanaka, Photocatalytic degradation of aqueous pollutants using Sand-modified TiO_2, *Water Res.*, **37** (2003) 3992-3996.

56. C.-F.Chi, Y.-L. Lee and H.-S. Weng, A CdS-modified TiO_2 nanocrystalline photoanode for efficient hydrogen generation by visible light, *Nanotechnology*, **19** (2008) 125704.

CHAPTER 5

NATURAL DYE SENSITIZERS OF TiO_2 IN METHYL ORANGE AND PHENAZOPYRIDINE PHOTO-DEGRADATION: SCREENING STUDY USING ANTHOCYANIN DYE

5.1 Introduction:

Dyes sensitized solar cells (DSSC) have been under extensive research for more than 40 years. Conversion efficiencies between 6-10% have been reached. The history of dye sensitized solar cell started in 1972 with chlorophyll sensitized zinc oxide electrode. An efficient photovoltaic cell was discovered by O'Regan and Gratzel [1-2], based on Ru-bipyridine dyes. The cell showed high efficiency with power conversions up to 10%. The idea of sensitizing the semiconductor to be excited under solar light was applied in water purification techniques [3]. As shown in earlier chapters, CdS dye is widely studied as TiO_2 sensitizer [4]. Most of synthetic dyes, like ruthenium and CdS are hazardous and costly. This makes synthetic dyes un favored in water purification. There remains the need for alternative photosensitizers in TiO_2-based photo-degradation of water contaminants. Therefore, finding safe, low cost and readily available sensitizers still remains a scientific challenge [5-6].

An alternative to synthetic dyes is to use natural dyes. In this work we present our screening study on one widely spread natural dye to be studied. Anthocyanin was a chosen here because it is available, easy to extract, applicable without further complicated purification and a non toxic natural dye that is commonly used as food additive. Scheme (5.1) shows the structural formula for anthocyanin molecule. Anthocyanins are responsible for several colors in the red–blue range depending on pH value. This pigment occurs in fruits, flowers and plant leaves. Efforts have been made by researchers to utilize natural dyes as sensitizers in solar cells [5-7], and to a lesser extent in water purification. Examples of natural dyes used in

solar cells are chlorophyll derivatives and natural porphyrins [5], anthocyanins [9]. Only the one layer of adsorbed dye molecules would attach to the semiconductor particle surface. The light harvesting efficiency of a single dye monolayer is thus expected to be small. Fortunately, that is not the case, because the effective surface area in powder semiconducting material is relatively large enough to compensate. Thus, sensitization is more efficient in nanoparticle semiconductors than in bulk counterparts.

In this work we present a preliminary screening study using anthocyanin as sensitizer for TiO_2 particles. The objective is to introduce a new area in which more detailed study be conducted on sensitization of TiO_2 with natural dyes.

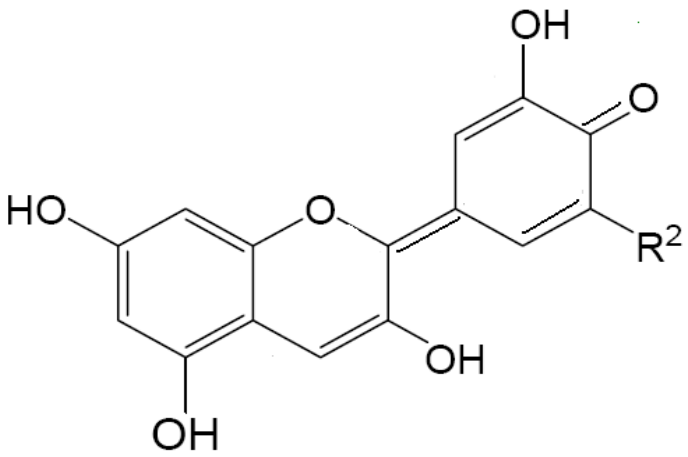

Scheme 5.1: Structural formula for anthocyanin.

In this work we use a natural dye (Anthocyanin) extracted from Karkade Plant flowers. The flower is available at local markets. It is commonly used as beverage, since it is rich with anthocyanins.

5.2 Theoretical Background:

In natural dye sensitization, the process involves excitation of dye molecules from ground state to an excited state by the absorption of a photon. In molecular terminology, an electron jumps from HOMO (Highest Occupied Molecular Orbital) to LUMO (Lowest Unoccupied Molecular Orbital). This is followed by relaxation through electron loss to the TiO_2 conduction band. The dye is then left as a surface-adsorbed cation. The dye cation conveys its positive charge to a redox species or an organic contaminant molecule. Spontaneously the electrons in the conduction band of the semiconductor will reduce species like O_2. The energy level of the LUMO must be higher (more negative) than the conduction band edge of the TiO_2, so that an electron can be injected during the relaxation process. The HOMO must be lower (more positive) than the reduction potential of the organic contaminant. In terms of photo-excitation, the HOMO-LUMO gap resembles band gap semiconductor energetic [10]. On the other hand, dye molecules may work as charge transfer mediators under UV irradiation. Elongation of time of electron-hole separation, which may lead to increasing in the efficiency of UV photodegradation, is also facilitated by dyes.

Anthocyanin has a band gap 2.3 eV (~ 530), which may suit such necessary energetic features. Moreover, anthocyanin has carbonyl and hydroxyl groups. Such groups may bind to the surface of TiO_2 particles, Scheme (5.2), making a bridge for electron transfer from the excited anthocyanin molecule to the conduction band of TiO_2 [7].

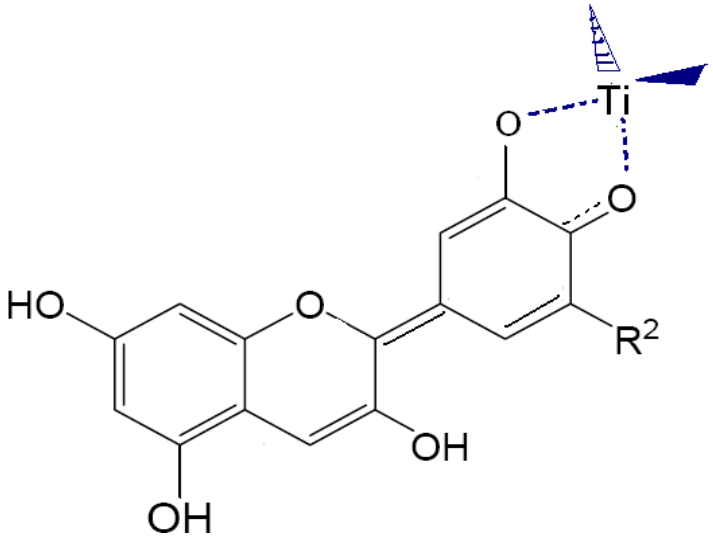

Scheme 5.2: Anthocyanin molecule attached to TiO_2 surface.

It is thus anticipated that supporting anthocyanin, and other suitable natural dyes, onto TiO_2 would sensitize it to visible light in water photo-degradation of water contaminants. Anthocyanin Scheme (5.1) was used here as an example of suitable natural dyes. Anthocyanin was extracted from *Hibiscus* [Karkade] flowers *vide infra*. Most fruits and leaves contain natural dyes, but not all are suitable for sensitizing TiO_2. One requirement for the dye is the presence of several carbonyl or hydroxyl groups capable of chelation to the Ti(IV) site on the TiO_2 surface [14]. For this reason, anthocyanin was chosen here.

5.3 Experimental:

5.3.1 Materials Preparation:

All common solvents and reagents used were of analytical grade and were purchased from Aldrich, Riedel or Merck.

5.3.1.1 Extraction of Anthocyanin Pigment:

The Karkade dried flowers were crushed in a juice mixer. The finely Karkade ground powder (10 g) was soaked in a 250 ml Erlenmeyer flask with 100 ml of ethanol. The solution was magnetically stirred gently at ~60 C^o for 20 minutes. The solution was then cooled for 20 minutes, and filtered. UV-vis spectra were measured for the extracted pigment in solution. The solution was transferred into a dark color glass bottle and stored in refrigerator for further applications.

5.3.1.2 Preparation of TiO_2/Anthocyanin:

Rutile TiO_2 (10 g) with particle size less than 5 µm were refluxed for half an hour with 30 ml of extracted anthocyanin ethanolic solution and 30 ml deionized distilled water. The mixture was then left to cool. It was chilled in ice for 15 minutes. The TiO_2/Anthocyanin was suction-filtered through sintered glass, and the solid powder was collected and washed with cold water. The solid was then dried in air and kept in dark for further use. Adsorption of anthocyanin on the surface of TiO_2 is a rapid reaction, displacing an OH groups at the Ti(IV) site that combines with a proton donated by the anthocyanin moiety. The reaction is accompanied with forming one molecule of H_2O (condensation reaction). A stable complex is thus formed (Scheme 5.2) [15-16].

5.3.1.3 Preparation of AC/TiO_2/Anthocyanin:

The preparation was a two-step process, starting first with AC/TiO_2 preparation, then with adsorption of anthocyanin on AC/TiO_2 surface. Commercial rutile structure TiO_2 (20 g) and 4 g Activated Carbon (AC) were mixed continuously in a container with 40 ml of water for an hour. The mixture was then suction-filtered. The composite solid of AC/TiO_2 was dried at 130°C for 2 hrs. The ratio of TiO_2:AC in the composite mixture was 10:2. The second step involved AC/TiO_2/Anthocyanin. Composite mixture AC/TiO_2 (10.0 g) was magnetically stirred in 20 ml of ethanolic anthocyanin solution for 1 hr, before suction-filtration through sintered glass. The solid was left to dry in the air for two days and was kept in the dark for further use.

5.3.1.4 Stock Solution Preparation:

The following stock solutions were needed for photocatalytic experiments:

1) Two stock solutions (1000 ppm each) for two contaminants were prepared. In each case 1.00 g the contaminant (Methyl Orange or Phenazopyridine) was dissolved in distilled water, and the resulting solution was then diluted to 1.0 L with distilled water.
2) Dilute solutions (0.05 M) for both HCl and NaOH were prepared. The solutions were used to adjust the acidity and basicity of the catalytic reaction mixtures as desired.

5.3.2 Characterization of TiO_2/Anthocyanin System:

5.3.2.1 Electronic Absorption Spectra:

The absorption spectrum for extracted anthocyanin in ethanol is shown in Figure (5.1). The spectrum shows an absorption at λ_{max} = 540 nm, which is consistent with literature spectrum of anthocyanin [24].

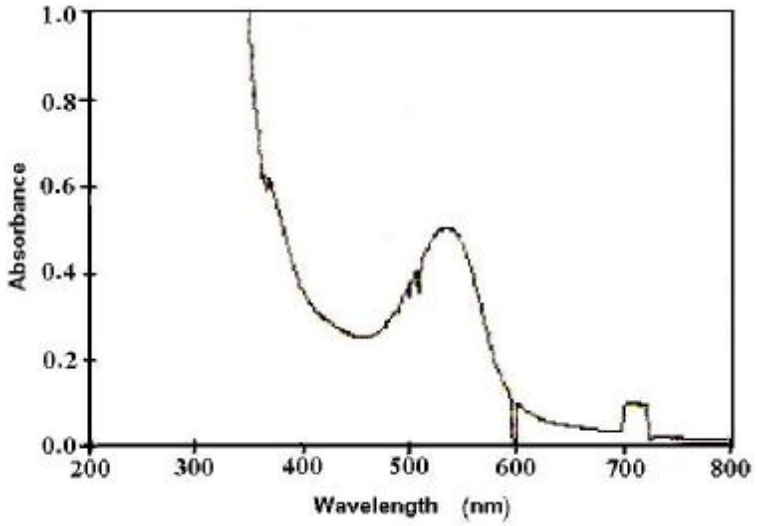

Figure 5.1: Anthocyanin UV-vis spectrum measured in ethanol.

UV-Visible electron absorption spectra were measured for the TiO_2/Anthocyanin particles suspended in toluene. Figure (5.2) shows absorption band at λ_{max} = 550 nm for anthocyanin. The other strong band starting at ~400 nm is assigned for TiO_2. The spectra show evidence of anthocyanin on the TiO_2 particles.

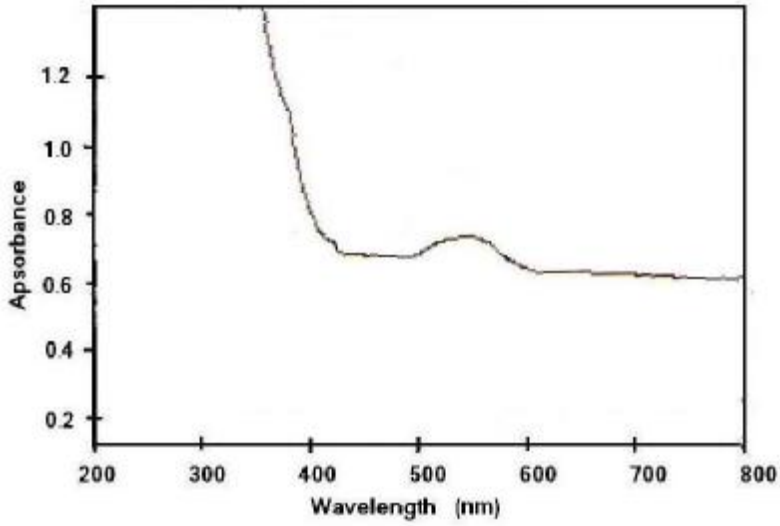

Figure 5.2: Solid state electronic absorption spectra measured for TiO_2/Anthocyanin dispersed as colloidal particles in toluene.

5.3.2.2 FT-IR for TiO_2/Anthocyanin:

Solid state FT-IR spectra were measured for TiO_2/Anthocyanin as KBr disc. When left over prolonged time periods (24 month) in the dark for 24 months the TiO_2/Anthocyanin showed no change in spectra, Figure (5.3). The peak at 1670 cm^{-1} is typical for carbonyl group. A broad band at 3400 cm^{-1} typical for hydroxyl groups was observed. The 1400 cm^{-1} band is assigned for unsaturated C=C bonds and for benzene ring. The FT-IR spectrum indicates the presence of anthocyanin onto TiO_2 particles. It also show the relatively high stability of anthocyanin with time.

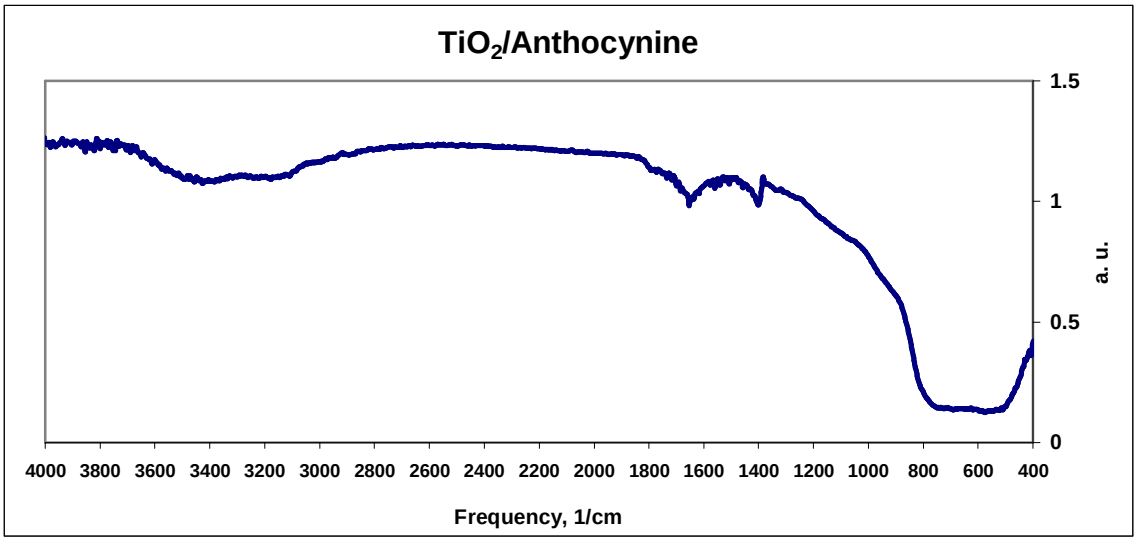

Figure 5.3: Solid state FT-IR spectrum of TiO_2/Anthocyanin measured as KBr disc.

5.3.2.3 Thermal Gravimetric Analysis (TGA) of AC/TiO_2/Anthocyanin:

TGA measurement of the AC/TiO_2/Anthocyanin was performed on a TA instrument 2950HR V5-3 TGA apparatus. The TGA showed a ~80% weight stile after 500°C, this weight is attributed to TiO_2, (Figure 5.4). The percent is parallel to catalyst nominal composition, which contained 83% TiO_2.

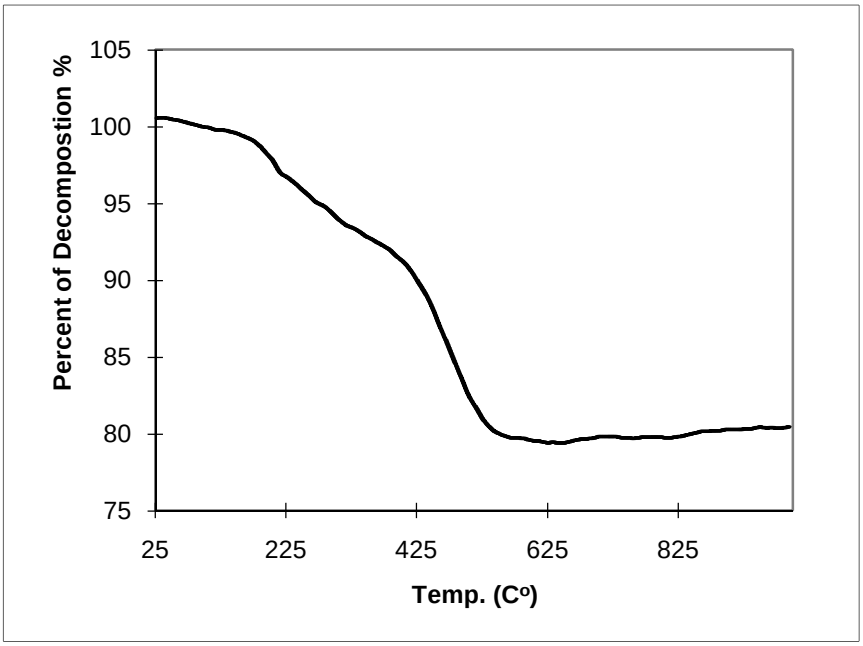

Figure 5.4: TGA thermograph for AC/TiO_2/Anthocyanin.

5.3.3 Photo-Catalytic Experiments:

Catalytic experiments were conducted in a 100 mL magnetically stirred thermostated glass beaker. The out-side walls of the beaker were covered with aluminum foil to reflect back astray radiations. The beaker was jacketed with controlled temperature water bath. Aqueous reaction mixtures (50 mL) of known nominal concentrations of contaminant and catalyst were placed in the beaker. The pH was controlled by adding a few drops of NaOH or HCl dilute solutions. Direct visible irradiation using a solar simulator halogen spot lamp (0.0212 W/cm^2) was applied to the photo-catalytic solution, (Figure 5.5). The spot lamp spectrum was comparable to solar light spectrum. The reaction mixture was exposed to incident irradiation directly coming out from the source lamp (adjusted

directly above the reaction mixture). The reaction mixture was exposed to air under continuous stirring.

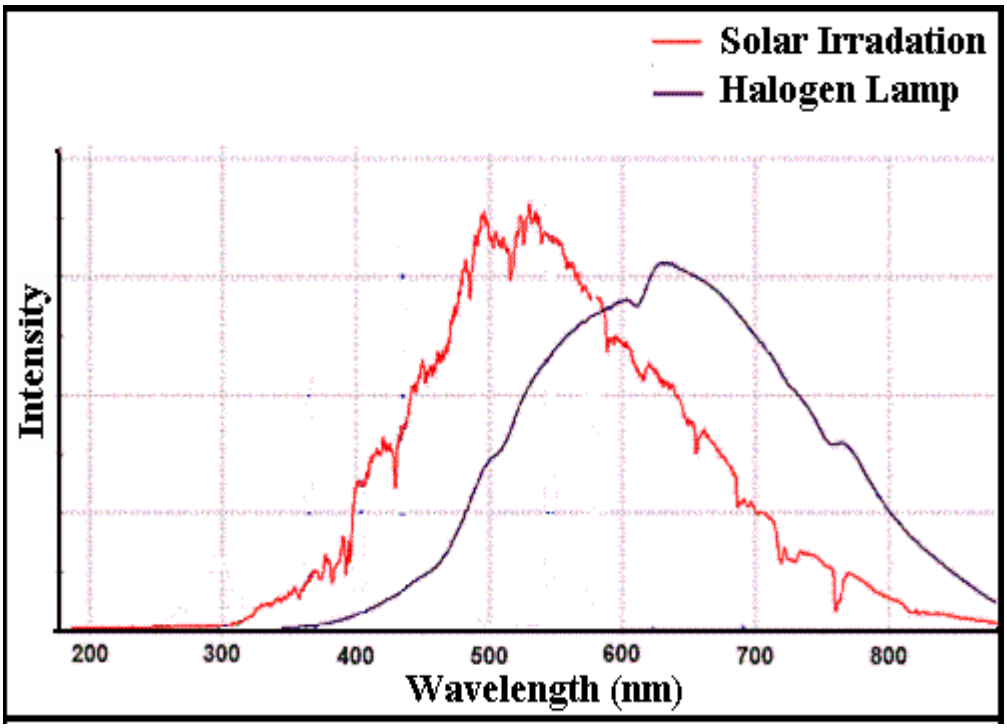

Figure 5.5: Solar radiation and Halogen spot lamp spectrum.

Different control experiments were conducted for different purposes. Known amounts of specific contaminant concentrations (50 ml), with added acid or base, were placed inside the reaction vessel. The solution was continually stirred for 90 min with no catalyst. The contaminant concentration was measured at different time intervals. This was to check if contaminant undergoes photolysis in absence of catalyst.

Anther control experiment was carried out by adding a known amount of catalyst, to the reaction mixture. The system was then continuously stirred in the dark for 90 min. The contaminant concentration was checked

periodically with time. The purpose was to know if contaminant loss occurs by adsorption onto solid systems.

A third control experiment was conducted using a UV screening filter. The filter was placed between the light source and the reaction mixture to block wavelengths of 400 nm or shorter. The experiment was conducted using TiO_2/Anthocyanin as a photo-degradation catalyst. The results of all control experiments will be discussed later.

The reaction progress was followed up by syringing out small aliquots, from the reaction mixture at different time intervals. Each aliquot was then immediately centrifuged (5000 rounds/min for 5 min) in dark, and the liquid phase was pipetted out for spectral analysis of the remaining contaminants at specific wavelength (λ_{480nm} for Methyl Orange and λ_{430nm} for Phenazopyridine). The reaction rate was measured based on analyzing remaining contaminant concentration with time. Values of turnover number (contaminant reaction moles per nominal TiO_2 mole after 60min) and quantum yield (contaminant reacted molecules per incident photon) were also calculated and used for efficiency comparison.

Recovery and reuse experiments were conducted using recovered catalyst, by filtration, after reaction completion. Recovered catalyst samples were re-used like fresh catalyst samples, as described above.

5.4 Results and Discussions:

5.4.1 Photo-degradation of Methyl Orange:

The systems TiO_2/Anthocyanins, AC/TiO_2/Anthocyanin, and naked TiO_2 were used as catalysts in photo-degradation of Methyl Orange, under solar

simulator radiations. Comparative study between catalyst systems was performed in order to assess the feasibility of anthocyanin as a safe future sensitizer. The efficiency of anthocyanin as a natural dye sensitizer was studied in terms of reaction rates, turnover number and quantum yield values. The effect of activated carbon support was also investigated.

5.4.1.1 Control Experiment Results:

The first control experiment was conducted under a halogen lamp radiation of 50 ml using Methyl Orange solution (5 ppm) in the absence of any catalyst systems with continued stirring. No significant change in Methyl Orange concentration occurred over a period of 90 min., (Figure 5.6). In the Second experiment, TiO_2/Anthocyanin (0.1 g) was added to Methyl Orange solution (50 ml, 5 ppm). The solution was stirred in dark for an hour to check for possible adsorption of Methyl Orange on the catalyst solid surface. The results, (Figure 5.6), indicated no observable contaminant adsorption on the TiO_2 or TiO_2/Anthocyanin system surfaces. In case AC/TiO_2/Anthocyanin (0.12 g) system, complete adsorption of Methyl Orange (5 ppm) on solid surface occurred in the dark. Therefore, the control experiment was repeated with higher Methyl Orange concentration (20 ppm). The purpose was to reach the equilibrium state of complete saturation of solid surface with contaminant. After 60 min of stirring in the dark, 5 ppm of Methyl Orange were adsorbed on the catalyst surface, and 15 ppm were left in solution. These results were considered while designing photo-degradation experiments using the

AC/TiO_2/Anthocyanin catalysts, *viz.* higher contaminant concentrations were typically used to account for adsorption of contaminant.

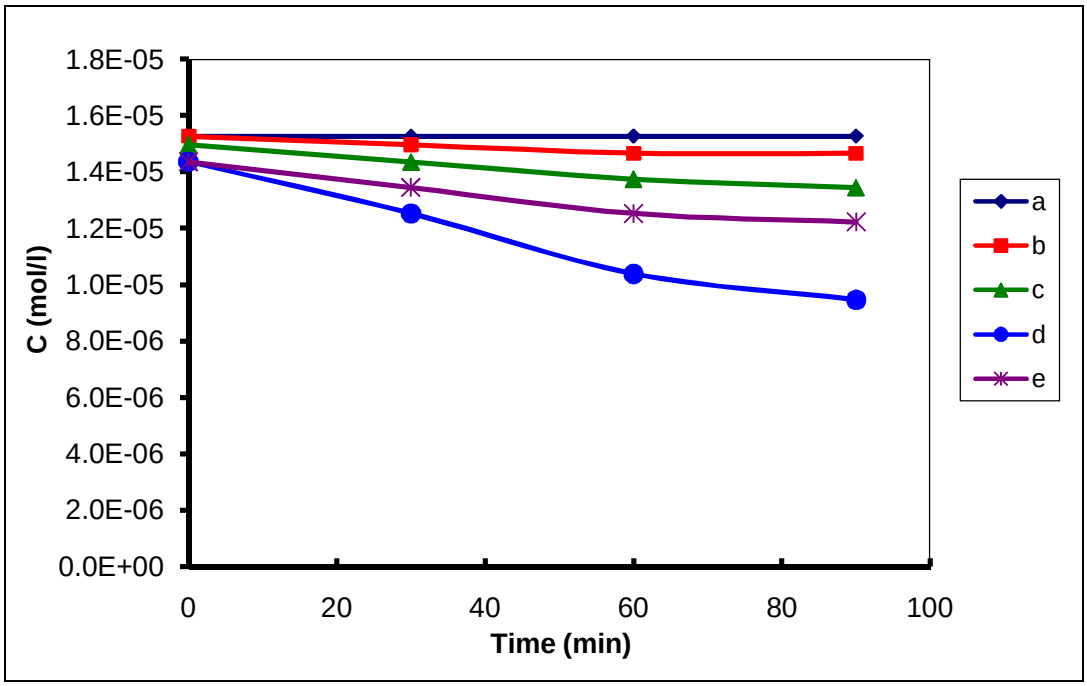

Figure 5.6: Results of control experiments: a) light with no catalyst b) TiO_2/Anthocyanin with no light c) TiO_2 with Visible light d) TiO_2/Anthocyanin with visible light e) TiO_2/Anthocyanin system with cut-off filter using. Experiments were conducted using 50 ml (5 ppm) Methyl Orange

The third control experiment was conducted to check the ability of anthocyanin to sensitize for TiO_2. For this purpose complete blockage of UV radiation was achieved by a cut-off filter that removes 400 nm (and shorter). Only visible light was allowed to pass. The results, Figure (5.6), show that the TiO_2/Anthocyanin catalyst functioned (with some decreased efficiency) under purely visible radiation. This indicates the sensitizing effect of anthocyanin in Methyl Orange photo-degradation with visible light.

5.4.1.2 Anthocyanin as Sensitizer:

Naked rutile TiO_2 powder failed to degrade Methyl Orange with a cut-of filter. The shortage in its efficiency is attributed to its wide band gap (3.2 eV), which needs photons with wavelengths shorter than 400 nm. With complete removal of waves shorter than 400 nm, no degradation occurred by the naked rutile TiO_2. The sensitized system (TiO_2/Anthocyanin) showed significantly higher efficiency (about 20% decomposition after 90 min with quantum yield 0.0000250 and turnover number 0.000076), (Figure 5.7). The results indicate the sensitizing ability of anthocyanin under visible light. The suggested mechanism will be discussed later.

About 13% decomposition occurred within 90 min radiation using TiO_2 under halogen lamp with no cut-of filter, (Figure 5.7). The quantum yield and the turnover number values were 0.000016 and 0.000049, respectively. The slight decomposition of Methyl Orange on TiO_2 is attributed to small UV fraction in the solar simulator spectrum.

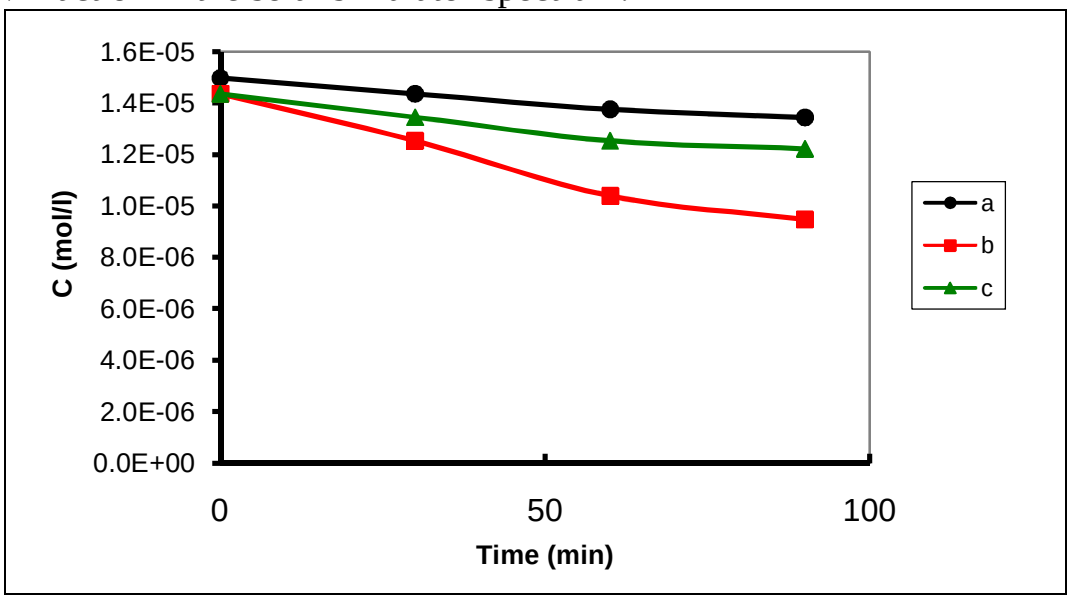

Figure 5.7: Effect of cut-off filter: a)TiO_2 under visible light, b) TiO_2/Anthocyanin under visible light, c) TiO_2/Anthocyanin using filter

400 nm. Q.Y & T.N: a) 0.000016 & 0.000049 b) 0.000053 & 0.000159 c) 0.0000250 & 0.000076. All experiments were conducted using 0.1 g catalyst on 50 ml 5 ppm MO.

About 40% of Methyl Orange decomposed after 90 min irradiation using TiO_2/Anthocyanin with no cut-of filter, giving values of quantum yield and the turnover number 0.000053 and 0.000159 respectively. The results show that photo-degradation occurs via two concurrent routes: the first route occurs by exciting TiO_2 itself with the small UV fraction, and the second occurs via sensitization mechanism. The fact that the TiO_2/Anthocyanin was more efficient in the absence of a filter is due to blockage of the first route.

In sensitization, photons excite anthocyanin electrons from HOMO to LUMO. Knowing that preliminary molecular orbital calculation using the Spartan software package indicate that, for the quinonoidal (type of anthocyanin) form complexd with the bare Ti(IV) ion, the LUMO electron density is located near the Ti end of the complex and the HOMO is located on the opposite side end. Such a configuration is favorable for electron injection. The excited electrons in the LUMO are quickly injected to the TiO_2 conduction band, leaving the HOMO of anthocyanin with positive cavity [12-13]. The electrons, injected in TiO_2 conduction band, behave as a reducing agent for O_2 to yield O_2^-. The positive cavity in the HOMO of the anthocyanin behaves as an oxidizing agent for the contaminant molecules (Methyl Orange). The mechanism is summarized in Scheme (5.3).

The sensitizing ability of anthocyanin has so far been evident. Study of different reaction parameters need to be studied. As this study is aimed to screen the effect of anthocyanin sensitization, we show here the effect of pH on photo-degradation processes.

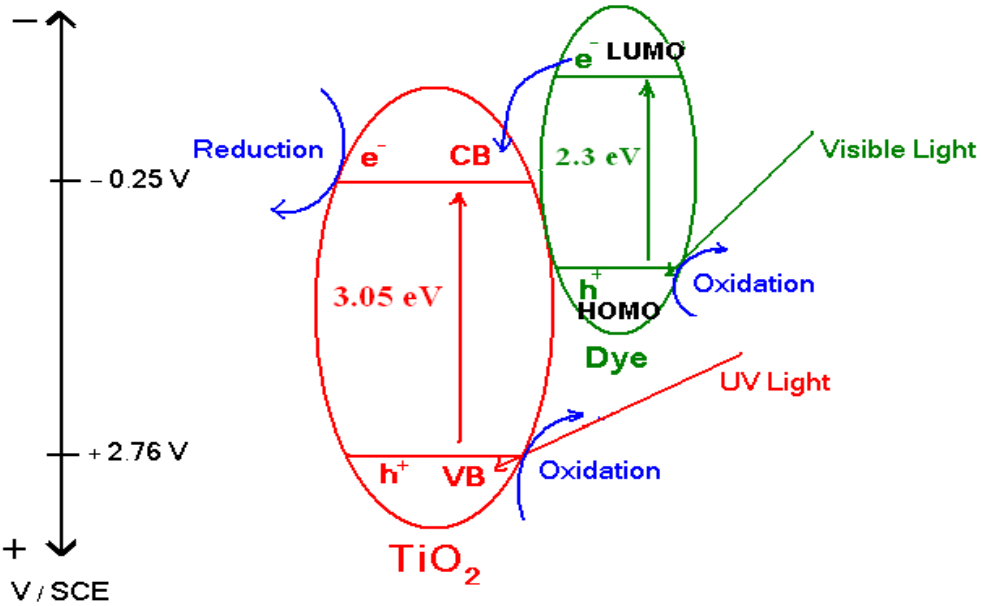

Scheme 5.3: Anthocyanin sensitizing of TiO_2 photo-degradation processes.

5.4.1.3 Effect of pH:

Aqueous solutions, pre-contaminated with Methyl Orange, at different pH values, were prepared. The acidic medium was adjusted to pH = 4.5 by adding drops of diluted $HCl_{(aq)}$ solution to the reaction container, while the basic medium was adjusted to pH = 11 by adding drops of diluted $NaOH_{(aq)}$ solution. Figure (5.8) shows the profiles of TiO_2/Anthocyanin catalyzed Methyl Orange degradation reactions. Efficiency of Methyl Orange degradation was affected by pH value. The efficiency is higher in acidic media. The behavior parallels earlier results observed for TiO_2 in decolorizing Methyl Orange and other contaminants [17-19]. Turnover

numbers and quantum yield values are comparable in neutral and basic media, but are higher in acidic media.

5.4.1.4 AC/TiO_2/Anthocyanin Catalytic System and pH:

In addition to TiO_2/Anthocyanin system, the AC/TiO_2/Anthocyanin was also investigated in Methyl Orange photo-degradation by solar simulator radiation. Our screening study here was focused on effect of pH on rate of degradation process. MO photo-degradation curves varied for different pH's values, (Figure 5.9). The photo-degradation rates were clearly higher as pH value was lowered. The calculated turnover frequency and quantum yield values showed such tendencies.

It should be noted here that the pH effect in case of AC/TiO_2/Anthocyanin system is more pronounced than in TiO_2/Anthocyanin.

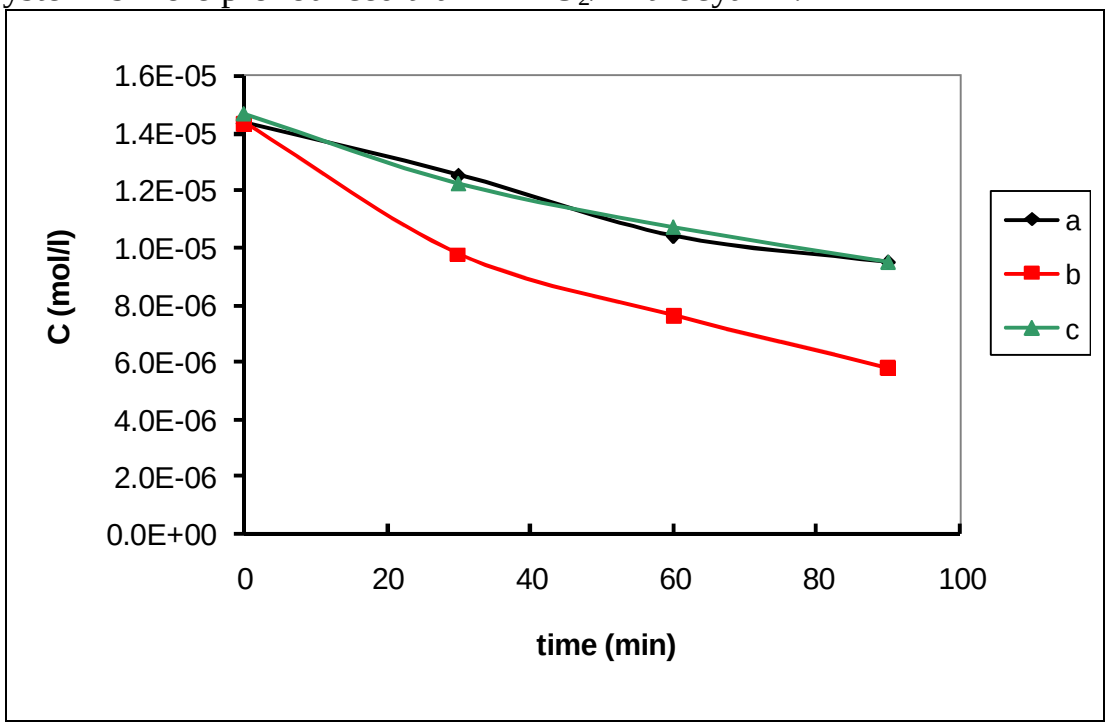

Figure 5.8: Effect of pH on photo-degradation rate of Methyl Orange using 0.1 g TiO_2/Anthocyanin stirred in reaction mixture (50 ml, 5 ppm MO): a) Neutral: b) Acidic pH = 4.5 c) Basic pH = 11.Values of T.N & Q.Y : a)

0.000159 & 0.000053 b) 0.000268 & 0.000089 c) 0.000160 & 0.000053. All measurements were conducted under solar simulator radiation (0.0212 W/cm^2).

This is understandable based on adsorption of contaminant molecules onto AC surface. In acidic media the Methyl Orange molecule undergoes protonation. The protonated molecule is easier to adsorb on AC. Thus the molecule becomes in closer proximity to the catalyst sites. This explains the special effect of pH value on degradation rate of Methyl Orange using AC/TiO_2/Anthocyanin system. Similar results were reported for different degradation systems [7,11].

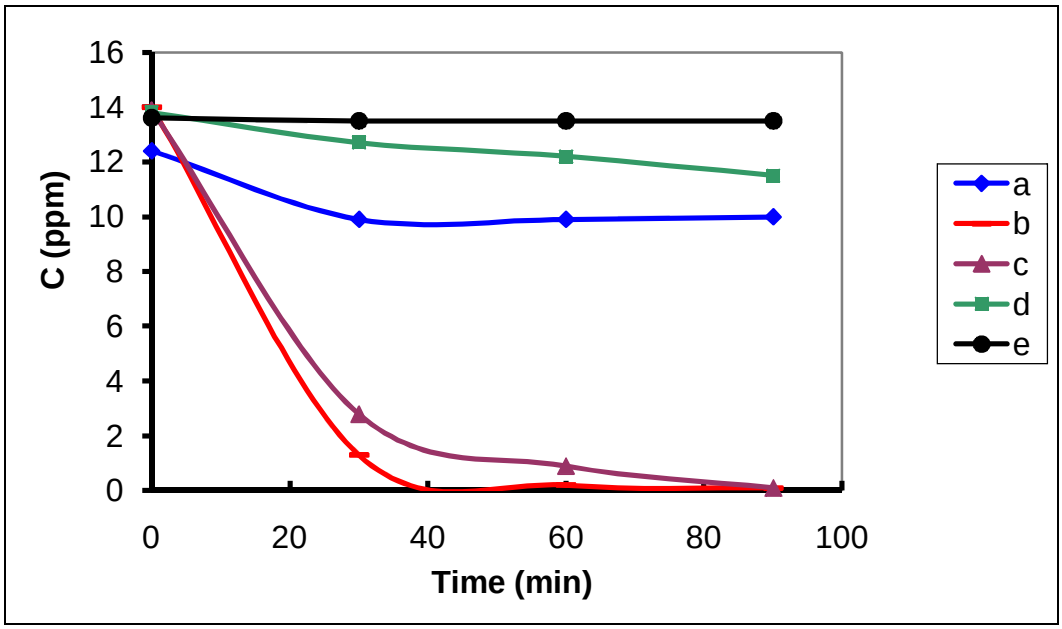

Figure 5.9: Effect of Medium pH on photo-degradation rate of Methyl Orange: 0.12 g AC/TiO_2/Anthocyanin on 50 ml 15 ppm MO, a) Neutral b) Acidic pH =3 c) Acidic pH=4.5 d) Basic pH=9.2 e) Basic pH= 11. T.N & Q.Y : a) 0.000306 & 0.000101 b) 0.001688 & 0.000560 c)0.001589 & 0.000527 d) 0.000196 & 0.000065 e) 0.000012 & 0.000004.

5.4.2 Photo-degradation of Phenazopyridine Hydrochloride:

The systems TiO_2/Anthocyanin, AC/TiO_2/Anthocyanin and naked TiO_2 were used as catalysts in photo-degradation of Phenazopyridine. Experiment were conducted under visible halogen spot lamp. Control experiments, as mentioned before in photo-degradation of Methyl Orange, were also conducted in photodegradation of Phenazopyridine. Turnover number and quantum yield were used to study catalyst efficiencies.

5.4.2.1 Control Experiments:

As in Methyl Orange degradation, control experiments were conducted here. The control experiments indicated that there was no reaction in the absence of light. Moreover, anthocyanin behaved as sensitizer for the TiO_2 system. The ability of AC to adsorb contaminant molecules was also manifested. Using a cut-off filter (400 nm and shorter wavelengths) proved the sensitizing effect of anthocyanin in degradation of Phenazopyridine. Results of control experiments are shown in Figure (5.10).

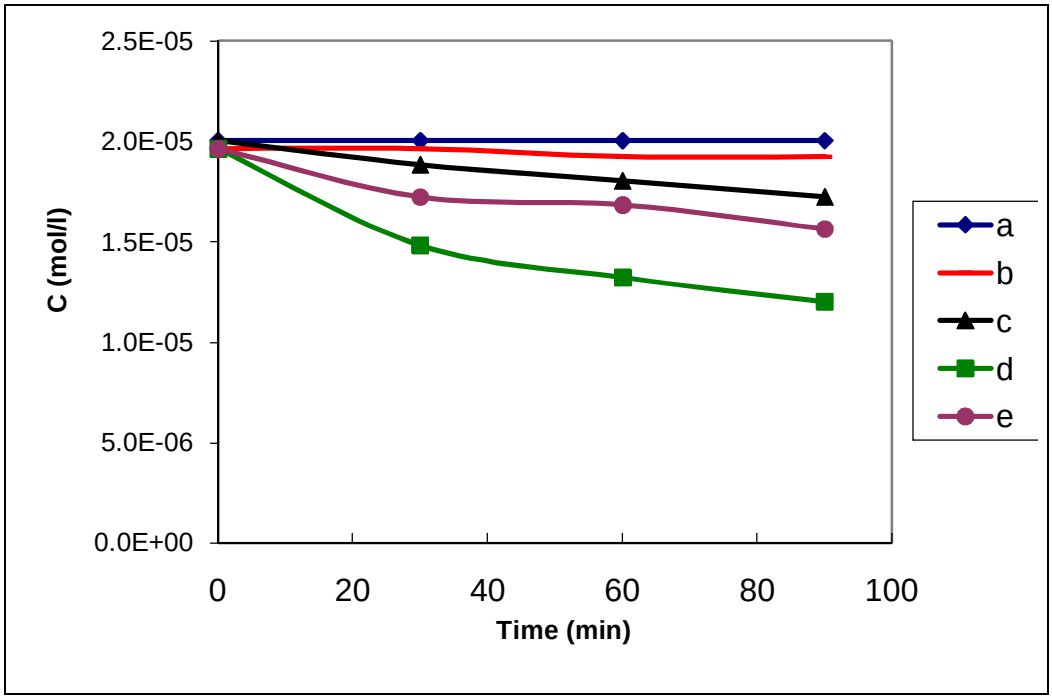

Figure 5.10: Results of control experiment on degradation of Phenazopyridine (50 mL, 5 ppm), a) light with no catalyst b) Catalyst with no light c) TiO_2 with light d) TiO_2/Anthocyanin with light e) Filter. TiO_2/Anthocyanin with light and cut-off filter (400 nm or shorter removed).
T.N & Q.Y: a) 0 & 0 b) 0.000016 & 0.0000050 c) 0.000080 & 0.000027 d) 0.000256 & 0.000085 e) 0.000112 & 0.000037

5.4.2.2 Anthocyanin as Sensitizer:

With complete removal of waves shorter than 400 nm using cut-of filter , no observable photo-degradation occurred by the naked rutile TiO_2. The TiO_2/Anthocyanin system showed significantly higher efficiency (about 25% decomposition after 90 min, with turnover number 0.000112 and quantum yield 0.000037). Figure (5.10) summarizes these results. The results indicate sensitization ability of anthocyanin under visible irradiation. About 17% decomposition occurred within 90 min irradiation using TiO_2 under halogen lamp without a cut-of filter, (Figure 5.10). Turnover number and quantum yield are 0.000080 and 0.000027

respectively. The slight decomposition of Phenazopyridine on TiO_2 is attributed to the very small UV fraction in the solar simulator spectrum. In case of TiO_2/Anthocyanin, with no cut-off filter, about 45% of Phenazopyridine decomposed within 90 min irradiation. The values of turnover number and quantum yield were 0.000256 and 0.000085, respectively. The proposed mechanisms for photo-degradation resembles that discussed above. Such a mechanism is widely accepted by researchers for different systems [12,22].

5.4.2.3 Effect of pH:

The effect of pH value on initial rate of photo-degradation of Phenazopyridine has been studied. Photo-degradation rate was measured in acidic (pH 4.5), basic (pH 9.5) and neutral (pH 7.0) media, Figure (5.11). The photo-degradation rate is higher in acidic media than in basic and neutral ones. The basic medium showed higher efficiency than the neutral one. The values of turnover number and quantum yield reflect the efficiency differences at different pH values.

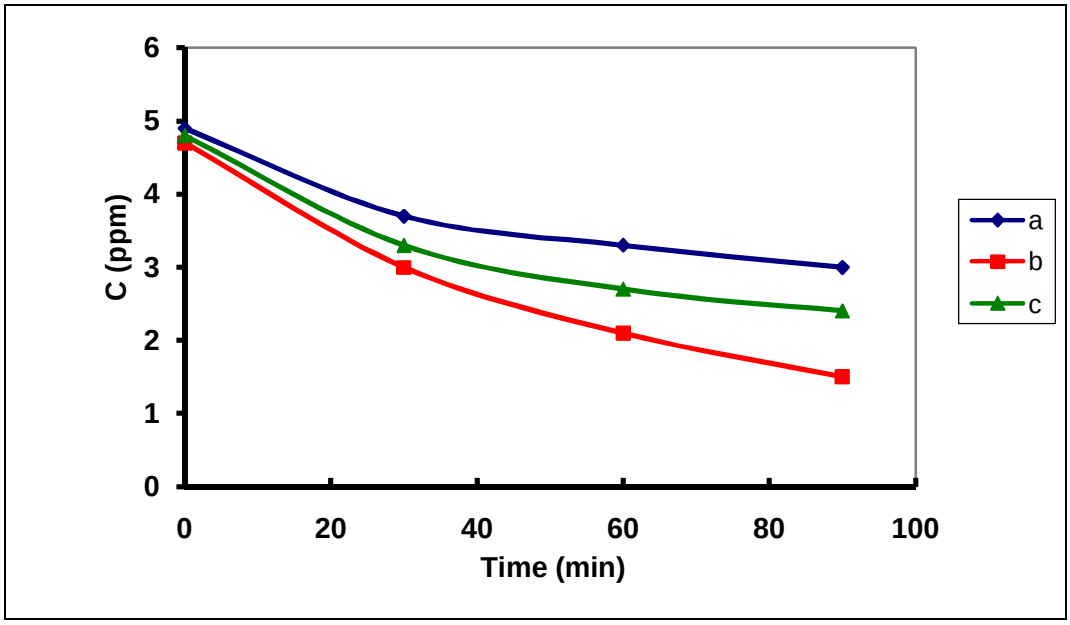

Figure 5.11: Effect of pH on photo-degradation rate of Phenazopyridine (50 mL, 5 ppm) using 0.1 g TiO_2/Anthocyanin: a) Neutral b) Acidic pH = 4.5 c) Basic pH = 11. T.N & Q.Y : a) 0.000256 & 0.000085 b) 0.000417 & 0.000138 c) 0.000336 & 0.000112 . All measurements were conducted using 0.0212 W/cm^2 radiation halogen lamp type.

5.4.2.4 AC/TiO_2/Anthocyanin Catalyst System and pH:

The effect of pH on photo-degradation rate was studied. Due to possible adsorption of contaminant on AC surface, a higher contaminant concentration (20 ppm) was used. Figure (5.12) shows that the highest values for turnover number and quantum yield occurred in basic media. The neutral medium showed higher activity than the acidic medium.

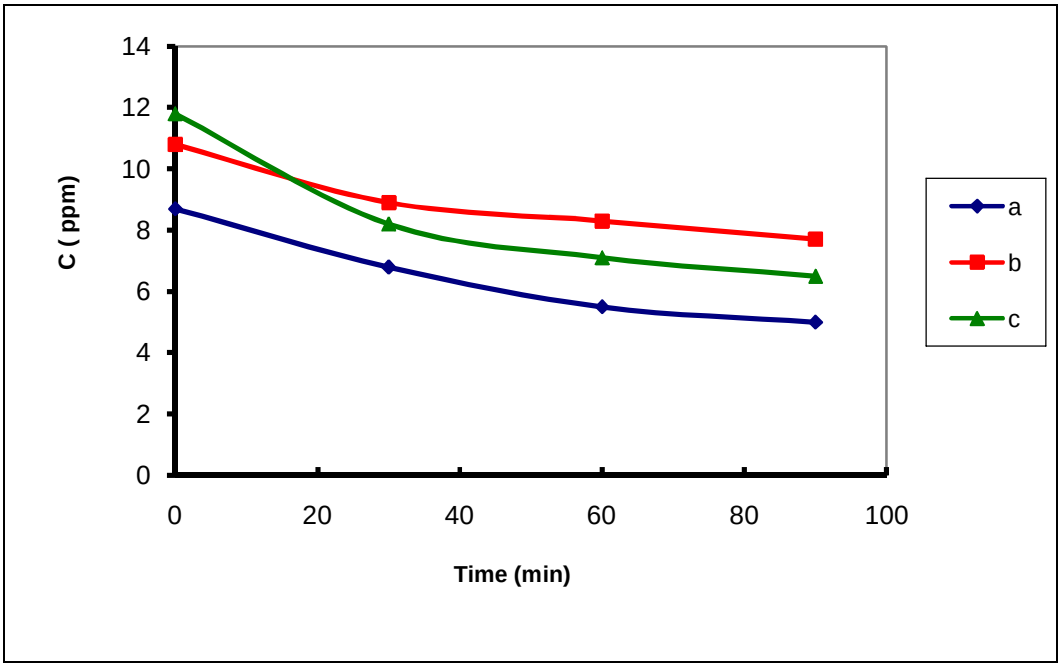

Figure 5.12: Effect of pH value on Phenazopyridine photo-degradation rate: 0.12 g AC/TiO_2/Anthocyanin on 50 ml 20 ppm PhPy, a) Neutral b) Acidic pH = 4.5 c) Basic pH = 11.
T.N & Q.Y: a) 0.000512 & 0.000170 b) 0.000404 & 0.000134 c) 0.000852 & 0.000282. All measurements were conducted using 0.0212 W/cm^2 radiation halogen lamp.

5.5 Conclusion:

Anthocyanin shows an observable efficiency towered sensitizing TiO_2 in visible region, the sensitized systems (TiO_2/Anthocyanin and AC/TiO_2/Anthocyanin) were used in photodegradation of both Methyl Orange and Phenazopyridine) under visible irradiation.

lower pH values (Except AC/TiO_2/Anthocyanin in photo-degradation Phenazopyridine) shows preference photo-degradation ability toward both Methyl Orange and Phenazopyridine, while AC/TiO_2/Anthocyanin shows a distinctive photo-degradation efficiency only toward Methyl Orange at lower pH values

References:

1- B. O. Regan, M. Grätzel, A low-cost, high-efficiency solar cellbased on dye-sensitized colloidal TiO_2 films. *Nature*, **353** (1991) 737–740.

2- K. Hara, *et al.*, Dye-sensitized nanocrystalline TiO_2 solar cellsbased on ruthenium(II) phenanthroline complex photosensitizers *Langmuir*, **17** (2001)5992–5999.

3- K. Tennakone, J. Bandara, Photocatalytic activity of dye-sensitized tin(IV) oxide nanocrystalline particles attached to zinc oxide particles: long distance electron transfer via ballistic transport of electrons across nanocrystallites, *Appl. Catalys A: Gen.*, **208** (2001) 335-341.

4- S. S. Srinivasan, J. Wade, E. K. Stefanakos, Visible Light Photocatalysis via CdS/TiO_2 Nanocomposite Materials, *J. Nanomat.*, **2006** (2006), 7 pages.

5- E. Yamazaki, M. Murayama, N. Nishikawa, N. Hashimoto, M. Shoyama, O. Kurita, Utilization of natural caroteniods asphotosensitizers for dye-sensitized solar cells. *Sol. Energy*, **81** (2007) 512–516.

6- K. Tennakone, A. R. Kumarasinghe, G. R. R. A. Kumara, K. G. U. Wijayantha, P. M. Sirimanne, Nanoporous TiO_2 photoanode sensitized with the flower pigment cyanadin. *J. Photochem. Photobiol. A*, **108** (1997) 193–195.

7- S. Hao, J. H. Wu, Y. Huang, J. Lin, Natural dyes as photosensitizers for dye-sensitized solar cells. *Sol. Energy*, **80** (2006) 209–214.

8- A. Kay, M. Gratzel, Artificial Photosynthesis. 1. Photosensitization of TiO_2 Solar Cells ith Chlorophyll Derivatives and Related Natural Porphyrines, *J. phys. Chem.*, **97** (1993) 6272-7.

9- K. Wongcharee, V. Meeyoo, S. CHavadej, Dye-sensitized solar cell using natural dyes extracted from rosella and blue pea flowers, *Sol. Energ. Mat. Sol. C.*, **91** (2007) 566-571.

10- M.Grätzel, A.J.McEvoy, Principles and Applications of Dye Sensitized Nanocrystalline Solar Cells (DSC), *Asian J. Energy Environ.*, **5** (2004) 197-210.

11- H.S. Hilal, L.Z. Majjad, N. Zaatar, A. El-Hamouz, Dye-effect in TiO_2 catalyzed contaminant photo-degradation: Sensitization vs. charge-transfer formalism, *Solid State Sci.* **9** (2007) 9-15.

12- N. J. Cherepy, G. P. Smestad, M. Graetzel and J. Z. Zhang, Ultrafast electron injection: Implications for a photoelectrochemical cell utilizing an anthocyanin dye sensitized $Ti0_2$ nanocrystalline electrode, *J. Phys. Chem. B*, **101** (1997) 9342-9351.

13- K. Dutta, S. Mukhopadhyay, S. Bhattacharjee, B. Chaudhuri, Chemical oxidation of methylene blue using Fenton-like reactions *J. Hazard. Mat.*, **84** (2001) 57–71.

14- L.G. Devi, S.G. Kumar, K.M. Reddy, C. Munikrishnappa, Photo degradation of Methyl Orange an azo dye by Advanced Fenton Processusing zero valent metallic iron: Influence of various reactionparameters and its degradation mechanism, *J. Hazard. Mat.*, **164** (2009) 459–467.

15- B. Neppolian, H.C. Choi, S. Sakthivel, B. Arabindoo, V. Murugesan, Solar UV-indiced photocatalytic degradation of hthree commercial textile dyes, *J. Hazard. Mat.*, **89** (2002) 303-317.

16- R.J. Davis, J.L. Gainer, G.O. Neal, I.W, Wu, Photocatalytic decolorization of wastewater dyes, *Water Environ. Res.*, **66** (1994) 50-53.

17- A.C. Coiffard, L.J.M. Coiffard and Y.M.R. De Roeck-Holtzhauer, Photo-degradation kinetics of acesulfame-K solutions under UV light: effect of pH, *Eur. Food Res. Technol.*, **208** (1999) 6-9.

18- Mo S. Al-Kahali, and Nada Al-Kata'a , pH effect on the photocatalytic degradation of the chloropyrifus from onsecticide morisban4 by ZnO in aqueous medium *Ass. Univ. Bull. Environ. Res*. **9** (2006) 23-31**.**

19- C.-H. Wu and C.-H. Yu, Effects of TiO_2 dosage, pH and temperature on decolorization of C.I. Reactive Red 2 in a UV/US/TiO_2 system, *J. Hazard. Mat.*, **169** (2009) 1179-1183.

20- F.-b. Li, G.-b. Gu, G.-f. Huang, Y.-l. Gu, H.-f. Wan, TiO_2-assisted photo-catalysis degradation process of dye chemicals, *J. Environ. Sci.*, **13** (2001) 64-68.

21- J.R. Colven, Binding of anions by denatured proteins, *Can. J. Chem.*, **30** (1952) 973-984.

22- P. A. Connor, K. D. Dobson, A. McQuillan, New Sol-Gel Attenuated total Reflection Infrared Spectroscopic Method forAnalysis of Adsorption at Metal Oxide Surfa ces in Aqueous Solutions. Chelation of TiO_2, ZrO_2, and Al_2O_3 Surfaces by Catechol, 8-Quinolinol, and Acetylacetone *J. Langmuir,* **11** (1995) 4193-4195.

23- K. Mehrotra, G. S. Yablonsky, and A. K. Ray, Macro Kinetic Studies for Photocatalytic Degradation of Benzoic Acid in Immobilized System, *Chemosphere*, **60** (2005) 1427-1436.

24- J. Fernando and G. Senadeera, Natural Anthocyanins as photosensitizers for dye-sensitized solar devices, *Curr. Sci. India*, **95** (2008) 663-666.

OVERALL CONCLUSION

1- Rutile TiO_2 particles were coated by CdS particles at the nano scale (17-20 nm) as confirmed by SEM. XRD indicated a cubic structure for CdS particles. The CdS effectively sensitized TiO2 under solar

simulator light in degradation of methyl orange and Phenazopyridine.

2- Electronic absorption spectra and voltametry confirmed complete mineralization of degraded contaminants.

3- Despite ability of CdS to sensitize TiO_2 in contaminant photodegradation, its tendency to degrade into soluble Cd^{2+} ions limits its applicability in water purification strategies.

4- Supporting TiO_2/CdS system onto sand lowered catalytic efficiency but made recovery feasible by simple filtration. Degradation of CdS was not terminated by the support.

5- A screening study using natural dyes (such as Anthocyanin) as sensitizers showed their potential as sensitizers in photo-degradation of Methyl Orange and Phenazopyridine. Supporting the TiO_2/Anthocyanin onto activated carbon, enhanced the reaction rates.

SUGGESTIONS FOR FURTHER WORK

1- Attempt to prevent CdS decomposition by covering the CdS particles with conducting polymer thin film. Use a composite catalyst of TiO_2 with CdS.

2- Replace CdS with other synthetic dyes.

3- Using other natural dyes to sensitize TiO_2 in different contaminant photo-degradations.
4- Study the effect of light concentration on photo-degradation rates and kinetics.
5- Degrade other water contaminants, such as drug formulations, fertilizers, chlorinated hydrocarbons, insecticides, pesticides, phenols and others using TiO_2/Anthocyanin systems.
6- Use other solid substrates (ceramics, clays, or glass pellets) in addition to activated carbon and sand to support TiO_2/Anthocyanin catalysts in water purification studies.

جدوى استخدام نانوحبيبات CdS في تنشيط TiO_2 لتحطيم الملوثات العضوية في الماء ضوئيا، والأصباغ الطبيعية كبدائل

اعداد : عـاهـد حسني عبد الرزاق زيــود

مشرف رئيسي: أ. د. حكمت هلال

مشرف ثاني: نضال زعتر

الملخص

تم في هذه الدراسة ترسيب دقائق كبريتيد الكادميوم CdS (17-20 نانوميتر) على حبيبات اوكسيد التيتيانيوم TiO_2 لتحضير الحفاز TiO_2/CdS، وتم استخدام حبيبات الرمل الطبيعي بعد معالجتها كسطوح لتثبيت الحفاز المحسن عليها لتحضير $Sand/TiO_2/CdS$. ولقد تم إجراء تشخيص لطبيعة كل من الحفازين من خلال اجراء مجموعة قياسات وتحاليل متقدمة لكل منهما. كما وتم استخدام الحفازين في تحطيم ملوثات عضوية (الميثيل البرتقالي المعروفة وعقار الفينازوبيريدين) في وسط مائي ، حيث اظهر استخدام الحفازات المحفزة بكبريتيد الكادميوم CdS قدرة عالية لتحطيم الملوثات باستخدام الإشعاعات المرئية. وتم كذلك دراسة تأثير تركيز كل من الحفاز والملوث وأثر درجة الحرارة ودرجة الحموضة على سرعة التفاعل. ورغم قدرة CdS على تنشيط TiO_2 على الحفز في الضوء المرئي الا أنه لوحظ تفككه الكامل خلال عملية تحطيم الملوثات مما أنتج ايونات الكادميوم Cd^{2+} في المياه المعالجة وبتراكيز مرتفعة ضارة صحيا، مما يضفي محاذير لاستخدام هذه الحفازات في عملية المعالجة، رغم أن كثيرا من الباحثين ما زال مهتما باستخدامها دون التطرق الى هذه المحاذير.

ولتجنب استخدام كبريتيد الكادميوم CdS في تنشيط اوكسيد التيتانيوم TiO_2 لجأنا الى استخدام صبغات طبيعية وآمنة كبدائل عن CdS حيث استخدمت الصبغة المستخرجة من أزهار الكركديه (Anthocyanin) من اجل هذا الغرض. هذا وقد تم تثبيت الحفازات المستخدمة على سطوح الكربون المنشط. وقد تم تشخيص هذا الحفاز من خلال اجراء مجموعة تحاليل وقياسات له. كما وتم دراسة تاثير تركيز كل من الحفاز والملوث وتأثير درجة الحموضة على نشاط الحفاز في تحطيم كل من الميثيل البرتقالي والفينازوبيريدين. وقد لوحظ اثر واضح في زيادة فعالية

الحفاز $AC/TiO_2/Anthocyanin$ في تحطيم الميثيل البرتقالي تحت الإشعاعات المرئية في المحاليل الحامضية.

يستنتج من هذه الدراسة أن استخدام CdS كمنشط للحفاز TiO_2 وان كان له حسنات واضحة الا أن له سيئات ومشاكل صحية وبيئية لم يتم تجنبها. وعليه فاننا نقترح أن يتم تركيز الباحثين مستقبلا على صبغات طبيعية أمنة متل صبغة الكركديه وغيره.

Appendix A

Appendix B

PUBLICATIONS AND CONFERENCES

- **Ahed H. Zyoud** and Hikmat S. Hilal*, Silica-Supported CdS-Sensitized TiO_2 Particles in Photo-Driven Water Purification: Assessment of Efficiency, Stability and Recovery Future Perspectives, *Chapter 5, Water Purification, Nova science Publ.*, (2009), https://www.novapublishers.com/catalog/product_info.php?products_id=10061, ISBN: 978-1-60741-599-2,

- **Ahed Zyoud**; Nidal Zaatar; Iyad Saadeddin; Cheknane Ali; DaeHoon Park; Guy Campet; HikmatS Hilal, Ph.D , CdS-sensitized TiO_2 in phenazopyridine photo-degradation:

Catalyst efficiency, stability and feasibility assessment. *Journal Hazardous Materials, Elsevier*, Finally accepted Aug. 19, 2009.

- Hikmat S. Hilal, Gahzi Y. M. Nour and **Ahed Zyoud**, Photo-Degradation of Methyl Orange with Direct Solar Light using ZnO and Activated Carbon-Supported ZnO, *Chapter 6, Water Purification, Nova science Publ.*, (2009), https://www.novapublishers.com/catalog/product_info.php?products_id=10061, ISBN: 978-1-60741-599-2,

- Hikmat S. Hilal, Rania M. A. Ismail, and Amer El-Hamouz, **Ahed Zyoud**, Iyad Saadeddin, Effect of cooling rate of pre-annealed CdS thin film electrodes prepared by chemical bath deposition: Enhancement of photoelectrochemical characteristics, *Electrochimica Acta, Accepted Manuscript*, 2009

- Hikmat S. Hilal, **Ahed Zyoud** and Ghazi Nour**,** Assessment of CdS as Sensitizer for TiO_2 and ZnO in Water Purification with Solar Light, *The 1st International Workshop on Advanced Material 22-24 Feb 2009 {IWAM-09} at Ras Al khaimah centre for advanced materials (RAK CAM)".*

- **Ahed Zyoud**, Hikmat Hilal, Photo-degradation of organic contaminants by CdS-sensitized TiO_2 supported onto insoluble support, *the Fourth Chemistry Conference / Alquds University/ 14-15th April* 2008.

- **Ahed Zyoud** and Hikma Hilal **,** Photo-degradation of Organic Contaminant by Dyes-Sensitized Nanoparticles of TiO_2 Supported onto Insoluble Supports, *the international conference for nanotechnology industries, King Abdullah Institute for nanotechnology, April 2009, King Saud University, Riyadh.*

- Hikmat S. Hilal and **Ahed Zyoud**, TiO_2 Nano-Particles Modified with Natural Dyes: Application in Photodegradation of Organic Contaminants, *Hybrid Materials 2009, (submitted to HYBRID MATERIALS 2009, First International Conference*

on Multifunctional, Hybrid and Nanomaterials 15-19 March 2009, Tours, France).

- Hikmat S. Hilal and **Ahed Zyoud**, Dye-Modified TiO_2 Particles In Water Purification With Solar Light, Conference on Energy and Renewable Energy Resources, *Fez, Maroco, Oct. 26-28, 2008, (Finally Accepted for oral presentation).*

- Hikmat S. Hilal, **Ahed Zyoud** and others, Preparation and modification of photoconversion efficiency and stability of CBD-based thin-film electrodes, 2nd International Workshop for Renewable Energies and its Applications (WIERA2009), 17-18 November 2009, Bejaia University, Algeria, (*Accepted for oral presentation).*

- Hikmat S. Hilal, **Ahed Zyoud** and Ghazi Nour, Dye-modified semiconductor nano-particles in water purification with solar light, Nanomaterials and Solar Energy Conversion (Solar'09), 10 - 14 January 2009, Luxor, Egypt, (*Accepted for oral presentation).*

- Hikmat S. Hilal, **Ahed Zyoud** and others, Simple Techniques to Enhance Semiconductor Characteristics in Solar Energy Conversion, International Conference on Nanotechnology and Advanced Materials (ICNAM 2009), 4-7 May (2009), Bahrain University, (*Accepted for oral presentation).*

- Hikmat S. Hilal, **Ahed Zyoud** and others, Enhancement of Monolithic and Thin-Film Based Solar Cells: Surface Modification with Charge Transfer Mediators, Nano/Molecular Photochemistry and Nanomaterials for Green Energy Development, (Solar'10), 15 - 17 February 2010, Cairo, Egypt, (*Accepted for oral presentation).*

جامعة النجاح الوطنية
كلية الدراسات العليا

جدوى استخدام نانوحبيبات CdS في تنشيط TiO_2 لتحطيم الملوثات العضوية في الماء ضوئيا، والأصباغ الطبيعية كبدائل

اعداد
عـاهــد حــســني عــبــد الــرزاق زيـــود

إشراف
أ. د. حكمت هلال
و
د. نضال زعتر

قدمت هذه الأطروحة استكمالا لمتطلبات درجة الدكتوراة في الكيمياء بكلية الدراسات العليا في جامعة النجاح الوطنية/ نابلس/ فلسطين

2009

جدوى استخدام نانوحبيبات CdS في تنشيط TiO_2 لتحطيم الملوثات العضوية في الماء ضوئيا، والأصباغ الطبيعية كبدائل

إعداد
عـاهــد حــســني عــبــد الــرزاق زيـــود

إشراف
أ. د. حكمت هلال
و
د. نضال زعتر

الملخص

تم في هذه الدراسة ترسيب دقائق كبريتيد الكادميوم CdS (17-20 نانوميتر) على حبيبات اوكسيد التيتيانيوم TiO_2 لتحضير الحفاز TiO_2/CdS، وتم استخدام حبيبات الرمل الطبيعي بعد معالجتها كسطوح لتثبيت الحفاز المحسن عليها لتحضير $Sand/TiO_2/CdS$. ولقد تم إجراء تشخيص لطبيعة كل من الحفازين من خلال اجراء مجموعة قياسات وتحاليل متقدمة لكل منهما. كما وتم استخدام الحفازين في تحطيم ملوثات عضوية (الميثيل البرتقالي المعروفة وعقار الفينازوبيريدين) في وسط مائي ، حيث اظهر استخدام الحفازات المحفزة بكبريتيد الكادميوم CdS قدرة عالية لتحطيم الملوثات باستخدام الإشعاعات المرئية. وتم كذلك دراسة تأثير تركيز كل من الحفاز والملوث وأثر درجة الحرارة ودرجة الحموضة على سرعة التفاعل. ورغم قدرة CdS على تنشيط TiO_2 على الحفز في الضوء المرئي الا أنه لوحظ تفككه الكامل خلال عملية تحطيم الملوثات مما أنتج ايونات الكادميوم Cd^{2+} في المياه المعالجة وبتراكيز مرتفعة ضارة صحيا، مما يضفي محاذير لاستخدام هذه الحفازات في عملية المعالجة، رغم أن كثيرا من الباحثين ما زال مهتما باستخدامها دون التطرق الى هذه المحاذير.

ولتجنب استخدام كبريتيد الكادميوم CdS في تنشيط اوكسيد التيتانيوم TiO_2 لجأنا الى استخدام صبغات طبيعية وآمنة كبدائل عن CdS حيث استخدمت الصبغة المستخرجة من أزهار الكركديه (Anthocyanin) من اجل هذا الغرض. هذا وقد تم تثبيت الحفازات المستخدمة على سطوح الكربون المنشط. وقد تم تشخيص هذا الحفاز من خلال اجراء مجموعة تحاليل وقياسات له. كما وتم دراسة تاثير تركيز كل من الحفاز والملوث وتأثير درجة الحموضة على نشاط الحفاز في تحطيم كل من الميثيل البرتقالي والفينازوبيريدين. وقد لوحظ اثر واضح في زيادة فعالية الحفاز $AC/TiO_2/Anthocyanin$ في تحطيم الميثيل البرتقالي تحت الإشعاعات المرئية في المحاليل الحامضية.

يستنتج من هذه الدراسة أن استخدام CdS كمنشط للحفاز TiO_2 وان كان له حسنات واضحة الا أن له سيئات ومشاكل صحية وبيئية لم يتم تجنبها. وعليه فاننا نقترح أن يتم تركيز الباحثين مستقبلا على صبغات طبيعية أمنة متل صبغة الكركديه وغيره.